UNIVERSITÀ DEGLI STUDI DI MILANO

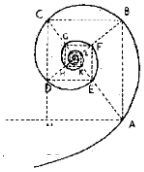

DOTTORATO IN MEDICINA MOLECOLARE

E TRASLAZIONALE

CICLO XXXI

Anno Accademico 2017/2018

TESI DI DOTTORATO DI RICERCA

MED/26 Neurologia

TDP-43 AND NOVA-1 RNA BINDING PROTEINS AS SPLICING REGULATORS OF *TNIK* GENE, A SCHIZOPHRENIA GENETIC RISK FACTOR

Dottorando : Valentina GUMINA

Matricola N° R11325

TUTORE: Dott.ssa Antonia RATTI

COORDINATORE DEL DOTTORATO: Prof. Riccardo GHIDONI

Abstract

TDP-43, a RNA-binding protein (RBP) involved in different steps of RNA metabolism, forms pathological aggregates in affected tissues of the majority of amyotrophic lateral sclerosis (ALS) patients and of a subset of frontotemporal dementia (FTLD) cases. Our group has recently demonstrated that TDP-43 regulates the alternative splicing of several pre-mRNAs related to neuronal metabolism, including *TNIK*, encoding for a Ser/Thr kinase highly expressed in the brain. TDP-43 promotes the skipping of *TNIK* alternative exon 15, which encodes for a 29-amino-acid sequence in a region of the protein with unknown function. The *TNIK* gene was found to be genetically associated to psychiatric disorders, such as schizophrenia, as a risk factor, and to intellectual disability for null-mutations. In neurons, TNIK is involved in regulating different processes, including synapse formation, dendrite arborization and neurogenesis.

In this study, our first aim was to investigate the regulation of *TNIK* exon 15 alternative splicing during neuronal differentiation in order to better characterize the role played by the ubiquitously expressed and ALS/FTLD-associated TDP-43 splicing factor in a neuronal context. Our second aim was to investigate if the specific expression of TNIK exon15-cointaining (TNIKex15) protein isoforms may be important to maintain TNIK physiological function in neurons, mainly focusing on its activity in neurite development.

We first observed that *TNIK* exon 15 alternative splicing was differently regulated in human adult tissues and *TNIKex15* isoforms were exclusively expressed in brain, spinal cord and skeletal muscle. Given the prevalent expression of *TNIKex15* isoforms in the central nervous system, we further investigated this alternative splicing event in *in vitro* models to evaluate its regulation during the neuronal differentiation process. We found a significant increase of *TNIKex15* transcripts in both SK-N-BE cells treated with retinoic acid and in human iPSCs differentiated into neurons. Moreover, TNIKex15 protein isoforms were specifically expressed in neuron-differentiated cells showing a prevalent perinuclear distribution in immunofluorescence analyses.

Since we previously showed that *TNIK* exon 15 inclusion increases upon TDP-43 knock-down, we measured TDP-43 protein content during neuronal differentiation *in vitro* but we found no changes. We therefore investigated the possible involvement of the neuron-specific splicing factor NOVA-1, specifically expressed in our neuron-differentiated cells, in regulating *TNIK* processing. In HEK293T cells, NOVA-1 over-expression increased *TNIK* exon 15 inclusion without negatively affecting TDP-43 protein content compared to mock-transfected cells. Furthermore, by minigene splicing assays we evaluated the NOVA-1 interplay with TDP-43 in regulating *TNIK* exon 15 splicing. In this analysis, we also included hnRNPA2/B1, an ubiquitous RBP that co-operates with TDP-43 in regulating its splicing activity and that we found to promote *TNIK* exon 15 skipping, similarly to TDP-43. In competition assay with TDP-

43 and hnRNPA2/B1, NOVA-1 completely abrogated their exon skipping activity on *TNIK* gene interacting with TDP-43 and hnRNPA2/B1 proteins in a RNA-dependent manner.

As our results suggested a neuronal relevance for TNIKex15 protein isoforms, we further investigated the specific function of these isoforms in neurite development in murine primary cortical neurons. *TNIKex15* over-expression negatively affected neurite development, reducing neurite number, as already describe in literature. When we analyzed TNIKex15-expressing neurons, we observed reduced filopodia number at growth cones, reduced soma area and filamentous actin (F-actin) levels compared to control cells. In contrast, upon *TNIK* exon 15-deleted (TNIKΔ15) over-expression, we found similar neurite development, soma and growth cones morphology and F-actin levels to control cells and also to TNIK KM, a TNIK mutant with a defective kinase activity. Moreover, *TNIKex15* over-expression affected cell spreading in HEK293T cells that showed a prevalent round morphology compared to control cells. In contrast, *TNIKΔ15*-expressing cells presented an intermediate phenotype.

In conclusion, our study has demonstrated that TNIKex15 isoforms are specifically expressed in neuronal tissues and during neuronal differentiation *in vitro* and that these isoforms show a specific function in regulating neurite development, influencing F-actin organization. Moreover, the neuron-specific splicing factor NOVA-1, probably promoting the formation of new ribonucleoprotein complex(es) with the ubiquitous splicing factors TDP-43 and hnRNPA2B1, acts as “silencer” of their splicing inhibitory activity on *TNIK* pre-mRNA.

These results suggest that investigating NOVA-1/TDP-43 competitive mechanism also for other TDP-43 splicing targets may further help the understanding of TDP-43 splicing activity in a neuronal environment and in ALS/FTD diseases.

Riassunto

TDP-43, una proteina legante gli RNA e coinvolta in diversi step del metabolismo degli RNA, forma aggregati patologici nei tessuti affetti della maggior parte dei pazienti colpiti da sclerosi laterale amiotrofica (SLA) e in un sottogruppo di pazienti con demenza frontotemporale (FTD). Il nostro gruppo ha recentemente dimostrato che la proteina TDP-43 regola lo splicing alternativo di diversi geni coinvolti nel metabolismo neuronale, compreso *TNIK*, che codifica per una serina/treonina chinasi, espressa ad alti livelli nel cervello. TDP-43 favorisce l'esclusione dell'esone alternativo 15 di *TNIK*, codificante per una sequenza di 29 amminoacidi contenuta in una regione della proteina con funzione ancora ignota. Il gene *TNIK* è stato geneticamente associato come fattore di rischio a disordini psichiatrici, come la schizofrenia, e come fattore causativo a ritardo mentale (ID). A livello neuronale, la proteina TNIK è coinvolta nella regolazione di diversi processi, come la formazione delle sinapsi, l'arborizzazione dendritica e la neurogenesi.

In questo studio, il nostro primo obiettivo è stato indagare la regolazione dello splicing alternativo dell'esone 15 di *TNIK* durante il differenziamento neuronale, al fine di caratterizzare ulteriormente il ruolo svolto dal fattore di splicing TDP-43, espresso in modo ubiquitario e associato a SLA/FTD, in un contesto neuronale. Inoltre, il nostro secondo obiettivo è stato indagare se l'espressione delle isoforme proteiche di TNIK che includono l'esone 15 (TNIKex15) possa essere importante per mantenere le funzioni svolte da TNIK nella regolazione dello sviluppo dei neuriti in neuroni corticali primari.

Abbiamo osservato che lo splicing alternativo dell'esone 15 di *TNIK* è regolato diversamente nei tessuti umani di adulto e che le isoforme *TNIKex15* sono espresse in modo esclusivo nel cervello, nel midollo spinale e nel muscolo scheletrico. Data la prevalente espressione di tali isoforme nel sistema nervoso centrale, abbiamo ulteriormente indagato questo evento di splicing alternativo in modelli *in vitro* per valutare la sua regolazione durante il processo di differenziamento neuronale. Abbiamo osservato un incremento significativo dell'espressione delle isoforme *TNIKex15* sia in cellule SK-N-BE trattate con acido retinoico che in cellule iPS differenziate in neuroni. Inoltre, a livello proteico, le isoforme TNIKex15 sono espresse in modo specifico nelle cellule neuronali differenziate, mostrando una localizzazione prevalentemente perinucleare in analisi di immunofluorescenza.

Nel nostro precedente studio avevamo dimostrato che, in condizioni di silenziamento di TDP-43, aumenta l'inclusione dell'esone 15 di *TNIK*. Durante il differenziamento neuronale *in vitro*, tuttavia, a fronte di un'aumentata espressione delle isoforme *TNIKex15*, non abbiamo osservato una riduzione del contenuto proteico di TDP-43. Pertanto abbiamo indagato il potenziale ruolo nella regolazione dell'esone 15 di *TNIK* del fattore di splicing neuronale specifico NOVA-1, espresso in modo specifico solo nelle nostre cellule neuronali differenziate dove è maggiore l'espressione delle isoforme *TNIKex15*. In cellule HEK293T, l'over-espressione di NOVA-1 determina

un aumento dell'inclusione dell'esone 15 di *TNIK* senza influenzare in modo negativo il contenuto proteico di TDP-43 rispetto alla condizione di controllo. Inoltre, mediante saggi di minigene, abbiamo valutato l'interazione di NOVA-1 con TDP-43 nella regolazione dello splicing dell'esone 15 di *TNIK*. In questa analisi, è stata inclusa anche hnRNPA2/B1, una proteina legante gli RNA ubiquitaria che coopera con TDP-43 per regolarne la sua attività di splicing, e abbiamo dimostrato che favorisce l'esclusione dell'esone 15 di *TNIK*, similmente a TDP-43. In saggi di competizione con TDP-43 e hnRNPA2/B1, la proteina NOVA-1 sopprime completamente la loro attività di inibitori di splicing, legando TDP-43 e hnRNPA2/B1 in modo RNA-dipendente.

Poiché i nostri risultati suggeriscono un'importanza a livello neuronale delle isoforme TNIKex15, abbiamo indagato ulteriormente la funzione specifica di tali isoforme proteiche durante lo sviluppo neuritico di neuroni corticali primari di topo. L'over-espressione dell'isoforma TNIKex15 influenza negativamente lo sviluppo neuritico, riducendo il numero di neuriti, come già osservato in letteratura. Inoltre, analizzando il soma e i coni di crescita dei neuroni esprimenti l'isoforma TNIKex15, abbiamo osservato una riduzione del numero dei filopodi dei coni di crescita, dell'area del soma e ridotti livelli di actina filamentosa (F-actina) rispetto ai neuroni di controllo. Diversamente, in condizione di over-espressione dell'isoforma di TNIK deleta dell'esone 15 (TNIKΔ15), lo sviluppo neuritico, la morfologia del soma e dei coni di crescita e i livelli di F-actina risultano comparabili a quelli di neuroni di controllo o transfettati con il costrutto TNIK KM mutagenizzato in modo da perdere l'attività chinasica. Inoltre, l'over-espressione dell'isoforma TNIKex15 determina cambiamenti della morfologia anche di cellule HEK293T, che mostrano una forma prevalentemente circolare rispetto alle cellule di controllo. Di contro, l'over-espressione dell'isoforma TNIKΔ15 mostra un fenotipo intermedio.

In conclusione, il nostro studio ha dimostrato che le isoforme TNIKex15 sono espresse in modo specifico nei tessuti neuronali e durante il differenziamento neuronale *in vitro* e che tali isoforme mostrano una specifica funzione nella regolazione dello sviluppo neuritico, influenzando l'organizzazione dell'actina filamentosa. Inoltre, il fattore di splicing neuronale specifico NOVA-1, probabilmente favorendo la formazione di nuovi complessi ribonucleoproteici con i fattori di splicing ubiquitari TDP-43 e hnRNPA2/B1, agisce come "silenziatore" della loro attività di splicing sul pre-mRNA di *TNIK*.

Questi risultati suggeriscono che un'indagine più approfondita del meccanismo di competizione tra le proteine NOVA-1 e TDP-43 anche in riferimento ad altri target di TDP-43, potrebbe chiarire ulteriormente l'attività di splicing di TDP-43 in un ambiente neuronale e in associazione alle patologie SLA e FTD.

Abbreviation

ALS	Amyotrophic lateral sclerosis
CTD	C-terminal domain
DISC1	Disrupted in schizophrenia 1
F-actin	Filamentous actin
FTLD	Frontotemporal lobar degeneration
hnRNP	Heterogeneous nuclear ribonucleoprotein
iPSCs	Induced pluripotent stem cells
NES	Nuclear export signal
NLS	Nuclear localization signal
NOVA	Neuro-oncologic ventral antigen
NSCs	Neural stem cells
NTD	N-terminal domain
RNP	RNA binding protein
RRM	RNA-recognition motifs
TDP-43	TAR-DNA Binding Protein 43 kDa
TNIK	Traf2- and NcK-interacting kinase

Contents

1 INTRODUCTION

1.1 The DNA/RNA binding protein TDP-43

1.1.1 TDP-43 protein structure and physiological functions

TAR-DNA Binding Protein 43 kDa (TDP-43) is a DNA/RNA binding protein (RBP) ubiquitously expressed and first described in 1995 as a transcriptional repressor of the Human Immunodeficiency Virus Type 1 (*HIV-1*) gene [1]. The human TDP-43 protein, encoded by the *TARDBP* gene located on chromosome 1p36.22, is composed of 414 amino acids and belongs to the heterogeneous nuclear ribonucleoprotein (hnRNP) family. Similarly to the hnRNP proteins, TDP-43 primary amino acid structure (Figure 1.1) includes an N-terminal domain (NTD, 1-106 amino acids), two RNA-recognition motifs (RRM), RRM1 (106-176 amino acids) and RRM2 (191-262 amino acids), and a C-terminal domain (CTD, 263-414 amino acids). The NTD, stably folded, is involved in TDP-43 homodimers formation and it is important for TDP-43 physiological functions, such as splicing activity [2–4]. TDP-43 binds the DNA/RNA targets preferentially recognizing the (TG)n/(UG)n consensus sequences with a minimum of six repeats and the binding affinity increases together with the repeat number [5]. The RRM1 domain has a higher affinity to DNA/RNA binding, while the RRM2 domain is less involved, in fact RRM2 deletion or mutations weakly affect TDP-43 ability to recognize the targets [5]. Although its role is not still completely clear, the RRM2 domain seems to be important for the correct TDP-43-RNA complex formation by interacting with the RRM1 domain [6].

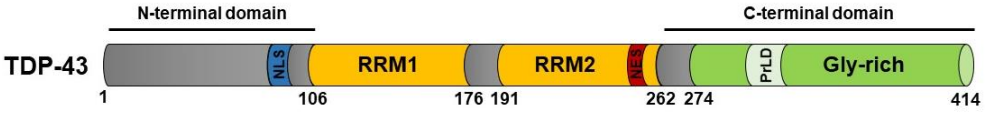

Figure 1.1 TDP-43 protein structure. Schematic representation of the TDP-43 protein that includes the nuclear localization signal (NLS) in the N-terminal domain, the two RNA recognition motifs (RRM1 and RRM2), the Glycine-rich (Gly-rich) region, including the prion-like domain (PrLD), within the C-terminal region and the nuclear export signal (NES) inside the RRM2 domain.

Within the NTD, a nuclear localization signal (NLS, 82-98 amino acids), important for TDP-43 nuclear import, is present, while a nuclear export signal (NES, 239-250 amino acids) located within the RRM2 domain is needed for TDP-43 export to the cytoplasm [7]. The CTD, including a Glycine-rich region (274-414 amino acids), has a low complexity composition and it is primarily disordered [8]. It is mainly involved in TDP-43 interaction with other proteins and in RNA processing [9,10]. This region is also rich in Glutamine (Q) and Asparagine (N) residues (321-366 amino acids) and it is described to act as a prion-like domain that promotes TDP-43 self-association and aggregation *in vitro* and both in yeast and in cellular cultures [11–15].

TDP-43 is mainly localized in the nucleus and only about 10% of the protein shows a cytoplasmic localization. It is involved in the regulation of several biological processes in both the nucleus and the cytoplasm, playing a crucial role in different steps of RNA metabolism (Figure 1.2).

The TDP-43 protein was first described to regulate the transcription process, mostly as a transcriptional repressor. In fact, TDP-43 represses the expression of the *HIV-1* gene when it binds to the viral TAR DNA sequence [1] and it also binds to the promoters of the murine testis-specific *Acrv1* gene and of the human and rat *VPS4B* gene to repress their expression [16,17].

The TDP-43 role in the regulation of transcription process is also supported by the described association of TDP-43 with euchromatinic region in both human brain [18] and cell cultures [19].

Besides this role as transcription regulator, TDP-43 is mostly characterized as an alternative splicing regulator and this function will be deeply described in the paragraph 1.1.2.

TDP-43 is also involved in the regulation of the non-coding RNAs, as microRNAs (miRNAs) and long-non-coding RNAs (lncRNAs). TDP-43 plays a role in miRNAs processing, as it is a component of both Drosha and Dicer complexes involved in miRNAs maturation in the nucleus and in the cytoplasm, respectively [20]. Moreover, our group demonstrated that TDP-43 knock-down in cellular models is associated to an increased *DICER1* expression both at transcript and protein levels [21]. TDP-43 regulates miRNAs processing also binding directly their precursors and many studies reported dysregulated levels of several miRNAs, such as let-7b, miR-9, miR-1/miR-206, miR-520, miR-132, miR-663, miR-588, miR-143, miR-NID1 and miR-574, in condition of TDP-43 depletion [20,22–26]. Nowadays, few lncRNAs were identified to be regulated by TDP-43, as *gadd7* [27], *MALAT1* [28,29], *NEAT 1_2* [28] and *lncLSTR* [30].

In the cytoplasm, TDP-43 participates to the regulation of mRNA stability, transport and translation. Like many RBPs, in order to regulate mRNA stability, TDP-43 binds to the 3'UTR of its mRNA targets, among which *VEGFA* and *GRN*, identified by our group [31], *Add2* [32] and *IL-6* [33] were experimentally validated.

TDP-43 role in mRNA transport is mostly studied in neurons, high polarized cells where mRNA transport into dendrites or axons is fundamental for the neuronal metabolism [34]. In primary murine motor neurons and human iPSC-derived motor neurons, TDP-43 was described to be transported along axons in RNA granules, where it colocalizes with other RBPs, such as SMN,

FMRP and Staufen, and with specific transcripts, including the neurofilament *NLF*, *βactin* and *CAMKII* mRNA [35–37].

TDP-43 role in mRNA transport is supposed to be closely associated to the regulation of local mRNA translation that is experimentally supported by proteomic studies that described TDP-43 association with the translation machinery [38]. Moreover, TDP-43 was described to repress translation in *in vitro* assay [35] and the *futsch* mRNA, the Drosphila homolog of mammalian *Map1b*, and the murine *Rac1* mRNA have been identified as specific TDP-43 targets, regulated at translational level [39-42]. Map1b and Rac1 play a important role in neuromuscular junction organization and spinogenesis, suggesting that TDP-43 regulatory activity is also involved in these neuronal processes. Another evidence of TDP-43 involvement in translation control is the observation that, under acute stress condition, TDP-43 protein is recruited into the stress granules (SGs) [43], cytoplasmic foci composed of mRNAs, ribosomal subunit 40S, translation initiation factors and other RBPs, that temporary sequester housekeeping mRNAs and block their translation to improve the stress-response proteins expression that helps the cells to effort the stress.

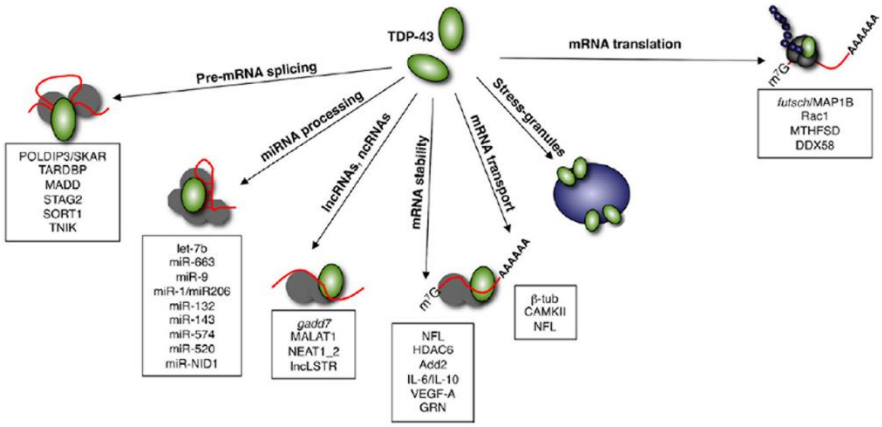

Figure 1.2 TDP-43 cellular functions. Schematic diagram of TDP-43 nuclear and cytoplasmic functions. The RNA targets of TDP-43 that have been validated are reported in the boxes below each function. This figure is adapted from Ratti and Buratti, Journal of Neurochemistry, 2016 (doi: 10.1111/jnc.13625)

1.1.2 TDP-43 protein as an alternative splicing regulator

Given its main nuclear localization, the TDP-43 protein is widely studied for its regulatory activity in the splicing process. The first identified TDP-43 splicing target was the human *CFTR* gene, as, in condition of TDP-43 depletion, the *CFTR* exon 9 inclusion increases [44]. Since in 2006, TDP-43 protein was described as the major component of the neuropathological aggregates present in the affected neurons of amyotrophic lateral sclerosis (ALS) and frontotemporal lobar degeneration (FTLD) patients [45,46], a plethora of high-throughput studies have attempted to define the splicing alterations following a TDP-43 dysfunction in ALS/FTLD human and murine disease models [28,47–49]. All these approaches defined that many alternative splicing events regulated by TDP-43 occur within transcripts with an important function in neuronal metabolism. Additionally, further gene-specific analyses and biological validation led to the identification of *apoA-II* [50], *POLDIP3/SKAR* [51, 52], *BCRA1, ETF1* [53], *STAG2*, *MADD* [54], *SORT1* [55,56] and *TNIK*, described by our group in [21], as direct splicing targets regulated by TDP-43. TDP-43 binds also its own pre-mRNA in the 3'UTR region [48,57] and it induces the spliceosome assembly at the normally silent intron 7 leading to a differential use of polyadenylation sites, that results in decreased TDP-43 mRNA and protein content [57–59]. Using this auto-regulatory mechanism, TDP-43 is able to maintain its own protein content at physiological levels in cells.

The TDP-43 RRM1 domain preferentially binds the pre-mRNA splicing targets at UG-rich sequences, repeated in tandem or in clusters, that are mainly localized in intronic regions [5]. The consensus binding sites seem to influence TDP-43 splicing activity based on their position [28], supporting the hypothesis of a position-dependent regulation similarly to the neuronal RBP NOVA-1 [60]. In fact, analysis of cross-linking clusters of TDP-43 RNA

targets suggests that TDP-43 preferentially promotes exon inclusion when it binds to UG-rich motifs located within the first 150 nucleotides of the downstream intron, while if these consensus binding sites are located in the first 150 nucleotides upstream from or within the regulated exon, TDP-43 seems to act promoting exon skipping [28]. In addition, UG-rich sites in a deep position (150-500 nucleotides) in the downstream intron are preferentially associated to TDP-43 exon skipping activity [28].

However, the TDP-43 splicing activity is not exclusively dependent on the consensus binding site position, but also the interplay with other RBPs modulates TDP-43 splicing regulation. Proteomic studies have identified more than 100 potential protein interactors of TDP-43 and most of them have a described function in RNA metabolism [38,61,62]. Among this array of interactors, many of the validated TDP-43 binding partners are members of the hnRNP family, such as hnRNPA2/B1, hnRNPA1 [9], hnRNPA2 [10], hnRNPH, hnRNPK and hnRNPQ [38, 61]. The TDP-43 ability to interact with the hnRNP proteins was shown to be associated with its inhibitory splicing activity, as described for *CFTR* exon 9 skipping that does not occur if TDP-43 interaction with hnRNPA2 is disrupted [9,10]. The Q/N-rich region (321-366 amino acids) of TDP-43 protein is indispensable for the interaction with the hnRNPs A2/B1 and A1, defining in this way a role also for the C-terminal tail in splicing regulation [9,10]. The interaction with hnRNP proteins seems to be less important when TDP-43 acts promoting exon inclusion, as described for the regulation of *POLDIP3/SKAR* exon 3 that is not affected by mutant TDP-43 deleted of the Q/N-rich region [51]. Moreover, the DAZAP1 protein was described as a TDP-43 splicing modifier competing with TDP-43 for the binding to the pre-mRNAs [63].

Recently, some studies have defined a role in TDP-43 splicing regulation for the NTD. Biochemical and biophysical approaches demonstrated that the NTD is able to form homodimers and tetradimers [3,64], and mutations in

NTD, disrupting TDP-43 monomeric folding and/or homodimerization, affect *CFTR* exon 9 inclusion mimicking the TDP-43 *loss-of-function* condition in cellular models [2–4].

Based on all these findings, TDP-43 splicing activity is defined by regulatory mechanisms including both the binding to specific RNA sequences of the targets and the interplay with several RBPs.

1.1.3 TDP-43 involvement in human diseases

TDP-43 protein has been widely associated to the neurodegeneration process since the wild-type form was described as a component of the neuropathological aggregates in the affected tissues of ALS and FTLD patients [45,46]. TDP-43-positive pathological inclusions are, in fact, observed in the majority of ALS patients (97%) and in about 45% of FTLD cases, independently on their familial or sporadic etiology [65]. The affected neuronal cells with TDP-43 aggregates usually show a concomitant depletion of the nuclear TDP-43 protein content [45,46]. It is still a debated issue if TDP-43 pathology is dependent on a loss of the nuclear TDP-43 functions (*loss-of-function*) or on a toxic effect of the cytoplasmic aggregates (*gain-of-function*) or if both mechanisms contribute to the pathology even if in a not temporally linked manner [66, 67]. The *loss-of-function* mechanism has been largely investigated by the *TARDBP* gene silencing in both cellular and animal models, studying the effects on the transcriptome (splicing and gene expression changes) [21,28,47–49]. As regards the *gain-of-function* hypothesis, unfortunately the molecular mechanisms that lead to the aggregates formation still remain unknown. The TDP-43 prion-like domain is mainly described to induce self-aggregation due to its biophysical properties [12], although recent studies identified a role also for the NTD [68,69]. Considering that TDP-43 is recruited into the SGs [43], one hypothesis is that

the aggregates would derive from SGs, that persist in the cytoplasm because of an impairment of their dynamics that may occur in condition of prolonged stress [70]. Recently, liquid-liquid phase separation (LLSP), a process that regulates the dynamics of membrane-less organelles, such as RNP granules, has been described to drive physiologically TDP-43 liquid droplets formation. A LLSP impairment would also lead to persistent TDP-43 liquid droplets, that may be precursors of the pathological TDP-43 aggregates [71]. According to another hypothesis, TDP-43 aggregation would be linked to many other cellular dysfunctions, such as an impairment of autophagic/proteasome pathways, an aberrant TDP-43 cleavage or an unbalanced increase of the physiological TDP-43 protein levels [72]. Furthermore, the maintenance of the physiological expression levels and of the correct balance of TDP-43 nucleo/cytoplasm protein content is finely regulated in healthy cells and alterations of nucleo-cytoplasm transport lead to a TDP-43 mislocalization in the cytoplasm that may represent the first step of pathological aggregate formation [73]. On another hand, few studies support the hypothesis of a protective role of the TDP-43 protein inclusions. In fact, especially in the first stage of the disease, the TDP-43 aggregates and the reduction of soluble nuclear protein could be protective, preventing TDP-43 aberrant binding and functions [74].

Additionally to the self-association, TDP-43 is also described to co-aggregate with other RNA-binding proteins, such as the RBM45 protein that colocalizes with TDP-43 inclusions in the affected tissues of ALS and FTLD patients [75] and the RPBs RBM14, NonO and PSF that co-aggregate with TDP-43 in cellular models of TDP-43 pathology [76]. Recently, Disrupted in schizophrenia 1 (DISC1), a key protein in schizophrenia pathology with a role in mRNA transport into dendrites and local translation [77,78], has been also described to co-aggregate with TDP-43 both in affected neurons of FTLD patients and in mice models with TDP-43 inclusions [78]. The sequestration

of other proteins in the pathological TDP-43 aggregates suggests that also these proteins may influence the neurodegenerative process, although the mechanisms involved are still unclear.

As TDP-43 contains a simil-prionic domain, the hypothesis that TDP-43 aggregates may propagate from the affected cells to the neighboring healthy ones through a prion-like mechanism is also supported, thus accounting for the spreading of the neurodegenerative process [79 ,80].

In the pathological aggregates, TDP-43 is post-translationally modified and, in particular, it is described to be ubiquitinated, phosphorylated, acetylated and cleaved in C-terminal fragments (25 kDa and 35 kDa) [45,46,81–83]. The role of these modifications in the process of aggregation is not well defined yet and need to be further studied.

In 2008, mutations in the *TARDBP* gene were discovered as causative of about 5% of familial ALS and FTLD forms and of very few sporadic ALS/FTLD cases, establishing a direct link between TDP-43 and ALS/FTLD pathogenesis [84–86]. To date, more than 50 *TARDBP* mutations have been reported occurring mostly in exon 6 that encodes for the CTD [87].The functional consequences of the *TARDBP* mutations appear to be mainly related to increased TDP-43 self-aggregation propensity and half-life or altered stress granules dynamics, TDP-43 subcellular distribution and protein-protein interaction [8,14,88,89]. Regarding the splicing activity, one group evidences dysregulation of a set of the TDP-43 splicing targets in a TDP-43-mutated mouse model [90], while other experimental findings described a very slight splicing alteration associated to *TARDBP* mutations [51,91] and we did not identify splicing dysfunction in fibroblasts derived from *TARDBP* mutated ALS patients [21].

TDP-43 protein is also associated to other diseases, as the presence of TDP-43 pathological inclusions has been described in Alzheimer's Disease [92], Guam Parkinsonism-dementia [93], Lewy bodies Disorders [94],

Hippocampal Sclerosis [95], Perry Sindrome [96], Corticobasal Degeneration, Facial Onset sensory and Motor Neuronopathy [97], Niemann-Pick C disease [98], Progressive Muscular Atrophy [99], Inclusion Body Myositis [100] and Fascioscapulohumeral Dystrophy [101].
Finally, in the brain tissues of a small group of aged healthy individuals, TDP-43 aggregates were described, suggesting a potential involvement of TDP-43 in the aging process [102].

1.2 The protein kinase Traf2- and NcK-interacting kinase (TNIK)

1.2.1 TNIK protein structure and its splicing regulation by TDP-43 protein

The human *TNIK* gene on chromosome 3q26.21 encodes for a serine/threonine kinase classified as member of the germinal center kinase (GCK) family, a subgroup of the Ste20 family. It is a 130 Kda protein with two functional domains, an N-terminal kinase domain (25-289 amino acids) and a regulatory citron homology domain (CNH) (1047-1334 amino acids) located in the C-terminal region (UniProtKB-Q9UKE5) (Figure 1.3). The N-terminal and C-terminal domains are linked by a long intermediate region (290-1046 amino acids) where no functional domains are annotated and whose biological significance is still unclear.
The human *TNIK* gene is composed of 33 exons, among which three alternative exons (exon 15, 17 and 22) encode for amino-acid sequences inserted *in frame* in TNIK intermediate region. The combination of the alternative splicing of these three exons results in eight different isoforms (Figure 1.3) described, for the first time, in 1999 by Fu et al [103]. To date,

no studies have identified the splicing regulation of the exon 17 (165 nucleotides) and 22 (24 nucleotides), while exon 15 (87 nucleotides) is regulated by TDP-43 RBP. By iCLIP-Seq, Tollervey et al identified an increase of *TNIK* exon 15 inclusion both in brain tissues of FTLD patients showing a TDP-43 pathology and in cellular models of TDP-43 depletion [28]. By exon array analysis, in condition of TDP-43 knock-down, mimicking a *loss-of-function* as in ALS disease, our group confirmed and further analyzed this alternative splicing event to demonstrate a direct effect of TDP-43 on *TNIK* exon 15 skipping [21]. By immunoprecipitation of endogenous TDP-43-ribonucleoprotein complexes in human neuroblastoma cells, we also demonstrated that TDP-43 binds *TNIK* pre-mRNA.

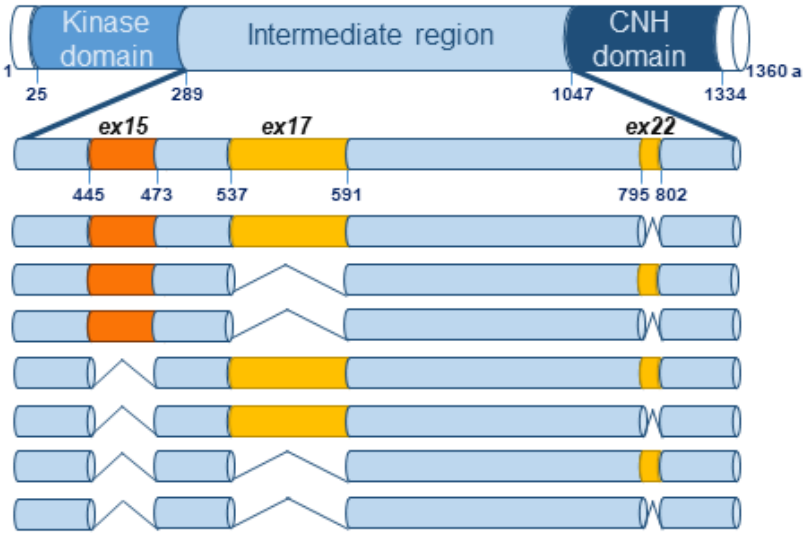

Figure 1.3 Schematic representation of TNIK protein isoforms. The graphic representation shows the functional domains of TNIK protein (N-terminal Kinase domain and C-terminal CNH domain) and the intermediate region. Three alternative exons (orange and yellow boxes) in the intermediate region are spliced in different combination and define eight different TNIK isoforms. Four of them contain the amino-acid region encoded by exon 15 (orange box).

We also observed that, in neuroblastoma cells silenced for TDP-43, the over-expression of siRNA-resistant TDP-43 plasmid was able to rescue the altered splicing and to restore *TNIK* exon 15 skipping. For the first time, we investigated this alternative splicing event also at protein level using a homemade antibody generated to recognize specifically the amino-acid region encoded by the *TNIK* exon 15. Upon TDP-43 knock-down, we described increased levels of the TNIK protein isoforms containing the exon 15 (TNIKex15) showing a peculiar subcellular localization in the neuroblastoma cells perinuclear region [21].

1.2.2 The neuronal functions of TNIK protein

TNIK plays several roles in neuronal metabolism (Figure 1.4) and all experimental findings regarding its functions are related to the full-length isoform, so the biological significance of the other protein isoforms remains to be investigated.

In human adult tissues, the *TNIK* gene is highly expressed in heart, skeletal muscle and brain [103] and in mouse and rat brain, *in situ* hybridization shows that *TNIK* mRNA is particularly enriched in cerebellum, dentate gyrus of hippocampus and cortex [104]. Moreover, TNIK protein is enriched in dendritic spines in murine cerebral cortex and striatum [105] and specifically localizes at the postsynaptic density (PSD), a region of the postsynaptic membrane specialized for plasticity and signaling [106,107]. Following studies have further described the TNIK role in the structural organization and the activity of synapses in murine and rat models [104,108,109] (Figure 1.4 A). In particular, in rat primary neurons, *TNIK* knock-down or its kinase activity inhibition was associated to reduced levels of PSD scaffold proteins, such as PSD-95 and stargazing, and to a decreased AMPAR currents due to a reduced GluR1 and GluR2 localization at the postsynaptic membrane

[104]. In the PSD, DISC1, a genetic rick factor for schizophrenia, interacts directly with TNIK inhibiting its kinase activity and this interaction is important for the synaptic composition and functionality [104]. Furthermore, from PSD fractions of mouse brain, TNIK has been also isolated in complex with NMDA receptors that seem able to decrease phosphorylation of TNIK serine 735, that may be necessary for its kinase activation [109]. Moreover, TNIK is also required for excitatory synaptic function, as in *TNIK* knock-out mice reduced mEPSCs frequency in CA1 pyramidal neurons was recorded [109].

In mammalian neurons, TNIK is also involved in the dendritic growth and arborization by regulating the actin cytoskeleton dynamics [110] (Figure 1.4 B). The first experimental findings describing TNIK function in cytoskeleton regulation came from studies in non-neuronal cells [103,111], where the activated Rap2A (GTP-Rap2A), a GTP-binding protein member of the Ras family, binds TNIK CNH domain promoting TNIK phosphorylation and kinase activity on effectors, such as Gelsolin, responsible of F-actin disassembly [103,111]. This pathway activation induces a change in cell morphology, that from a flat and spreading one, becomes round with a reduced adhesion to the substrate [103,111]. In neurons, Nedd4-1, an ubiquitin ligase with a positive regulatory effect on dendritic arborization, also participates in this mechanism by binding to the TNIK intermediate region and forming a ternary complex with TNIK and Rap2A. This complex is necessary to inactivate Rap2A activity by Nedd4-1-dependent ubiquitination, thus promoting dendrites arborization [110]. Furthermore, both *TNIK* silencing and over-expression in murine cortical and hippocampal neurons are responsible of dendrite retraction and immature neurites formation [110], suggesting that a fine regulation of TNIK protein content is important for a proper dendrite organization.

Through the intermediate region, TNIK also interacts with NcK, an adaptor protein with a role in the cytoskeleton organization and with Traf2 protein,

involved in JNK (cJun N-terminal kinase) pathway activation [103] (Figure 1.4 C). In neurons, during the synaptic depotenziation, TNIK, interacting with Rap2A, determines JNK pathway activation that promotes synaptic membrane removal and AMPA receptors internalization and degradation [112]. Furthermore, TNIK together with MINK and MAP4K4 proteins, two other members of the Ste20 family, acts as an upstream regulator of DLK (dual leucine zipper kinase) that is required for stress-induced activation of JNK pathway in neurons [113].

TNIK plays a role also during the dentate gyrus neurogenesis [109] (Figure 1.4 D), that requires the Wnt proteins and β catenin expression [114,115]. In mice, TNIK knock-out is associated to a reduction of differentiating and newly born neurons in murine dentate gyrus, due to increased GSK3β levels that highly phosphorylate the transcriptional factor NeuroD1, inhibiting the Wnt/β catenin transcription [109].

To date, few TNIK kinase substrates are known, among which TNIK itself has been the first described and its autophosphorylated form is required for its kinase activity [103]. Two serine residues, p.S764 and p.S769, identified by proteomic studies of the human kinome [116,117] are proposed as autophosphorylation sites. In *in vitro* kinase assay, TNIK phosphorylates Gelsolin, a F-actin fragmenting protein [103], and, recently, Wang Q et al have identified p-120-catenin, δ-catenin, armadillo repeat gene deleted in velo-cardio-facial syndrome (ARCVF) and formin-like protein 2 (FMNL2), as endogenous substrates of TNIK kinase, in neurons [118]. By a phosphopeptide sequence analysis, they defined also three putative phosphorylation consensus sequences for TNIK such as pT/S-L/I/V-D/E-x-x-x-K/R, pT/S-L/I/V-x-K/R, and pT/S-L-P/Q-L/I-x-x-K/R [118].

As the majority of the identified TNIK substrates have a role in actin regulation mechanisms, the TNIK function in cytoskeleton dynamics is further supported.

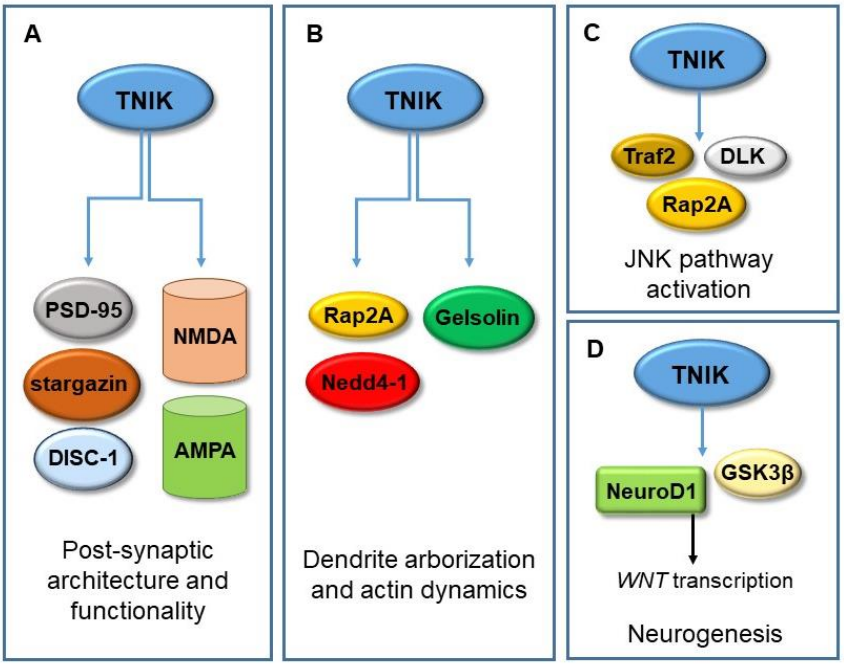

Figure 1.4 TNIK neuronal functions. Schematic representation of the main TNIK neuronal functions (***A***, post-synaptic architecture and functionality; ***B*** dendrite arborisation; ***C*** JNK pathway activation; ***D***, neurogenesis). The experimentally validated TNIK effectors, interactors and other proteins cooperating with TNIK are indicated.

1.2.3 TNIK involvement in neurological diseases

Biological and genetic evidences support a TNIK role in the pathogenesis of psychiatric disorders, like schizophrenia and bipolar disorders and recently also in intellectual disability.

The *TNIK* gene knockout is associated with both defects of dentate gyrus neurogenesis and NMDA and AMPA postsynaptic signaling in mice that show also an impairment of the pattern separation and the object-location paired associates learning [109]. The dentate gyrus neurogenesis and the NMDA and AMPA receptors signaling result impaired in schizophrenia

patients [119–121] that may present also a compromised object-location paired associates learning [122]. Another biological evidence that supports the potential TNIK role in pathogenic mechanisms of psychiatric disorders is TNIK interaction with DISC1 [104], the genetic risk factor for schizophrenia, bipolar disorders and autism [123].

Furthermore, genetic studies support a direct link between *TNIK* and psychiatric disorders, as *TNIK* was identified as a genetic risk factor for schizophrenia in different genome-wide association studies (GWAS). The five associated SNPs (single-nucleotide polymorphisms) including rs2088885, rs7627954 [124], rs13065441 [125], rs260769 and rs12639373 [126] map in intronic regions (intron 2 and 3) of *TNIK* gene and no functional studies have further investigated their biological significance. Interestingly, a recent Chinese GWAS identified a new SNP (rs6444970) in the intergenic region upstream the *TNIK* gene associated to the antipsychotic treatment that is usually somministrated to manage the symptoms of schizophrenic patients [127]. In post mortem dorsolateral prefrontal cortex of schizophrenic patients, gene expression analysis showed increased levels of *TNIK* [128] which negatively correlated with the mRNA content of its interactor DISC1 [129], suggesting that *TNIK* gene expression is altered in schizophrenia brain. Increased expression of the *TNIK* gene was also reported in lymphoblastoid cell lines from bipolar disorder patients, further supporting a role of this gene in disease pathogenesis [130].

A recent exome sequence analysis of two consanguineous families with non-syndromic intellectual disability has identified a truncating mutation (c.538C>T) in the *TNIK* gene in a homozygous state that lead to the total loss of TNIK protein levels [131].

All these findings underline that *TNIK* dysregulation or depletion in brain may be responsible of dysfunctions that may manifest in both psychiatric and mental disorders.

1.3 Alternative splicing in neurons

1.3.1 Alternative splicing mechanism

In mammals, the alternative splicing, a post-transcriptional process important for pre-mRNA maturation, occurs in 95% of human genes [132]. Different alternative splicing forms, including cassette exon, mutually exclusive exons, alternative 5' or 3' splice site recognition, intron retention and alternative promoter or polyA site are described and among them, the cassette exon is the alternative splice event more frequent in the humans [133]. The alternative splicing process is regulated by *cis-acting* elements, including specific intronic or exonic sequences in the pre-mRNA, and by *trans-acting* splicing regulators, including RNA binding proteins, among which the best characterized ones are the members of the SR (serine/ariginine rich) or the hnRNP families. The complex interplay of both *cis-* and *trans-acting* regulators defines the splicing event, which depend on the accessibility and binding of spliceosome machinery to the target pre-mRNA [134]. Furthermore, other biological mechanisms, such as transcription and chromatin organization, may also influence the alternative splicing process [135,136].

By the alternative splicing, a single gene may generate alternative transcripts with different mRNA stability encoding for protein isoforms with specific structures and biological functions, subcellular localization and biochemical properties [137]. In this way, the alternative splicing determines the single cells proteomic complexity and specificity, playing an important role during the different tissues development, where the alternative splicing regulation is mainly the result of an integrated activity of ubiquitous and tissue-specific splicing factors [138]. Among the different tissues, the higher number of alternative splicing events occurs in the brain and these events are highly

conserved along the vertebrates evolution [139–141], suggesting that the alternative splicing may give an important contribution to the high complexity of the human nervous system.

1.3.2 Alternative splicing in neurons and during neuronal differentiation

All stages of neuronal development, from the neural stem cells differentiation into neurons to the axon and dendrite formation, synapses maturation and neuronal plasticity, are spatio-temporally regulated by many mechanisms among which the alternative splicing process seems to play an essential role [142,143].

In developing and mature neurons, the neuronal activity may act as a splicing regulator that contributes to synaptic remodeling [144]. The activity-dependent splicing regulation include pre-mRNAs encoding for neurotransmitter receptors (NMDA receptor 1; [145]), ion-channels (BK channels; [146]), and post-synaptic (Homer 1; [147]), pre-synaptic (SNAP25; [148]) and cell adhesion (NCAM, Neurexin, [149]; Neuroligin, [150]) proteins. Splicing changes in all these factors modulate the synaptic function, representing an example of how alternative splicing may be regulated by synaptic signaling and in turn modify the neuronal physiology.

The alternative splicing is also regulated by the combinatorial control of more than one RBP and this is particularly evident in the nervous system where the regulatory activity of ubiquitous splicing factors is integrated by neuronal RBPs defining specific splicing patterns for pre-mRNAs [151,152]. The splicing factors known to act during neuronal development and in mature neurons include the nSR100 protein and the members of RBFOX (RNA-binding Fox), PTB (Polypyrimidine Tract-binding protein), Hu/Elav and NOVA (neuro-oncologic ventral antigen) families. The nSR100 (neural specific SR

related protein of 100 kDa) protein is highly expressed in neurons, where it regulates the processing of transcripts, such as *PTB2* and the *REST/NRSF*, necessary for neurogenesis and neuronal differentiation [153,154]. The members of the RBFOX family (RBFOX1, 2 and 3) are also specifically expressed during neuronal development and they control splicing of genes up-regulated during this process [155,156]. PTB1 and PTB2 are members of the PTB family and during differentiation of neural progenitors into post-mitotic neurons, a switch from the non-neuronal PTB1 to the neuronal PTB2 expression occurs with a consequent alternative splicing regulation of several genes important for the neuronal differentiation process [157,158]. The Hu/ELAV family includes four members, HuA (HuR), ubiquitously expressed, and HuB, HuC and HuD specifically expressed in neurons [159]. Although the neuronal Hu proteins have been mainly described to regulate mRNA stability by binding to the 3'UTR of their targets [160], one study reported also a role as competitors of the ubiquitous RBPs TIA-1 and TIAR in regulating *calcitonin/CGRP* gene splicing to produce the neuropeptide CGRP transcript in neurons [161].

1.3.3 The neuron-specific splicing factors NOVA

The members of NOVA family, NOVA-1 and NOVA-2 RBPs, were the first neuron-specific splicing factors described and they are specifically expressed in neurons of the central nervous system [162–164]. NOVA-1 and NOVA-2 were firstly identified as autoantigens in patients affected by the paraneoplastic opsoclonus myoclonus ataxia (POMA), an autoimmune syndrome [162,163].

NOVA-1 knockout mice show important motor defects and post-natal death (7-10 days after birth) due to an extensive apoptosis of motor neurons in spinal cord and brain stem [164]. Instead, NOVA-2 depletion in mice model

is responsible of inhibitory synapses impairment in hippocampus [165]. Mice with a double knockout of NOVA proteins are paralyzed and die within few days from birth [166].

The human *NOVA-1* and *NOVA-2* genes encode for proteins with high identity that are classified as K-homology (KH) RBPs. Structurally, they present a NLS in the N-terminal region and three KH domains (KH1-2-3) that are RNA binding elements. The first two KH domains are in tandem arrangement and are connected by a large linker sequence to the KH3 domain, located in the C-terminal region (Figure 1.5). NOVA proteins bind the pre-mRNA targets recognizing a stem-loop RNA sequence, that contains a minimum of three YCAY-clusters (Y=pyrimidine) in the loop region [167]. How the KH-domains act together in the RNA recognition is not well defined yet.

In the post-natal mouse brain, NOVA-1 protein is particularly enriched in the hindbrain and the ventral spinal cord, while NOVA-2 is expressed at high levels in the hippocampus and the neocortex [163]. At the cellular level, NOVA proteins are mainly localized in the nucleus and more weakly in the cytoplasm of neurons [168]. In particular, in somatic and dendritic cytoplasm of murine ventral horn neurons, NOVA proteins have been described to colocalized with the inhibitory *glycine receptor α2 subunit (GlyRα2)* mRNA [169], one of the first described NOVA-1 target [167].

Figure 1.5 NOVA-1 and NOVA-2 protein structure. Schematic representation of NOVA-1 and NOVA-2 protein primary structure. Both proteins contain a NLS in the NTD and three RNA binding domains (KH1, KH2 and KH3). NOVA-1 (UniProtKB - P51513) and NOVA-2 (UniProtKB - Q9UNW9).

High-throughput approaches have identified several NOVA proteins splicing targets that play important role in synaptic architecture, function and axon guidance. Many of these targets are synaptic proteins, such as neurotransmitter receptors, scaffold and adhesion proteins [60,170–172].

NOVA proteins splicing activity is regulated by the YCAY binding motifs in a position-dependent manner [60]. In particular, if NOVA-1 binds exonic YCAY-elements, it blocks spliceosome assembly and promotes the exon skipping, whereas NOVA binding to intronic YCAY-clusters improves exon inclusion by favoring the spliceosome assembly [60]. NOVA proteins may also regulate the alternative splicing of its targets in a combinatorial control with other tissue-specific or ubiquitous splicing factors. For example, NOVA-2 promotes exon 19 inclusion of the *NMDA receptor 1* pre-mRNA in the murine neocortex, while in the spinal cord, where similar expression levels of both NOVA proteins were detected, *NMDAR1* exon 19 is mainly skipped [171]. This finding suggests a possible interplay with other splicing factors, such as the hnRNPA1 that is also described as a *NMDAR1* exon 19 regulator [173]. Another example of splicing combinatory control involving NOVA proteins is the regulation of the *Dopamine D2 receptor (DR2*) pre-mRNA. In particular, both NOVA-1 and the ubiquitous hnRNPM bind the *DR2* exon 6 and compete to regulate its splicing in an opposite direction [174].

All these findings support that NOVA proteins, through the alternative splicing regulation of several transcripts, play an important role in neuronal metabolism.

2 AIM

In this study, we aimed to investigate the regulation of *TNIK* exon 15 alternative splicing during the neuronal differentiation, in order to better characterize the role played by the ubiquitously expressed and ALS/FTD associated TDP-43 splicing factor in a neuronal context. To address this issue, we analysed *TNIK* exon 15 splicing in human adult tissues and in two distinct models of neuronal differentiation *in vitro*, such as human neuroblastoma cells treated with retinoic acid (RA) and human iPSCs differentiated into neurons. Assuming that, in neurons, tissue-specific splicing factors may play a role in *TNIK* splicing regulation together with TDP-43, we investigated the RBP NOVA-1 as a neuron-specific *TNIK* splicing regulator, evaluating the possible interplay with TDP-43.

Since TNIK plays an important role in neuronal metabolism and all literature data about TNIK functions are referring only to the full-length protein, our second aim was to investigate if the specific expression of TNIKex15 isoforms may be important to maintain TNIK physiological functions in neurons, mainly focusing on its activity on F-actin organization. In this view, we studied the already described effect of the full-length TNIK isoform on cell morphology in comparison to the effect of exon 15-deleted isoform, in murine primary cortical neurons.

3 MATERIALS AND METHODS

3.1 Cell cultures

The human neuroblastoma SK-N-BE cells were maintained in RPMI-1640 (Thermo Fisher Scientific) medium supplemented with 10% fetal bovine serum (FBS, SigmaAldrich), 2 g/l glucose, 2 mM L-glutamine (Gibco), 1 mM sodium pyruvate (Gibco), 100 U/ml penicillin and 100 µg/ml streptomycin (Gibco).

Human embryonic kidney (HEK) 293T cells were cultured in DMEM (Thermo Fisher Scientific) medium supplemented with 10% FBS, 100 U/ml penicillin and 100 µg/ml streptomycin.

Human inducent pluripotent stem cells (iPSCs) were previously obtained in our laboratory by reprogramming fibroblasts from healthy donors with Sendai virus (Thermo Fisher Scientific) and were maintained in E8 essential medium (Thermo Fisher Scientific) in wells coated with Matrigel (Corning). The iPSCs were characterized by RT-PCR and immunofluorescence (both described later) for the expression of the pluripotency markers Oct 3/4, Sox 2, Nanog and TRA1-60. All iPSCs lines presented a normal karyotype [175].

Primary cortical neurons were isolated from wild-type murine embryos (E14.5 or E15.5) and seeded on glass coverslips coated with 0.125 mg/mL of poly D-Lysine Hydrobromide (Sigma) and 5 ug/mL of laminin (Corning) at the concentration $4x10^5$ cells/well in 6-well plates. Primary cortical neurons were maintained in Neurobasal (Thermo Fisher Scientific) medium supplemented with 2% B-27 (Gibco), 2 mM GlutaMAX (Gibco) and 100 U/ml penicillin and 100 µg/ml streptomycin (Gibco).

3.2 Plasmid constructs and cell transfection

For NOVA-1 over-expression experiments, HEK293T cells were transfected with the pCGN-ha-tagged-NOVA-1 plasmid (a kind gift of Prof. E. Battaglioli, Università degli Studi di Milano) or empty vector using Lipofectamine 2000 (Life Technologies) according to the manufacturer's instructions and harvested after 24 h for the following analysis.

The TNIKex15 minigene construct (pTBminigene_TNIKex15) already described [21] and containing the genomic region of *TNIK* exon 15 (87 bp) along with part of 5′ (141 bp) and 3′ (126 bp) flanking introns, was used.

The pFLAG-CMV2 human full-length and mutated (ΔRRM1, ΔC-term, 4FL) TDP-43 constructs or pFLAG-CMV2 human hnRNPA2B1 (all kind gifts from Dr. E. Buratti, ICGEB, Trieste) were co-transfected with ha-tagged-NOVA-1 in HEK293T cells using Lipofectamine 2000 and harvested after 24 h for the co-immunoprecipitation (co-IP) assays.

The human TNIK full-length (TNIK FL) and human TNIK kinase mutant (TNIK KM) pCI-ha-tagged plasmids were kindly provided by Prof. Ken-ichi Kariya (Graduate School of Medicine, University of the Ryukyus, Japan). The ha-tagged TNIKΔ15 plasmid was obtained by mutagenesis of ha-tagged TNIK FL as described below. For morphological cell assay, HEK293T cells were seeded on glass coverslips in 24-well plates and transiently co-transfected with 3 µg of green fluorescent protein (GFP) and the different TNIK constructs in a 1:3 ratio. Cells were fixed after 24 h for images analyses.

To analyse neuronal arborization, primary murine cortical neurons were seeded on glass coverslips in well of 12-well plate and at DIV4 were transiently transfected with 1.3 µg DNA using Lipofectamine 2000. A ratio of 1:3 was used for GFP and TNIK constructs. Three days after transfection cells were fixed for the following analysis.

3.3 Site-directed mutagenesis

The ha-tagged TNIK FL plasmid was mutagenized using the QuikChange II Site-Directed Mutagenesis Kit (Agilent Technologies) with the two oligos 5'-CGTGCGGAGCATGAACAGGAATATAAGCGCAAACAA-3' and 5'-TTGTTT GCGCTTATATTCCTGTTCATGCTCCGCACG-3' to delete exon 15 nucleotide-sequence and obtain the human TNIKΔ15 construct. Briefly, the QuickChange Primer Design program (www.agilent.com/genomics/qcpd) was used to design primer pairs and the PCR reaction was performed using 10 ng of template ha-tagged TNIK FL plasmid, 125 ng of each primer, 2.5 U di PfuUltra HF DNA polymerase in a final volume of 50 µl (annealing: 58°C for 1 min; extension: 68°C for 10 min; 18 cycles). 10 U of *Dpn*I restriction enzyme were added to the amplification reaction to digest the parental supercoiled dsDNA at 37°C for 1 h. Subsequently, 4ul of *Dpn*I-treated amplicons were used to transform the One Shot TOP10 chemically competent *E. coli* cells (Life technologies) according to the manufacturer's instruction. The obtained colonies were screened by DNA sequencing and one mutagenized clone was amplified and used for cell transfection.

3.4 Neural and neuronal differentiation

The human neuroblastoma SK-N-BE cells were treated with 10 uM of RA for six days to induce neuronal differentiation. The medium was replaced every two days and the cells were analysed before treatment (T0) and after two (T2), four (T4) and six (T6) days. The neuronal differentiation was evaluated by immunofluorescence using the neuronal cytoskeleton marker βIII-Tubulin staining.

The human iPSCs were differentiated into neural stem cells (NSCs) using PSC Neural Induction Medium (Thermo Fisher Scientific). Briefly, iPSCs were seeded at low density on Matrigel-coated wells and maintained in Neural Induction Medium for six days, replacing the medium every two days. On day 7 cells were harvested, seeded on Geltrex (Thermo Fisher Scientific)-coated wells and expanded for two passages before being characterized. Neural induction into neural stem cells (NSCs) was evaluated by immunostaining with the NSC marker Nestin.

iPSCs were differentiated into neurons (iPSC-neurons) using a modified protocol from Amoroso et al. [176]. Briefly, iPSCs were seeded in low adhesion dishes and were grown in suspension in HuES (Thermo Fisher Scientific) medium supplemented with 20 ng/ml basic fibroblast growth factor (FGF) (Peprotech) and 20 µM Rho-associated kinase (ROCK) inhibitor Y27632 (Selleckchem) for the first 2 days in order to induce embryoid bodies (EBs) formation. The third day neuralization was induced by the addition of 10 µM SB431542 and 0.2 µM LDN193189 (both from Stemgent). The fourth day, EBs were switched to neural induction medium (DMEM/F12, 2 mM L-glutamine, 10 U/ml penicillin, 10 µg/ml streptomycin, 0.1mM MEM NEAA, 2 µg/ml heparin (Sigma-Aldrich), 1% N2 supplement (Thermo Fisher Scientific), supplemented with 20 µM ROCK inhibitor, 0.4 µg/ml ascorbic acid (AA) (Sigma-Aldrich), 1 µM RA (Sigma-Aldrich), 10 ng/ml brain-derived neurotrophic factor (BDNF) (Peprotech) to induce caudalization. SB431542 and LDN193189 were added until day 7 when cultures were supplemented with the ventralizating factors smoothened agonist (1 µM; Merck) and purmorphamine (0.5 µM; Sigma-Aldrich). EBs were grown for additional ten day with a medium change every alternate day and at day 17, they were dissociated with 0.05% trypsin (Sigma-Aldrich) and plated on poly-D-Lysine (Sigma-Aldrich)/laminin (Thermo Fisher Scientific)-coated coverslips in 24-well plates at a concentration of $5x10^5$ cells/well. Cells were cultured in neural

differentiation medium (Neurobasal (Thermo Fisher Scientific), 2 mM L-glutamine, 10 U/ml penicillin, 10 µg/ml streptomycin, 0.1 mM MEM NEAA, 1% N2 supplement), supplemented with 2% B27 (Thermo Fisher Scientific), 1 µg/ml laminin, 25 µM glutamate (Sigma-Aldrich), 0.4 µg/ml ascorbic acid, 10 ng/ml glial-derived neurotrophic factor (GDNF) and 10 ng/ml ciliary neurotrophic factor (CNTF) (both from Peprotech). Neurons were allowed to differentiate for 10 days and then were characterized by immunostaining with the βIII-Tubulin and the anti-neurofilament SMI-312 markers.

3.5 RNA isolation and RT-PCR assay

RNA samples from human adult tissues (brain, spinal cord, skeletal muscle, kidney, testis, liver and lung) were purchased by Clontech and were pools of three different healthy donors. Whole RNA was isolated from cells using TriZol reagent (Thermo Fisher Scientific) according to the manufacturer's instructions. RNA samples were quantified using a ND-1000 NanoDrop spectrophotometer (NanoDrop Technologies) and 5 µg or 3 µg of total RNA from cell lines or from human tissues, respectively, were treated with 1 U of *DNase*I (Roche) for 20 min at 37°C and then retro-transcribed using 1 U of SuperScript II-RT (Thermo Fisher Scientific) and oligodT. Specific primers for *TNIKex15* (exons 14-16), *TNIKex17* (exons 16-18), *TNIKex22* (exons 21-23) splicing isoforms were designed. RT-PCR was performed using 300nM of each primer and GoTaq G2 DNA polymerase (Promega) for 26-35 cycles. Amplicons were visualized on 2% agarose gel. For data normalization, *GAPDH* gene was used in cell cultures RT-PCR, while *RPL10a* gene was used in tissue analysis because of the high tissue-variability of *GAPDH* gene expression. All primer sequences are reported in Table 3.1. By densitometric analyses performed using Image J software (NIH), the *TNIK* isoforms relative

amount in human tissues and *TNIKex15* inclusion in neuronal-differentiated cells were quantified.
The *TNIK* alternative exons nomenclature is referred to the database EASANA FAST DB 2010_2.

3.6 Quantitative real-time PCR

Total RNA from differentiated SK-N-BE cells and HEK293T cells transfected with ha-tagged NOVA-1 plasmid or empty vector was retro-transcribed as already described and real-time PCR (qPCR) was performed for 45 cycles with SYBR Green PCR Master mix (Applied Biosystems) and specific primers for *TNIK* gene total (exons 30-31) and exon 15-containing isoforms (for primer sequences see Table 3.1). Reactions were run in duplicate for each sample on ABI Prism 7900HT (Applied Biosystems) and a dissociation curve was generated at the end. Threshold cycles (Ct) for each tested gene were normalized on the housekeeping *RPL10a* gene Ct value (ΔCt) and every experimental sample was referred to its control (ΔΔCt). Fold change values were expressed as $2^{-\Delta\Delta Ct.}$

3.7 Minigene assay

HEK293T cells were transiently co-transfected with pTBminigene_TNIKex15 and flag-tagged TDP-43, flag-tagged hnRNPA2/B1, ha-tagged NOVA-1 plasmids or empty vectors, alone or in combination with each other, using Lipofectamine 2000 (Life Technologies) according to the manufacturer's instructions. After 24h-transfection, cell were harvested and divided for protein and RNA extraction. Total RNA was extracted 24 h after transfection

and retro-transcribed as described above. RT-PCR reactions were carried out using specific primers (a2-3 For and Bra2 Rev) designed on pTB plasmid (Table 3.1) and *GAPDH* gene was used for sample normalization. Proteins were extracted as described above and used for western blot analysis to assess the transfection efficiency.

Table 3.1 Primer sequences for RT-PCR and qPCR assays.

Gene	Foward primer	Reverse primer	Ref	Assay
TNIK(ex15)	CAAAGGCGAGAGAAGGAGCTG	CTGATGCTGAAGGGAAACTAAG	[21]	RT-PCR
TNIK(ex17)	CTTCAGCATCAGCGGCAGGAGC	ACTGACTGGGAGGCGGTCAAG	-	RT-PCR
TNIK(ex22)	CAGAAGAATCCAGGGACATTAC	CACCTTCTTCATTGGGCGGTTTG	-	RT-PCR
RPL10a	CAAGAAGCTGGCCAAGAAGTATG	TCTGTCATCTTCACGTGAC	-	RT-PCR
GAPDH	TCCCCACTGCCAACGTGTCAGTG	ACCCTGTTGCTGTAGCCAAATTCG	[21]	RT-PCR
MINIGENE	CAACTTCAAGCTCCTAAGCCACTGC	GGTCACCAGGAAGTTGGTTAAATCA	[177]	RT-PCR
OCT3/4	GACAGGGGGAGGGGAGGAGCTAGG	CTTCCCTCCAACCAGTTGCCCCAAAC	[178]	RT-PCR
SOX2	TTGCGTGAGTGTGGATGGGATTGGTG	GGGAAATGGGAGGGGTGCAAAAGAGG	[178]	RT-PCR
NANOG	CAGCCCTGATTCTTCCACCAGTCC	GTTCTGGAACCAGGTCTTCACCTG	-	RT-PCR
TNIK(ex15)	AATACATCAGGCGACAGTTAG	GCTTATATTCCAGAAGTAGAGCT	-	qPCR
TNIK(Total)	ACATACCATCTCATATTCAGGGC	CATTCCATCTGTTTTAGGCAAGA	[175]	qPCR
RPL10a	GAAGAAGGTGTTATGTCTGG	TCTGTCATCTTCACGTGAC	[21]	qPCR

3.8 Immunofluorescence and image acquisition

Cells were fixed with 4% paraformaldehyde in phosphate buffered saline (PBS, pH 7.4) for 15 min at room temperature (RT), permeabilized with 0.3% Triton X-100 and blocked with 10% normal goat serum (NGS) in PBS (blocking solution) for 20 min at RT. Incubation with primary antibodies was performed in blocking solution for 2 hr at 37°C. The fluorescent-tagged secondary antibodies Alexa Fluor 488 and 555 (Thermo Fisher Scientific) (dilution 1:500) were used for detection. DAPI staining was used to visualize nuclei. Coverslips were mounted onto glass slides using FluorSave mounting medium (Calbiochem). Images were acquired using the confocal inverted microscope (Nikon Eclipse C1). Images were acquired as Z-stacks (0.2 µm step size) using a 60X magnification.

Murine primary cortical neurons were fixed as described above. Fixed cells were treated with hot 10mM citrate buffer pH 6 for 20 min and permeabilized with 0.2% Triton X-100 for 5 min at RT. Cells were blocked with 5% bovine serum albumin in PBS for 45 minutes at RT and hybridized with primary antibodies overnight at 4°C. Anti-mouse goat secondary antibody and phalloidin, conjugated with Alexa Fluor 647 and Alexa Fluor 546 (Thermo Fisher Scientific) respectively, were incubated for 1h at RT. Coverslips were mounted onto a glass slide using Prolong Gold mounting medium (Thermo Fisher Scientific) and images were acquired using an epifluorescence microscope (Nikon Ti E) equipped with a cooled CMOS camera (Andor Zyla). Images were acquired as a single focal plane using a 20X magnification or as Z-stacks (0.2 µM step size) using a 60X magnification. Primary antibodies used are listed in Table 3.2.

3.9 Western blot assay

Cells were homogenized in lysis buffer (20 mM Tris–HCl pH 7.5, 150 mM NaCl, 1 mM EDTA, 1 mM EGTA, 1% Triton X-100 (Sigma-Aldrich), protease inhibitor cocktail (Roche)), sonicated and incubated 15 min on ice. Protein lysates were quantified by BCA protein assay (Thermo Fisher Scientific) and 25 µg protein samples were resolved by SDS-PAGE on 10% NuPAGE Bis-Tris pre-cast polyacrylamide gels (Thermo Fisher Scientific) and transferred to nitrocellulose membranes. Immunoblots were performed with specific primary antibodies (listed in Table 3.2), diluted in 5% milk in TBS with 0.1% Tween-20. The Novex ECL kit (Thermo Fisher Scientific) was used for detection. Densitometric analyses were performed using Image J software (NIH).

Table 3.2 Primary antibodies for immunofluorescence and western blot assays.

Antibody	Source	Assay
βIII Tubulin (1:800)	Abcam_ab52623	Immunofluorescence
TNIK exon 15 (1:500)	home-made (mouse)	Immunofluorescence
TRA1-60 (1:500)	Invitrogen_14-8863-80	Immunofluorescence
NESTIN (1:200)	Chemicon_MAB5326	Immunofluorescence
SMI 312 (1:700)	Covance_SMI-312R	Immunofluorescence
TNIK (1:500)	Gene Tex_GTX13141	Immunofluorescence
HA (1:200)	Sigma aldrich_H6908	Immunofluorescence
Alexa Fluor 546 Phalloidin (1:500)	ThermoFisher_A22283	Immunofluorescence
TDP-43 (1:1000)	Protein Tech_10782-2-AP	Western blot
NOVA-1 (1:1000)	Thermo Fisher Scientific_PA5-21459	Western blot
GAPDH (1:1000)	Santa Cruz_sc-47724	Western blot
HA-Peroxidase (HRP) (1:10000)	Miltenyi biotec_130-091-972	Western blot
FLAG-Peroxidase (HRP) (1:1000)	Sigma-Aldrich_A8592	Western blot
hnRNPA2B1 (1:500)	Santa Cruz_sc-32316	Western blot
α Tubulin (1:500)	Santa Cruz_sc-8035	Western blot

3.10 UV-Cross-linking and immunoprecipitation

PCR amplicons containing the genomic region of *TNIK* exon 15 (87 bp) with 141 bp of 5′ (TNIK A) or 126 bp of 3′ (TNIK B) flanking introns were cloned into the TA TOPO vector (Thermo Fisher Scientific) downstream of the T7 promoter. TNIK A and TNIK B plasmids were linearized by 30 U of *Hind*III restriction enzyme and radio-labeled riboprobes were obtained by transcribing 0.5 µg of each linearized construct with 20 U T7 RNA polymerase, 20 µCi α-[^{32}P] UTP, 0.5 mM NTPs, and 20 U RNase inhibitor. After template DNA removal by *DNase*I digestion, the resulting 32^{P}-labeled riboprobes were purified on ProbeQuant G-50 microcolumns. UV-Cross-linking and immunoprecipitation (UV-CLIP) experiments were performed as previously described [179]. Briefly, 300,000 cpm riboprobes were incubated with 200 µg of protein lysates of HEK293T cells transfected with flag-tagged-TDP-43 or ha-tagged-NOVA-1 constructs in 25 µl ligation buffer (1.3 mM MgCl2, 19 mM HEPES-KOH pH 7.4, 1.5 mM ATP, 19 mM Creatine phosphate) for 10 min at 30 °C. After addition of 5 µg tRNA, samples were

irradiated with UV light for 5 min and RNase A treated (25 U) for 30 min. Immunoprecipitation (IP) was then conducted by the addition of 2 µg of the selected antibody (anti-ha, -flag or the irrelevant IgG (Santa Cruz Biotechnology) pre-coated to protein G Dynabeads (Thermo Fisher Scientific). Immunocomplexes were washed several times in PBS with 0.02% Tween-20, run on a 10% SDS-PAGE and analyzed by autoradiography.

3.11 Co-immunoprecipitations

HEK293T cells transiently transfected as described above, were harvested after 24 h, lysed in lysis buffer (see above) by sonication and treated with RNAse inhibitor (10 U/100 µ protein lysate) or RNAse A (5 µg/100µ protein lysate). For immunoprecipitation, 2 ug of anti-ha (Sigma Aldrich), anti-flag (Sigma Aldrich) or the irrelevant IgG (Santa Cruz Biotechnologies) antibody were pre-coated to 450 ug of Dynabeads protein G (Thermo Fisher Scientific) and incubated with 200 ug of cell lysate for 45 min at room temperature. Immunocomplexes were washed four times in PBS with 0.02% Tween-20, eluted in 20µl 3x sample loading buffer (50mM Tris-HCL pH 6.8, 2% SDS, 0.1 % bromophenol blue, 10% glycerol) and 200mM DTT, resolved on 10% SDS-PAGE and processed for western blot as described above.

3.12 Cell morphological analyses

To measure the cell circularity, HEK 293T, transiently co-transfected with GFP and ha-tagged TNIK constructs, were fixed and stained to detect ha-TNIK expression. GFP was used to visualize the whole cell shape. Confocal

images were acquired as Z-stacks (0.2µm step size) using a 40X magnification. Using the software ImageJ (NIH), images were pre-processed to eliminate noise and, after applying a threshold, cellular circularity was measured using the shape descriptor "circularity" ($4\pi(\text{area}/\text{perimeter}^2)$). At least 25 cells/group were analyzed in three biological replicates.

To analyse neuronal arborization, primary murine cortical neurons, transiently transfected with GFP and ha-tagged TNIK constructs were fixed at DIV7 and stained for HA and F-actin (phalloidin) markers. For morphological analysis, epifluorescence images as individual focal planes were acquired using 20X lens, while cells bodies and growth cones were imaged as Z-stacks (0.2µm step size) using a 60X lens. Immunofluorescence images acquired at 60X were deconvolved using an adaptive blind deconvolution algorithm (Autoquant X3, Media Cybernetics) before analysis. Sholl analysis was used to describe the cortical neurons neuronal arbors, by ImageJ software. Images of isolated neurons were pre-processed to eliminate noise and background fluorescence, were segmented by applying an appropriate threshold and the binary images obtained were skeletonized. Concentric circles were drawn at 7.5 µm intervals around a common center in the cell body and the numbers of crossing neurites were counted at each of these circles starting from the second circle (15µm radius). To quantify F-actin levels in cell body or in the growth cone, the phalloidin fluorescence intensity was measured. The specific signal was thresholded to eliminate the background fluorescence and the integrated densities were measured into the cell body and growth cone marked as ROI (Region of interest) and normalized on the appropriate area. Raw values were normalized to the mean of the control condition for each replicates. At least 20 cells/group were analyzed in four biological replicates.

3.14 Statistical analysis

Statistical analyses were conducted with PRISM 5 software package (GraphPad). The D'Agostino & Pearson Omibus test was used to evaluate normality of the samples and the appropriate parametric or non-parametric tests were used to assess significance, according to the data normality. Student's t-test and one-way analysis of variance followed by appropriate *post-hoc* tests were applied to compare two or multiple groups, respectively. Data are presented as mean±s.e.m. Significance value was defined as $p < 0.05$.

4 RESULTS

4.1 *TNIK* alternative splicing in human adult tissues

We previously showed that in human neuroblastoma cells the RBP TDP-43 negatively regulates the inclusion of *TNIK* exon 15, encoding for a 29 aminoacid-long region [21]. In different human adult tissues, we evaluated *TNIK* exon 15 alternative splicing by RT-PCR analysis (Figure 4.1 A). We found *TNIK* exon 15 inclusion as the only splicing event occurring in brain, spinal cord and skeletal muscle (Figure 4.1 B), while in the other tissues we observed the expression of both *TNIK* containing-exon15 isoforms (*TNIKex15*) and the skipped ones (*TNIKex14-16*). Moreover, *TNIKex14-16* isoforms were more abundant than *TNIKex15* ones, except in liver where *TNIK* exon 15 inclusion was higher (Figure 4.1 B).

As *TNIK* gene is alternatively spliced also in exons 17 (55 amino-acid sequence) and 22 (8 amino-acid sequence), we tested their alternative splicing by RT-PCR assay (Figure 4.2). The *TNIK* isoforms containing the alternative exon 17 (*TNIKex17*) were mainly expressed in all tissues analyzed, while the exon 17 skipped isoforms (*TNIKex16-18*) were weakly expressed, excluding skeletal muscle where they are absent (Figure 4.2 A). Moreover, in all tissues analyzed we found the concomitant expression of *TNIK* isoforms including and skipping exon 22 (*TNIKex22* and *TNIKex21-23*, respectively), except in liver where *TNIKex22* isoforms were missing (Figure 4.2 A). Interestingly, exon 22 was differently regulated in the neuronal tissues analysed, as exon 22 inclusion was prevalently in brain, while in spinal cord, it is mainly skipped (Figure 4.2 A). The relative ratio of *TNIK*ex17/*TNIK*ex16-

18 and *TNIK*ex22/*TNIK*ex21-23 was quantified and represented in Figure 4.2 B.

These data suggest a specific neuronal role of *TNIKex15* isoform, as all *TNIK* isoforms expressed in both brain and spinal cord always include exon 15, unlike for exon 22 that is contemporary included or skipped and exon 17 that is mainly expressed not only in neuronal, but in all tissues analyzed.

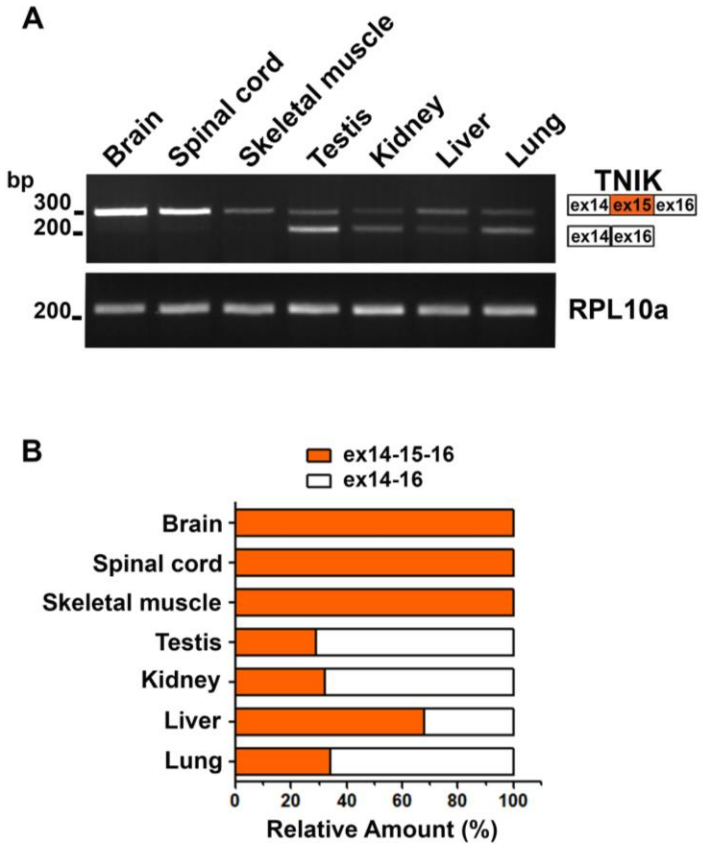

Figure 4.1 Analysis of *TNIK* exon 15 alternative splicing in different human adult tissues. ***A)*** Agarose gel images of semi-quantitative RT-PCR analysis of the *TNIK* exon 15 alternative splicing in the indicated tissues (upper band: *TNIKex15* isoforms, lower band: *TNIKex14-16* isoforms). *RPL10a* was used for sample normalization. ***B)*** Densitometric analysis of the relative amount of the two alternative splicing isoforms for each tissue analyzed.

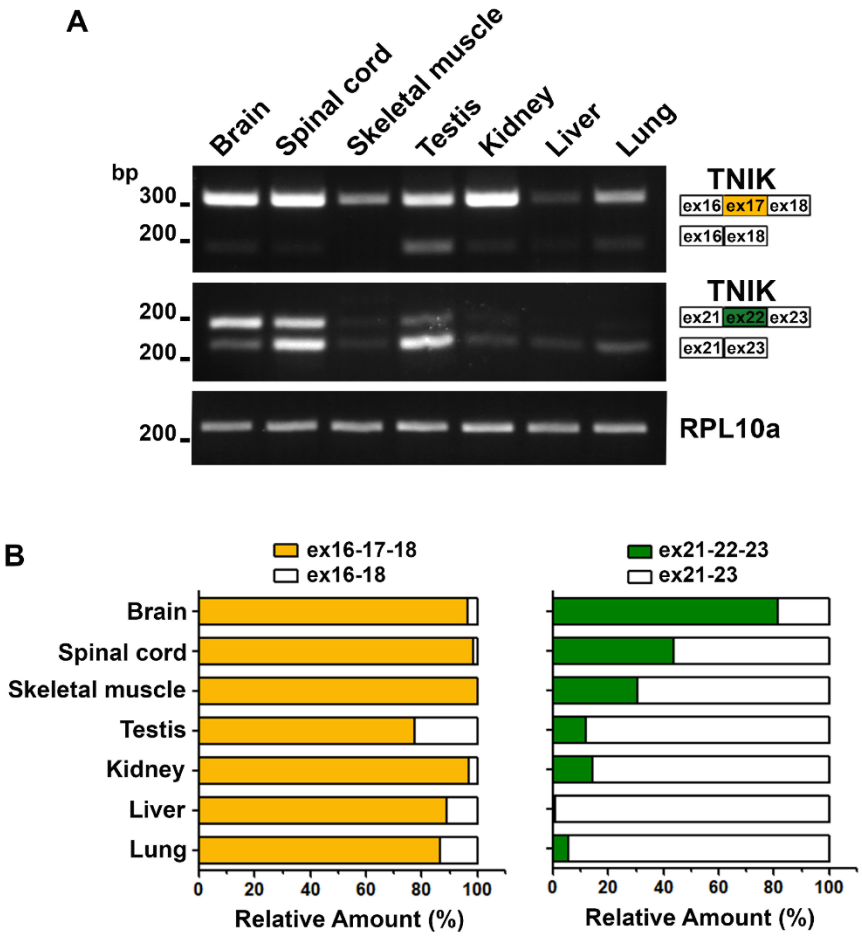

Figure 4.2 Analysis of *TNIK* exon 17 and 22 alternative splicing in different human adult tissues. ***A)*** Semi-quantitative RT-PCR analysis of the *TNIK* exon 17 (upper panel) and exon 22 (middle panel) alternative splicing in the indicated tissues. For both alternative splicing events, the upper band indicates exon inclusion (*TNIKex17* or *TNIKex22* isoforms), while the lower band represents exon skipping (*TNIKex16-18* or *TNIKex21-22* isoforms). *RPL10a* was used for sample normalization. ***B)*** Densitometric analysis representing the relative amount of *TNIKex17* and *TNIKex16-18 (left panel)* and of *TNIKex22* and *TNIKex21-23 (right panel)* isoforms in the analyzed tissues.

4.2 *TNIK* exon 15 alternative splicing during human neuroblastoma cell differentiation *in vitro*

As *TNIKex15* isoforms showed a prevalent expression in central nervous system, we further investigated this alternative splicing event in a cell model of neuronal differentiation *in vitro* to evaluate its regulation during the differentiation process. Since in human neuroblastoma SK-N-BE cells *TNIK* exon 15 skipping is physiologically prevalent (Figure 4.3 A), we investigated whether this alternative splicing event is regulated upon SK-N-BE neuronal differentiation.

By treating SK-N-BE cells with RA for a time-frame of 6 days, we observed an increase of *TNIK* exon 15 inclusion by RT-PCR analysis, although not statistical significant (Figure 4.3 A, B). However, quantification by real-time PCR showed a significant increase of *TNIKex15* isoforms expression from T0 to T4, with mRNA levels at T6 comparable to T4 (Figure 4.3 C). Using primers designed on *TNIK* exons 31-32, we observed that the all *TNIK* isoforms expression was also significantly up-regulated during neuronal differentiation (Figure 4.3 C).

Immunofluorescence analysis (IF) using a custom-made anti-TNIKex15 antibody, previously described [21], showed the appearance of the TNIKex15 protein isoforms specifically at 6 days post-differentiation (T6) (Figure 4.4), when βIII-tubulin staining showed a concomitant increase in neuronal outgrowth and branching, less evident already at 4 days post-differentiation (T4) (Figure 4.4). In differentiated neuroblastoma cells, TNIKex15 protein isoforms localized in the cytoplasm showing a prevalent localization in the perinuclear region (Figure 4.4).

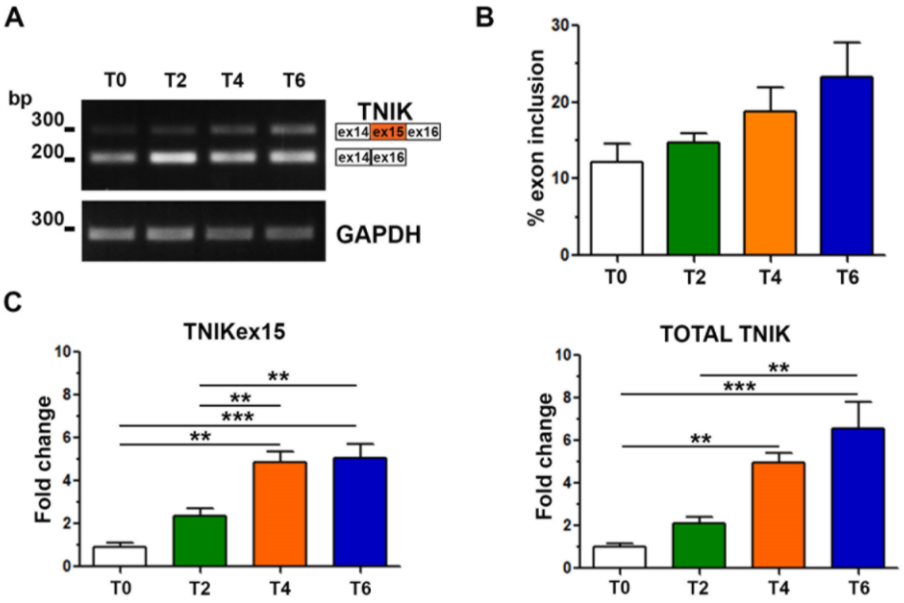

Figure 4.3 Analysis of *TNIK* exon 15 splicing during SK-N-BE cells neuronal differentiation. SK-N-BE cells were differentiated with RA (10μM) and analysed before treatment (T0), after two (T2), four (T4) or six days (T6). ***A)*** Representative agarose gel image of RT-PCR of *TNIK* exon 15 alternative splicing isoforms. *GAPDH* was used for data normalization. ***B)*** Densitometric and statistical analysis of *TNIK* exon 15 inclusion (mean ± s.e.m.; n = 3 independent experiments; one-way ANOVA and Tukey post hoc test). ***C)*** Real-time PCR assay of *TNIKex15* isoforms (*left*) and total *TNIK* (*right*). Fold change values were calculated versus T0 stage (mean ± s.e.m.; n = 3 independent experiments; one-way ANOVA and Tukey post hoc test; ** $p < 0.01$, *** $p < 0.001$).

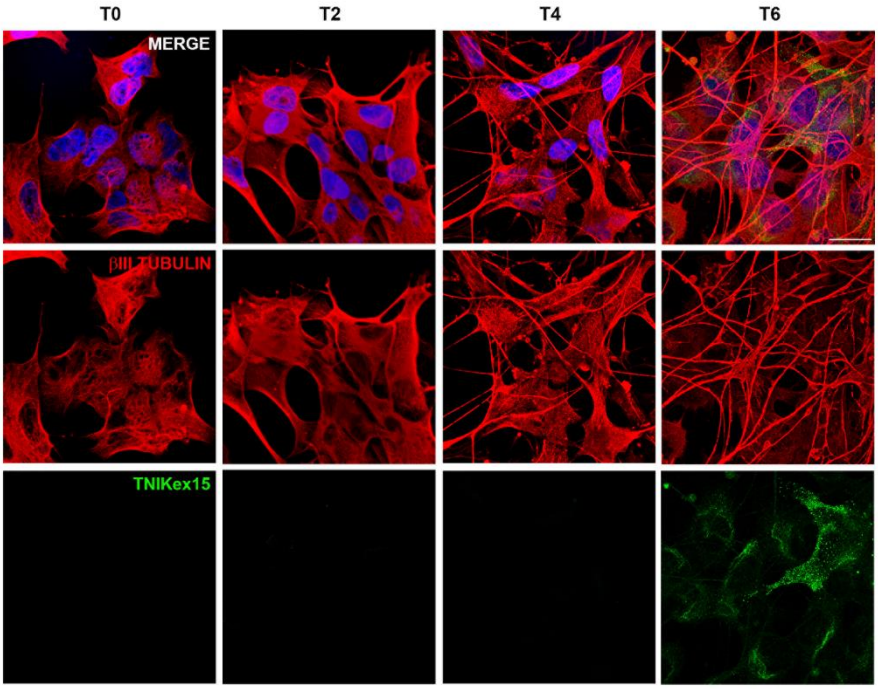

Figure 4.4 TNIKex15 protein expression during SK-N-BE cells neuronal differentiation. Representative IF images of βIII-Tubulin (red) and TNIKex15 (green) immunostaining in SK-N-BE cells at T0, T2, T4 and T6. Nuclear staining is indicated in blue (DAPI) in the merged images. Bar, 20 μm.

4.3 Analysis of *TNIK* exon 15 alternative splicing in human iPSC-derived neural stem cells and neurons

The alternative splicing of *TNIK* exon 15 was also studied in an alternative differentiation cell model, including human iPSCs committed into neural stem cells (NSCs) or differentiated into neuronal cells (iPSC-Neurons). We used iPSCs already available in our laboratory and derived from the reprogramming of three healthy control fibroblasts that were characterized by immunofluorescence and RT-PCR for the expression of the pluripotency markers TRA1-60, Oct 3/4, Sox 2 and Nanog (Figure 4.5 A, B).

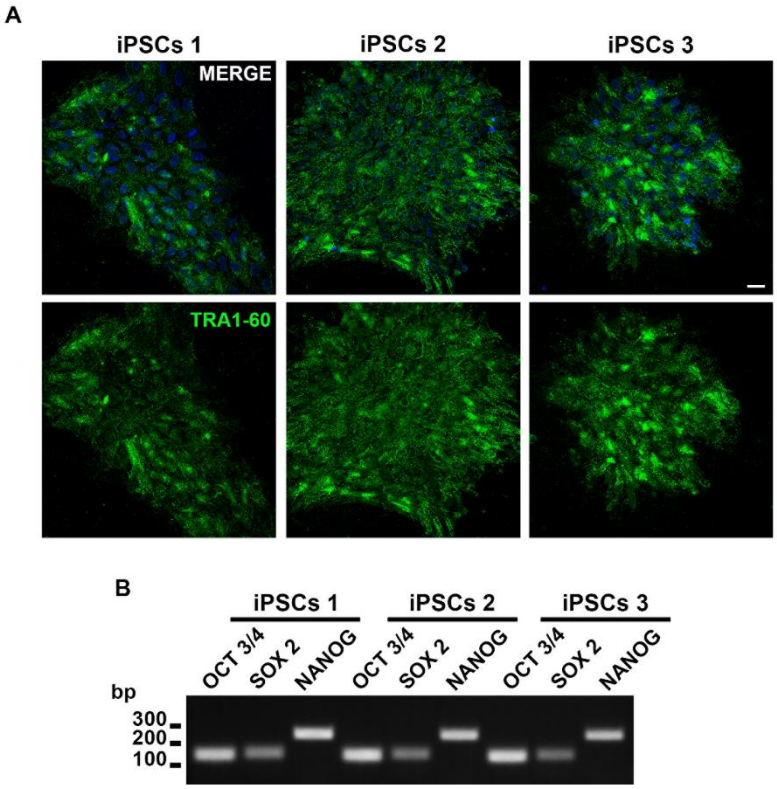

Figure 4.5 Characterization of pluripotency of human iPSCs. Pluripotency of the three human healthy iPSCs lines was evaluated ***A)*** by IF analysis of TRA-1-60 (green) and ***B)*** by RT-PCR assay of *OCT 3/4*, *SOX 2* and *NANOG* staminal markers. In the representative IF images the nuclear staining is indicated in blue (DAPI) in the merged images. Bar, 20 μm.

Culturing iPSCs in a commercial medium for one week, we obtained a neural population that showed 100% of Nestin-positive cells when characterized by immunofluorescence analysis (Figure 4.6 A). iPSC differentiation into neurons, performed by a modified protocol of Amoroso et al. [176], was assessed by the expression of the neuronal βIII-tubulin and the neurofilament SMI-312 cytoskeleton markers in immunofluorescence images. We obtained a neuronal population with 100% βIII-tubulin-positive cells and ~80% of SMI-312-positive cells for all the three differentiated iPSC lines (Figure 4.6 B).

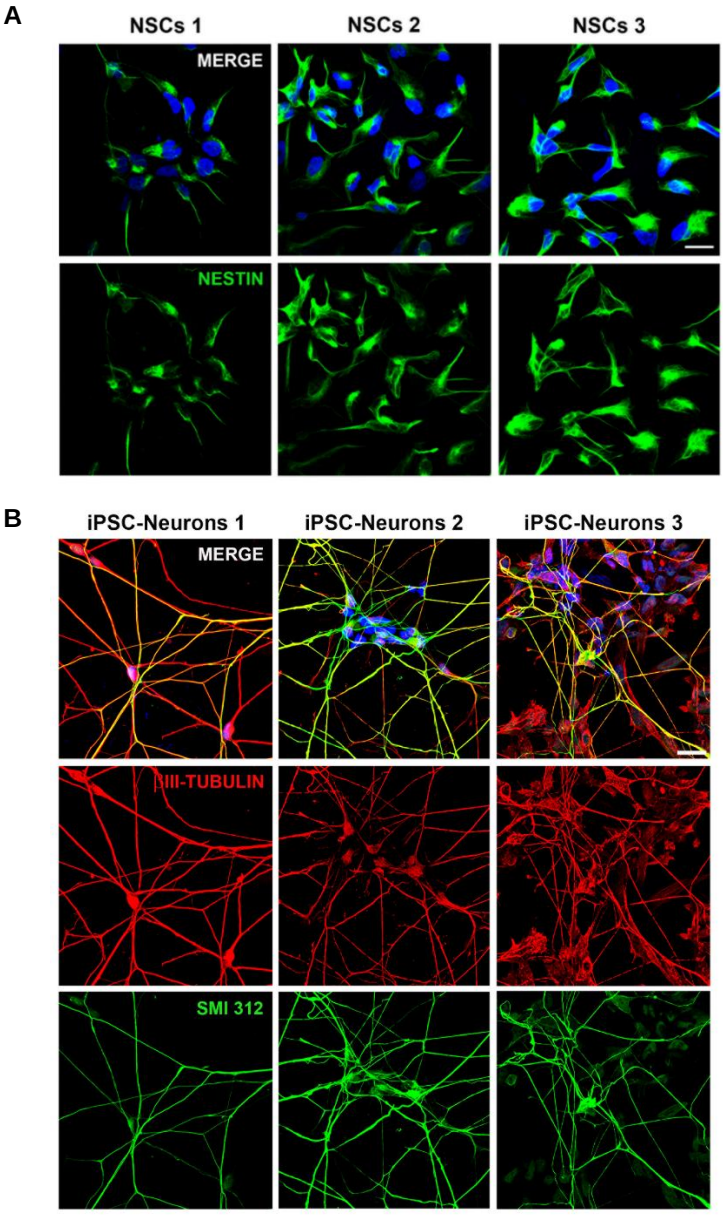

Figure 4.6 Characterization of iPSCs neural and neuronal differentiation. Three human healthy iPSCs lines were differentiated into neural stem cells (NSCs 1-2-3) and were characterized by IF analysis of the neural marker Nestin (green) showed in the representative images ***A)***. The three iPSCs lines were also differentiated into neurons (iPSC-Neurons 1-2-3) and the neuronal differentiation efficiency was evaluated by IF analysis of the neuronal βIII-Tubulin (red) and the neurofilament SMI 312 (green) markers ***B)***. Nuclear staining is indicated in blue (DAPI) in the merged images. Bar, 20 μm.

Quantitative analysis of *TNIK* exon 15 alternative splicing by RT-PCR showed that in iPSCs the *TNIKex14-16* isoforms were prevalent with only 5.8% of exon 15 inclusion, while during neuronal differentiation the inclusion of exon 15 significantly increased to 25% in NSCs and to 50% in iPSC-Neurons (Figure 4.7 A, B).

Immunofluorescence analyses confirmed the exclusive expression of TNIKex15 protein isoforms in iPSC-Neurons (Figure 4.7 C), but not in iPSCs and in NSCs (data not shown). The cellular distribution of TNIKex15 protein was prevalent in the cytoplasm, particularly enriched in the perinuclear region, as observed in SK-N-BE differentiated cells, but also distributed along few neurites. The TNIK protein, detected with a commercial antibody generated against an amino acidic region common to all the isoforms, was mainly distributed like the TNIKex15 isoforms but showed a weak diffuse staining also in other cytoplasmic regions (Figure 4.7 C).

Our results from both human neuroblastoma and iPSCs *in vitro* models suggest that *TNIK* exon 15 inclusion is up-regulated and that the TNIKex15 protein isoforms are specifically present in differentiated neuronal cells.

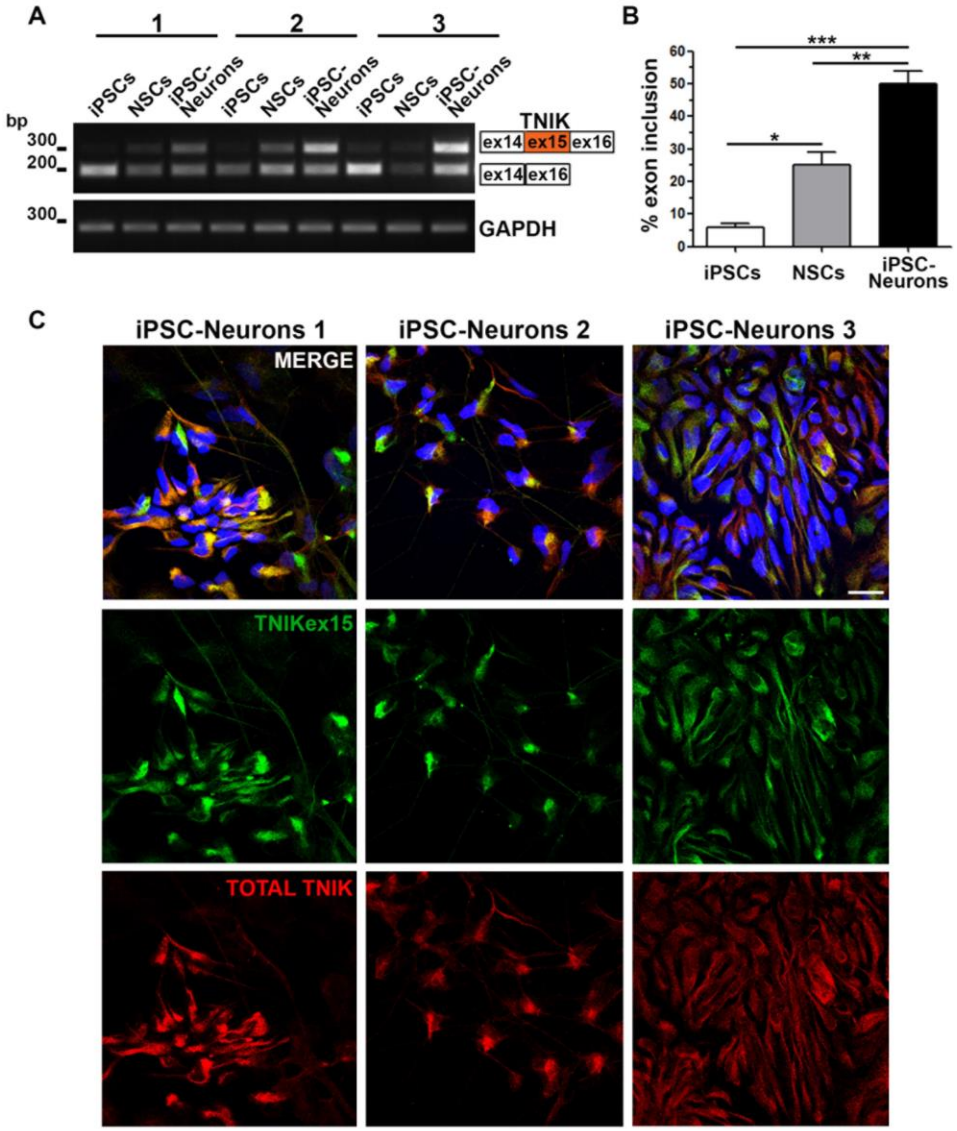

Figure 4.7 Analysis of *TNIK* alternative splicing during neuronal differentiation of human iPSCs. ***A)*** RT-PCR analysis of *TNIK* exon 15 alternative splicing in three differentiation stages: before differentiation (iPSCs), in the intermediate stage of neural stem cells (NSCs) and in the late stage of iPSC-Neurons. ***B)*** Densitometric and statistical analysis of RT-PCR assay showed in A (mean ± s.e.m, one-way ANOVA and Tukey post hoc test; n=3 is referred to the differentiation of three human healthy iPSC lines; * $p<0,05$; ** $p<0,01$; *** $p<0,001$). ***C)*** Representative IF images of TNIKex15 (green) and TNIK (red), detected with a home-made and a commercial antibody, respectively, in differentiated iPSC-Neurons. Nuclear staining is indicated in blue (DAPI) in the merged images. Bar, 20 µm.

4.4 Regulation of *TNIK* exon 15 inclusion by the neuronal-specific splicing factor NOVA-1

As TDP-43 acts by inhibiting *TNIK* exon 15 inclusion, we assessed whether TDP-43 protein content changes during neuronal differentiation to account for the observed increase in *TNIK* exon 15 inclusion. By Western blot (WB) analyses, TDP-43 protein levels were comparable both in all stages of neuroblastoma differentiation (Figure 4.8 A) and during differentiation of iPSC into NSCs and iPSC-neurons (Figure 4.8 B). Moreover, immunofluorescence analysis showed that TDP-43 mainly localized in the nucleus of both neuron-differentiated cells, excluding a loss of TDP-43 nuclear function (data not shown).

We therefore investigated whether *TNIK* splicing is regulated by other splicing factors in neuronal cells. We focused on NOVA-1, which is reported to be expressed specifically in neurons and to regulate the alternative splicing of a wide array of genes involved in synapse architecture and functioning [170]. NOVA-1 protein content significantly increased in differentiated neuroblastoma cells at T6 by WB analysis (Figure 4.8 A). During iPSCs differentiation, NOVA-1 was detected only in iPSC-neurons (Figure 4.8 B), confirming literature data about its neuron-specific expression.

To test if NOVA-1 RBP can regulate *TNIK* pre-mRNA splicing, we first assessed *TNIK* exon 15 alternative splicing upon NOVA-1 over-expression. In non-neuronal HEK293T cells, not physiologically expressing the *NOVA-1* gene, *TNIK* exon 15 was prevalently skipped as showed by RT-PCR analysis (Figure 4.9 A), while we observed an increased exon 15 inclusion upon ha-tagged NOVA-1 over-expression (Figure 4.9 A). We confirmed these findings by quantitative real-time PCR that showed a significant three-fold increase of *TNIK* exon 15 isoforms together with unchanged levels of all *TNIK*

isoforms (*Total TNIK*) (Figure 4.9 B). We also tested if NOVA-1 over-expression influenced TDP-43 protein levels by WB analysis (Figure 4.9 A) that showed unchanged TDP-43 content in NOVA-1 over-expressing cells in comparison to the mock-transfected ones (Figure 4.9 C).

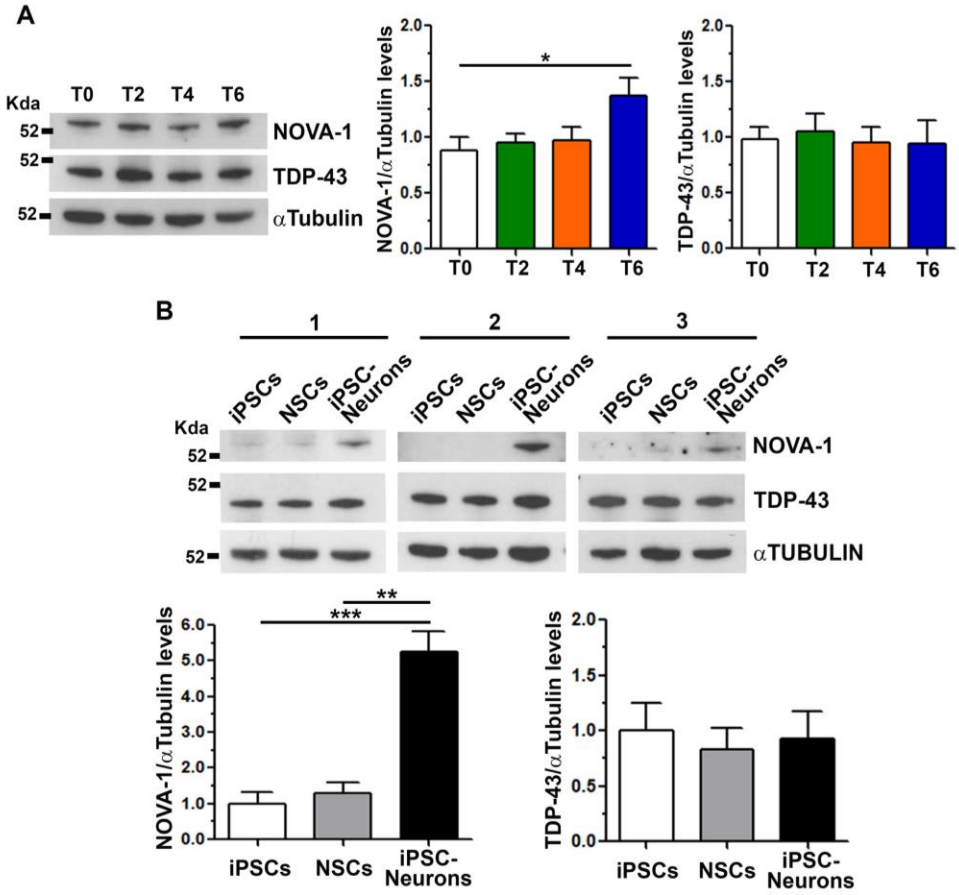

Figure 4.8 NOVA-1 and TDP-43 protein levels in neuronal differentiation models *in vitro*. Representative WB images and densitometric analysis of TDP-43 and NOVA-1 protein levels ***A)*** during SK-N-BE neuronal differentiation (mean ± s.e.m.; n = 3 independent experiments; one-way ANOVA and Tukey post hoc test; * p <0.05) and ***B)*** in iPSCs, neural stem cells (NSCs) and iPSC-Neurons (mean ± s.e.m.; n = 3 is referred to the differentiation of three human healthy iPS cells; one-way ANOVA and Tukey post hoc test; ** p <0.01, *** p<0.001).

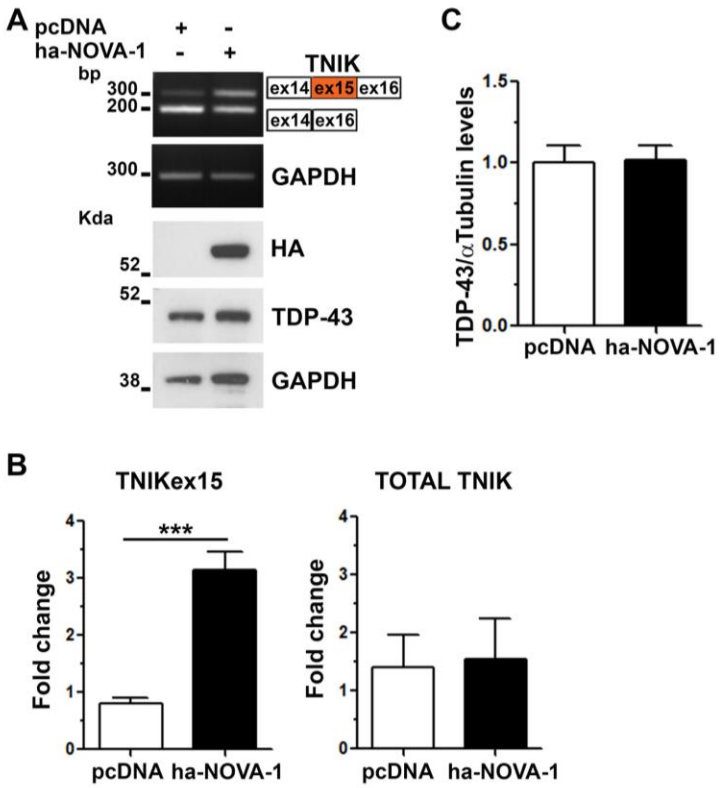

Figure 4.9 *TNIK* exon 15 alternative splicing and TDP-43 protein levels upon NOVA-1 over-expression in HEK293T cells. ***A)*** Representative RT-PCR image of *TNIK* exon 15 splicing upon ha-tagged NOVA-1 or empty vector (pcDNA) over-expression in HEK293T cells *(Upper panel)*. Representative WB images to assess ha-tagged NOVA-1 transfection efficiency and endogenous TDP-43 protein levels *(Lower panel)*. GAPDH was used for data normalization. ***B)*** Real-time PCR of *TNIKex15* isoforms and total *TNIK* gene. Fold change values were calculated versus mock-transfected cells (pcDNA) (mean ± s.e.m.; n = 3 independent experiments; Unpaired *t-test*; *** $p < 0.001$). ***C)*** Densitometric analysis of TDP-43 protein levels showed in A (mean ± s.e.m.; n = 3 independent experiments; Unpaired *t-test*).

To further investigate if NOVA-1 may act as a *TNIK* exon 15 splicing regulator, we performed a minigene assay that we previously used to demonstrate TDP-43-mediated splicing of *TNIK* [21]. *TNIK* exon 15 (87bp) and part of its flanking 5' (141bp) and 3' (126bp) intronic regions were cloned into the pTB minigene system as already described [21]. Figure 4.10

schematically reports the pTB minigene system and the full *TNIK* sequence cloned, highlighting the TDP-43 consensus binding motif $(TG)_{18}$ within the intronic region downstream exon 15.

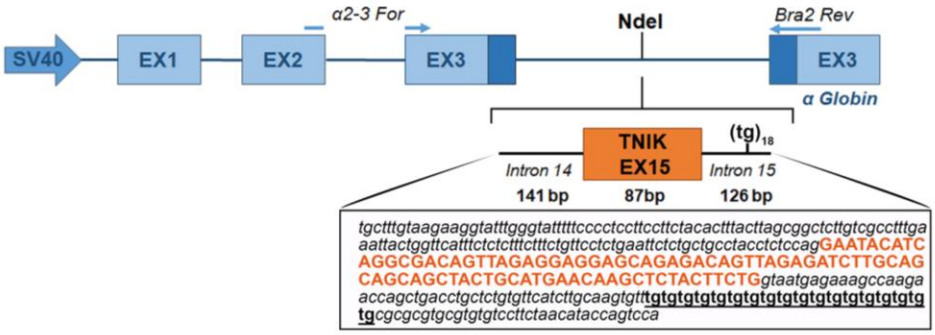

Figure 4.10 *TNIK* exon 15 minigene construct. Schematic representation of the pTB minigene system. *TNIK* exon 15 (orange box) along with parts of 5' (141 bp) and 3' (126 bp) introns were subcloned into the NdeI restriction site of the pTB vector. The sequence of the subcloned region is reported highlighting exon 15 sequence (orange) and the TDP-43 consensus motif (underlined bolt). The primers used for the RT-PCR are also indicated (a2-3 For; Bra2 Rev).

In our analysis, we also included hnRNPA2/B1, an ubiquitous RBP that is known to interact directly with TDP-43 and to co-operate in regulating its splicing activity [9]. Therefore, in HEK293T cells upon the over-expression of the splicing factors TDP-43, NOVA-1 and hnRNPA2/B1 alone or in combination with each other, we evaluated the exon 15 inclusion/skipping of *TNIK*-minigene construct (Figure 4.11 A). When TDP-43 was over-expressed, *TNIK* exon 15 inclusion decreased to 53.5% compared to mock-transfected cells (88.2%), as already shown [21] (Figure 4.11 A *lane 1, 2*; B). Similar results were obtained upon transfection of flag-tagged hnRNPA2/B1 showing a 68.8% of exon 15 inclusion (Figure 4.11 A *lane 4*; B). Transfection with ha-tagged NOVA-1 showed a slight, although not significant, increase of exon 15 inclusion (92.2%) compared to mock-transfected cells even if *TNIK* exon 15 inclusion is almost complete in these cells (Figure 4.11 A *lane 3, 1*; B). In competition experiments, by co-expression of NOVA-1 with TDP-

43 or hnRNPA2/B1, we observed that NOVA-1 completely abrogated both TDP-43 and hnRNPA2/B1 skipping activity on exon 15 (90.8% and 92.8% exon inclusion, respectively) (Figure 4.11 A *lane 5, 6*; B). The co-expression of TDP-43 and hnRNPA2/B1 synergistically decreased to 32.2% the exon 15 inclusion (Figure 4.11 A *lane 7*; B), while the presence of NOVA-1 was able to completely inhibit TDP-43/hnRNPA2/B1 splicing activity by restoring *TNIK* exon 15 inclusion (93.5%) similarly to control cells (88.2%) (Figure 4.11 A *lane 8*; B). WB analyses assessed that the recombinant proteins content was comparable in all minigene splicing assays (Figure 4.11 A).

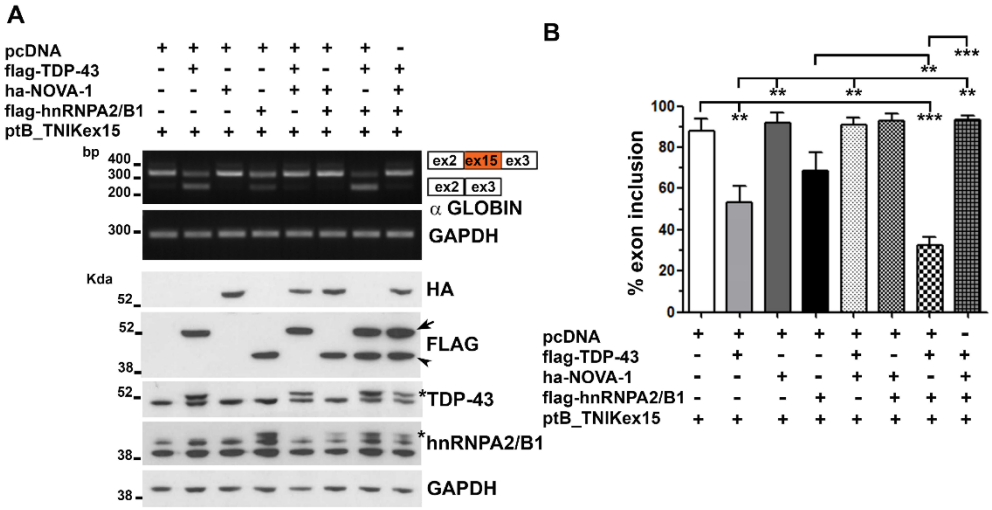

Figure 4.11 *TNIK* exon 15 minigene assay in HEK293T cells *A)* Representative RT-PCR image of the splicing pattern of *TNIKex15*-minigene in HEK293T cells co-transfected with pTBminigene_TNIKex15 and flag-tagged TDP-43, flag-tagged hnRNPA2/B1, ha-tagged NOVA-1 or empty vector (pcDNA) as indicated *(Upper panel)*. The scheme of *TNIKex15* inclusion (ex2-ex15-ex3) and skipping (ex2-ex3) in α-globin gene is indicated. Representative WB images to evaluate transfection efficiency of the different constructs *(Lower panel)*. GAPDH was used for data normalization in WB and RT-PCR analysis. Arrow, flag-TDP-43; arrowhead, flag-hnRNPA2B1; asterisk, recombinant flag-tagged TDP-43 or hnRNPA2/B1 protein.
B) Densitometric and statistical analysis of *TNIKex15*-minigene inclusion data (mean ± s.e.m, one-way ANOVA and Tukey post hoc test; n=3 independent experiments; ** p< 0,01; *** p< 0,001).

4.5 NOVA-1 and TDP-43 interplay in regulating *TNIK* alternative splicing

According to our minigene results, a competitive mechanism between TDP-43 and NOVA-1 is suggested in the regulation of *TNIK* exon 15 splicing. We previously showed by RNA-immunoprecipitation (RIP) assay that TDP-43 binds the *TNIK* pre-mRNA in human neuroblastoma cells [21].

We tested NOVA-1 binding by UV-CLIP experiments using protein lysates of HEK293T cells transfected with ha-tagged NOVA-1 or flag-tagged TDP-43 and two riboprobes, *TNIK A* and *TNIK B*, encompassing specifically the *TNIK* intronic regions included in the minigene assay and exon 15, as schematically reported in Figure 4.12 A. While we confirmed TDP-43 binding to *TNIK*, demonstrating that specifically recognizes intron 15, containing the UG-consensus binding motif, we failed to detect NOVA-1 binding to the intron14-exon15-intron15 selected region (Figure 4.12 B), although the recombinant NOVA-1 protein was recovered successfully in the immunoprecipitation (IP) assay (Figure 4.12 C). This result was also supported by *in silico* analysis using the RBPmap software (http://rbpmap.technion.ac.il/; [180]) of *TNIK* pre-mRNA that did not identify the canonical NOVA-1 specific consensus motif (YCAY clusters) within the selected *TNIK* sequence also used in the minigene assay (data not shown).

Excluding a direct binding of NOVA-1 on *TNIK* pre-mRNA, we tested if this RBP binds to TDP-43 protein and if this interaction is RNA-mediated. Co-immunoprecipitation (co-IP) experiments on HEK293T lysates co-transfected with flag-tagged TDP-43 and ha-tagged NOVA-1 constructs showed that NOVA-1 bound TDP-43 only if RNA was preserved by adding a ribonuclease (RNAse) inhibitor in the cell lysates (Figure 4.13). This result was further supported by the reduced NOVA-1 interaction with TDP-43 in cell lysates treated with RNAse A to digest the RNA component (Figure 4.13).

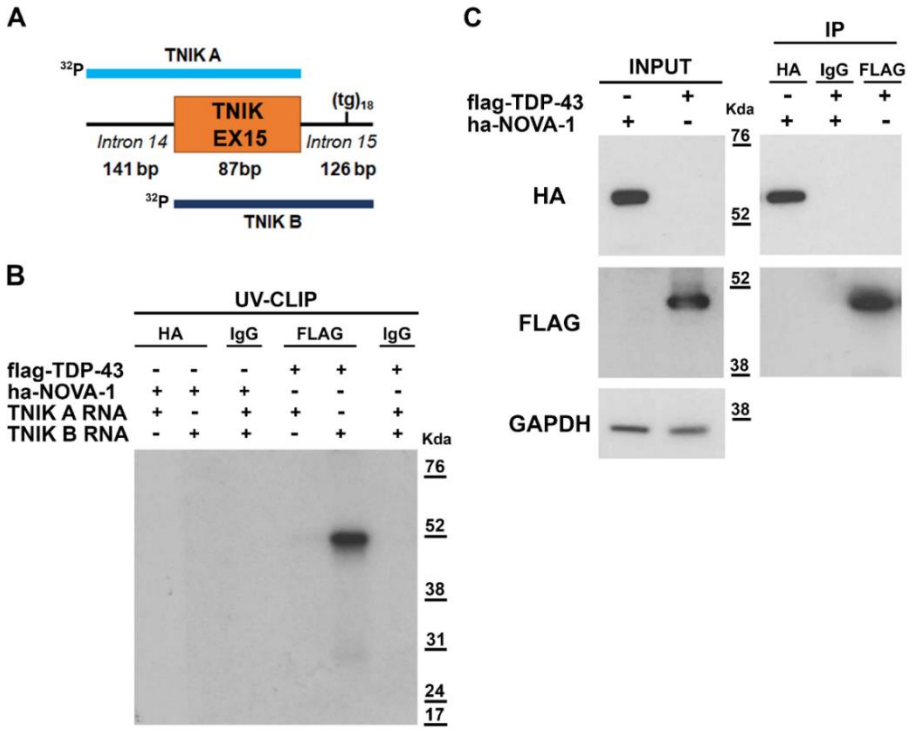

Figure 4.12 Analysis of NOVA-1 interaction to *TNIK* pre-mRNA. ***A)*** Schematic representation of *TNIK A* and *TNIK B* riboprobes designed for the UV-CLIP assay. *TNIK A* riboprobe includes 141 bp-intron14 and exon15 region, while exon15 and 126bp-intron15 sequence is contained in *TNIK B*. ***B)*** SDS-PAGE of UV-CLIP experiment with anti-ha (*first and second lanes*) anti-flag (*fourth and fifth lanes*) antibody and radiolabeled *TNIK* A (*first and fourth lanes*) or *TNIK* B (*second and fifth lanes*) riboprobes. The irrilevant IgG antibody was used as a negative control (*third and sixth lanes*). ***C)*** WB representative images of IP samples to check the transfection efficiency (INPUT) and the ha-tagged NOVA-1 and flag-tagged TDP-43 recovery in IP assay. GAPDH was used to data normalization.

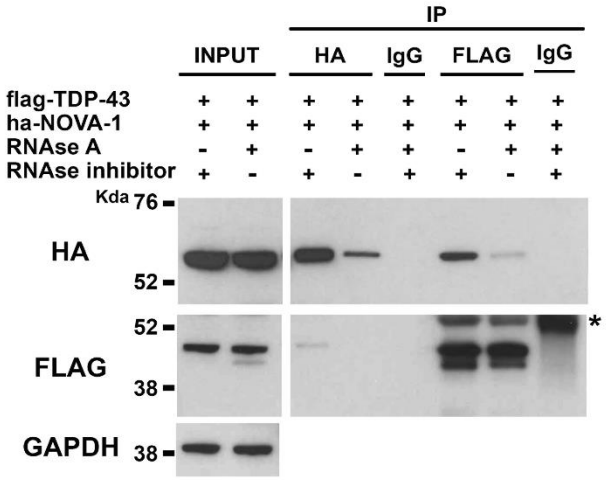

Figure 4.13 NOVA-1 protein interaction with TDP-43. Representative WB image of co-IP on HEK293T cell lysates transfected with ha-tagged NOVA-1 and flag-tagged TDP43 constructs and treated with RNAse A or RNAse inhibitor to digest or preserve RNA, respectively. Anti-flag or anti-ha antibody was used to immunoprecipitate the recombinant proteins and their complexes (n=3 independent experiments); asterisk, indicate IgG heavy chain.

In order to confirm that this interaction occurs only in a RNA-dependent manner and to map TDP-43 protein region involved in the binding, we performed co-IP assay on HEK293T cell lysates, co-transfected with ha-tagged NOVA-1 and flag-tagged full-length or mutated TDP-43. We used two TDP-43 constructs unable to bind the RNA targets, such as the flag-tagged TDP-43 ΔRRM1, where the entire RRM1 domain was deleted, and flag-tagged TDP-43 4FL, where four phenylalanines residues (p.F147 and p.F149 in RRM1 and p.F229 and p.F231 in RRM2 domain), indispensable for the binding to RNA, were mutated into lysines [5]. As the C-terminal TDP-43 domain is described to be mainly involved in protein-protein interaction, we also used a C-terminal deleted TDP-43 construct (flag-tagged TDP-43 ΔC) to assess if this region may be involved in TDP-43/NOVA-1 interaction (Figure 4.14 A). Co-IP experiments on lysates treated with RNAse inhibitor confirmed NOVA-1 binding to TDP-43 only if the TDP-43 ability to recognize

RNA was preserved, as NOVA-1 failed to bind both TDP-43 ΔRRM1 and TDP-43 4FL protein (Figure 4.14 B). The NOVA-1 interaction with the mutant TDP-43 ΔC was maintained, indicating that TDP-43 C-terminal domain is not necessary for NOVA-1 binding (Figure 4.14 B).

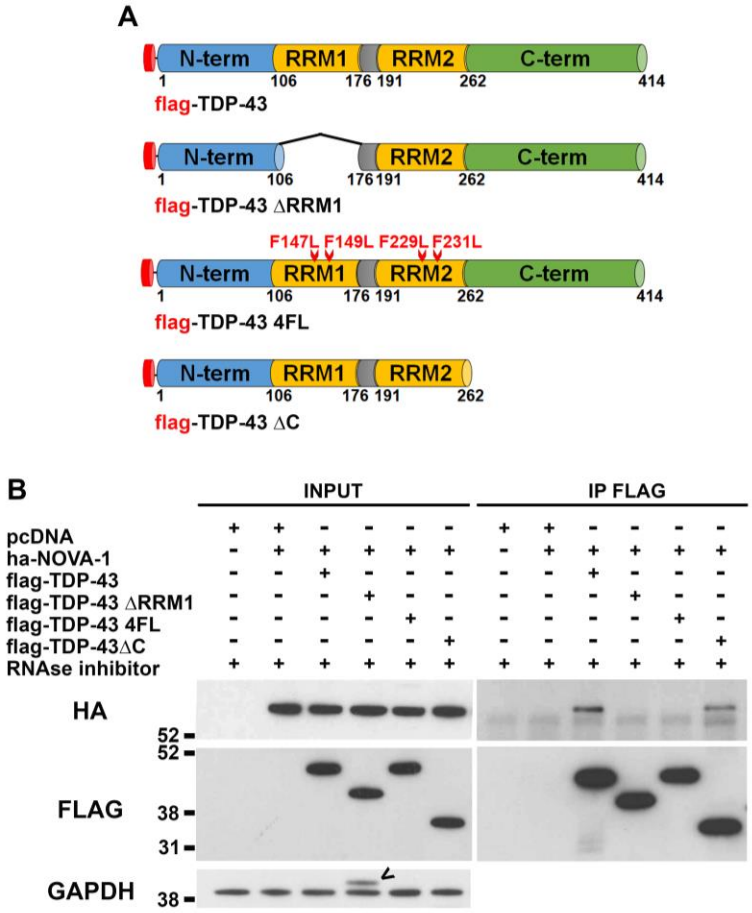

Figure 4.14 Mapping of TDP-43 protein region interacting with NOVA-1. ***A)*** Graphical representation of the flag-tagged full-length and mutant TDP-43 constructs used in B. ***B)*** Representative WB image of co-IP using anti-flag antibody on HEK293T lysates transfected with ha-tagged NOVA-1 or flag-tagged TDP-43 plasmids, showed in A, as indicated to assess TDP-43 protein region involved in NOVA-1 binding (n=3 independent experiments). **<** indicate residual flag signal from the previous hybridization.

As our minigene data showed that NOVA-1 also abrogated hnRNPA2/B1 exon skipping activity on *TNIK* exon 15, we tested if NOVA-1 also binds to this RBP by co-IP experiments. Similarly to TDP-43, NOVA-1 bound hnRNPA2/B1 only if RNA was preserved with a RNAse inhibitor compared to RNAse A treatment (Figure 4.15). Immunoprecipitation using anti-ha, the NOVA-1-tag, antibody failed to isolate protein complexes including hnRNPA2B1 (Figure 4.15), probably because the ha-sequence may be masked in these complexes. This may be also valid to explain the reduced NOVA-1/TDP-43 interaction observed when anti-ha antibody was used to IP (Figure 4.13).

These results suggest that the RNA-dependent interactions between the tissue-specific NOVA-1 and the ubiquitous TDP-43 and hnRNPA2B1 RBPs may play a role in regulating *TNIK* exon 15 alternative splicing in neurons.

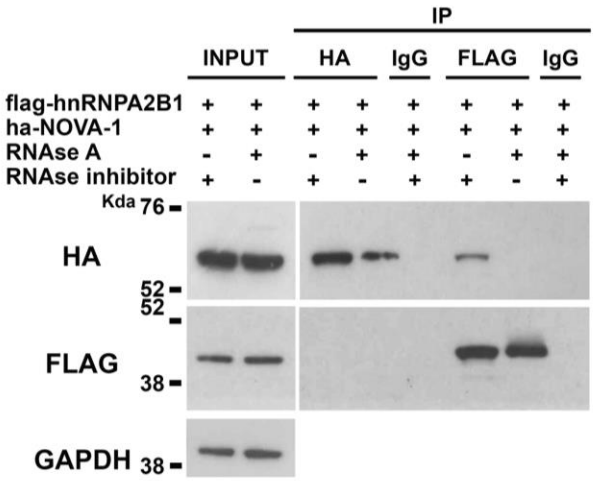

Figure 4.15 NOVA-1 protein interaction with hnRNPA2B1. Western blot image representative of co-IP experiments using anti-flag and anti-ha antibody to check for NOVA-1 binding to hnRNPA2B1. HEK293T cells were transfected with ha-tagged NOVA-1 or flag-tagged hnRNPA2B1 and lysates treated with RNAse A or RNAse inhibitor to determine if the binding was RNA-mediated (n=3 independent experiments).

4.6 Role of TNIKex15 protein isoform on cell spreading in HEK293T cells

The full-length TNIK over-expression has already been described to affect cell spreading and morphology through the disruption of the filamentous actin (F-actin) network [103,111]. This effect has been associated with TNIK kinase activity, as the over-expression of a TNIK construct mutated in the N-terminal domain (K54R) with a defective kinase activity did not show cell spreading and morphological defects [103,111].

To evaluate if also the 29-amino-acid region encoded by exon 15 is necessary to affect cell spreading, we transiently over-expressed the human full-length TNIK (TNIK FL) and TNIK exon 15-deleted (TNIKΔ15) constructs in HEK293T cells, to analyze their effect on cell morphology by measuring the cell circularity parameter by ImageJ NIH software (Figure 4.16). In our analysis, we included also the kinase mutant TNIK construct (TNIK KM), as a negative control (Figure 4.16 A). Our analysis showed that the TNIK FL over-expression significantly increased cell circularity compared to control cells, while TNIK KM-transfected cells showed a cellular shape comparable to mock-transfected ones, as expected [103] (Figure 4.16 B). Moreover, TNIK FL circularity resulted significantly increased also compared to TNIK KM condition, confirming that the kinase activity is important to affect cell spreading (Figure 4.16 B). The TNIKΔ15-expressing cells showed circularity values closer to the control cells and significantly different from both TNIK full-length and TNIK KM transfected cells (Figure 4.16 B), thus showing an intermediate phenotype.

These results suggest that the amino acidic sequence encoded by *TNIK* exon 15 is required to inhibit cell spreading in HEK293T cells.

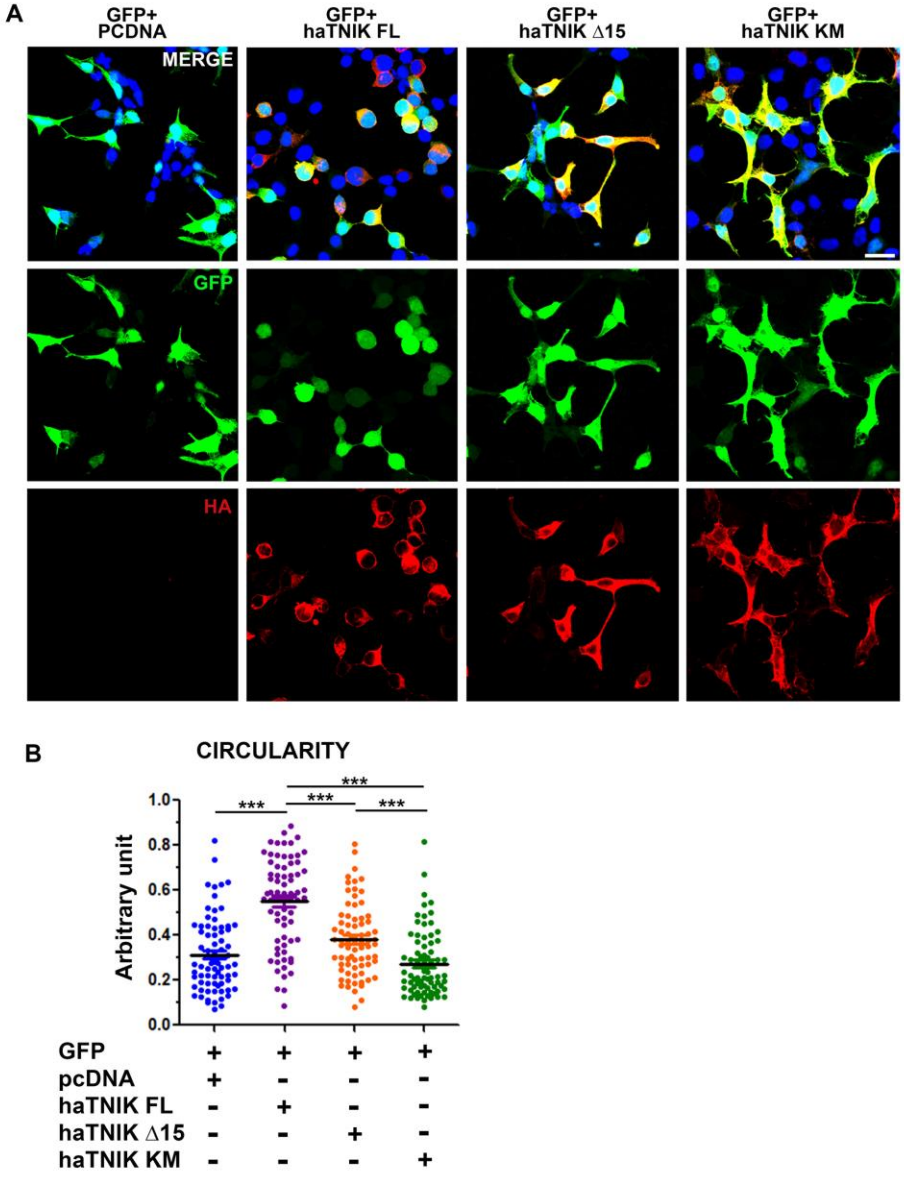

Figure 4.16 TNIK effect on cell spreading in HEK293T cells. ***A)*** Representative IF images of HEK293T cells transfected with human TNIK constructs (ha-tagged TNIK FL, ha-tagged TNIKΔ15 and ha-tagged TNIK KM) (red) or empty vector. GFP was co-transfected to label cell morphology and the nuclear staining is showed in blue in the merged images (DAPI). Bar 20μM. ***B)*** Cell circularity analysis performed by ImageJ NIH software. Blue circles, mock-transfected cells; purple circles, TNIK FL cells; orange circles, TNIKΔ15 cells; green circles, TNIK KM cells (mean ± s.e.m.; n = 3 independent experiments; 75 cells for condition were analysed; one-way ANOVA Kruskal-Wallis, Dunn's post hoc test; *** $p < 0.001$).

4.7 Role of TNIKex15 protein isoform in neurite development in primary cortical neurons

As our results showed a specific expression of *TNIK* exon 15 in neuronal tissues and during neuronal differentiation *in vitro*, we hypothesized that the amino acidic region encoded by this alternative exon may be important to define TNIK neuronal functions. Among the different biological process in which TNIK is involved in neurons, its role in regulating dendrite arborization has been documented and the TNIK FL over-expression was described to negatively affect neurite development in primary rat neurons [110].

We analyzed the effect of human TNIK FL in comparison to TNIKΔ15 over-expression on neurite development in DIV7 primary murine cortical neurons (Figure 4.17 A). Also in this analysis we included the already described kinase mutated TNIK construct [103]. By Sholl analysis, that counted the number of neurites crossing concentric circles drawn at 7.5 μm intervals around the neurons, we observed a decreased number of crossing neurites in TNIK FL-expressing neurons already at 15 μm distance from the cell body center compared to the mock-transfected cells (Figure 4.17 B). TNIKΔ15 and TNIK KM-transfected neurons showed a similar behavior to control cells (Figure 4.17 B). When we compared the more proximal neurites emerging from the cell body at 15 μm distance, a significant decrease in TNIK FL-transfected cells (crossing neurites mean number: 8.4) was observed compared to both control (10.2) and TNIK KM-expressing (10.7) neurons (Figure 4.17 C). The same trend, although not statistical significant, was observed versus TNIKΔ15-transfected cell (9.9) (Figure 4.17 C). No differences were observed in the cellular distribution of the transfected constructs in the primary cortical neurons analysed, as all TNIK transfected proteins localized in the cytoplasm, enriched in the perinuclear region and weaker along neurites (Figure 4.17 A), resembling the endogenous TNIK

distribution that we observed in neurons differentiated from iPSCs (Figure 4.7 C).

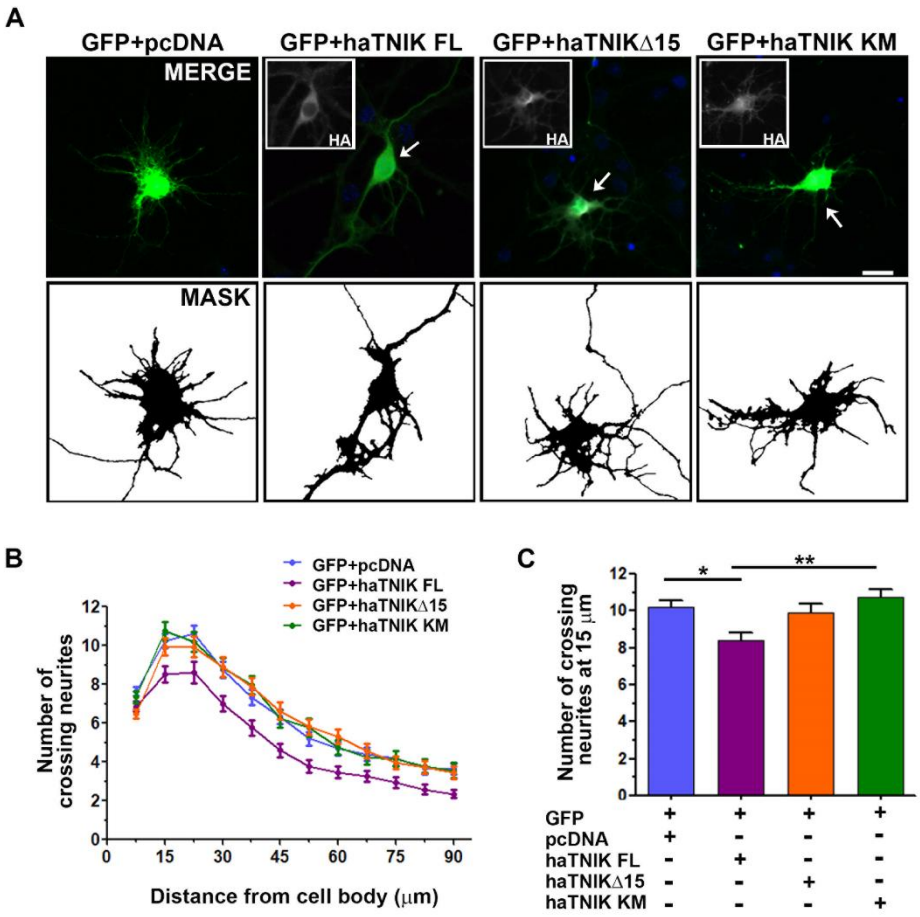

Figure 4.17 Neurite development in human TNIK-overexpressing primary murine cortical neurons. ***A)*** Representative IF images of DIV7 cortical neurons transfected with human TNIK constructs (ha-TNIK FL, ha-TNIKΔ15 and ha-TNIK KM) (grey) or empty vector. GFP was co-transfected to label cell morphology and is showed in the merged images together with the nuclear staining (DAPI, blue). Bar, 20μM. ***B)*** Sholl analysis of transfected neurons. Blue circles, mock-transfected neurons (n=72); purple circles, TNIK FL neurons (n=59); orange circles, TNIKΔ15 neurons (n=72), green circles, TNIK KM neurons (n=59) (mean ± s.e.m; n is referred to all the cells analysed for each condition from four independent experiments). ***C)*** Crossing neurites number at 15 μm from the cell body in all transfected neurons analysed (mean ± s.e.m.; n = 4 independent experiments; one-way ANOVA Kruskal-Wallis, Dunn's post hoc test; * $p < 0.05$, ** $p<0.01$).

As neurite development is tightly dependent on actin dynamics and as TNIK kinase activity is described to affect actin polymerization [103,111], we quantified F-actin levels at growth cones (Figure 4.18) and in the soma (Figure 4.19) of transfected neurons.

Our growth cone analysis showed that TNIK FL over-expression significantly reduced F-actin levels compared to control cells (Figure 4.18 A, B) and led to a significantly lower filopodia number (Figure 4.18 D), but no changes in growth cones area (Figure 4.18 C). In contrast, upon TNIKΔ15 or KM over-expression, F-actin levels, growth cones morphology and filopodia number were unchanged compared to control cells (Figure 4.18 A, B, C).

When we analysed the soma of TNIK FL-expressing neurons, F-actin levels were not altered (Figure 4.19 A, B), however, we observed a significant smaller area (Figure 4.19 A, C). TNIKΔ15 over-expression did not change soma morphology and F-actin levels, while, surprisingly, TNIK KM-expressing neurons showed a significant increase of F-actin levels (Figure 4.19 A, B) albeit the soma area was unchanged compared to control cells (Figure 4.19 A, C).

All these findings evidence that in primary murine cortical neurons TNIK FL over-expression has a different effect on neurite development and actin dynamics compared to TNIKΔ15 ones. Our data also suggest that 29-amino-acid sequence encoded by exon 15 may be necessary for TNIK kinase activity, as the TNIKΔ15 and TNIK KM-expressing neurons showed a comparable effect on both neurite development, growth cones and soma morphology and F-actin levels.

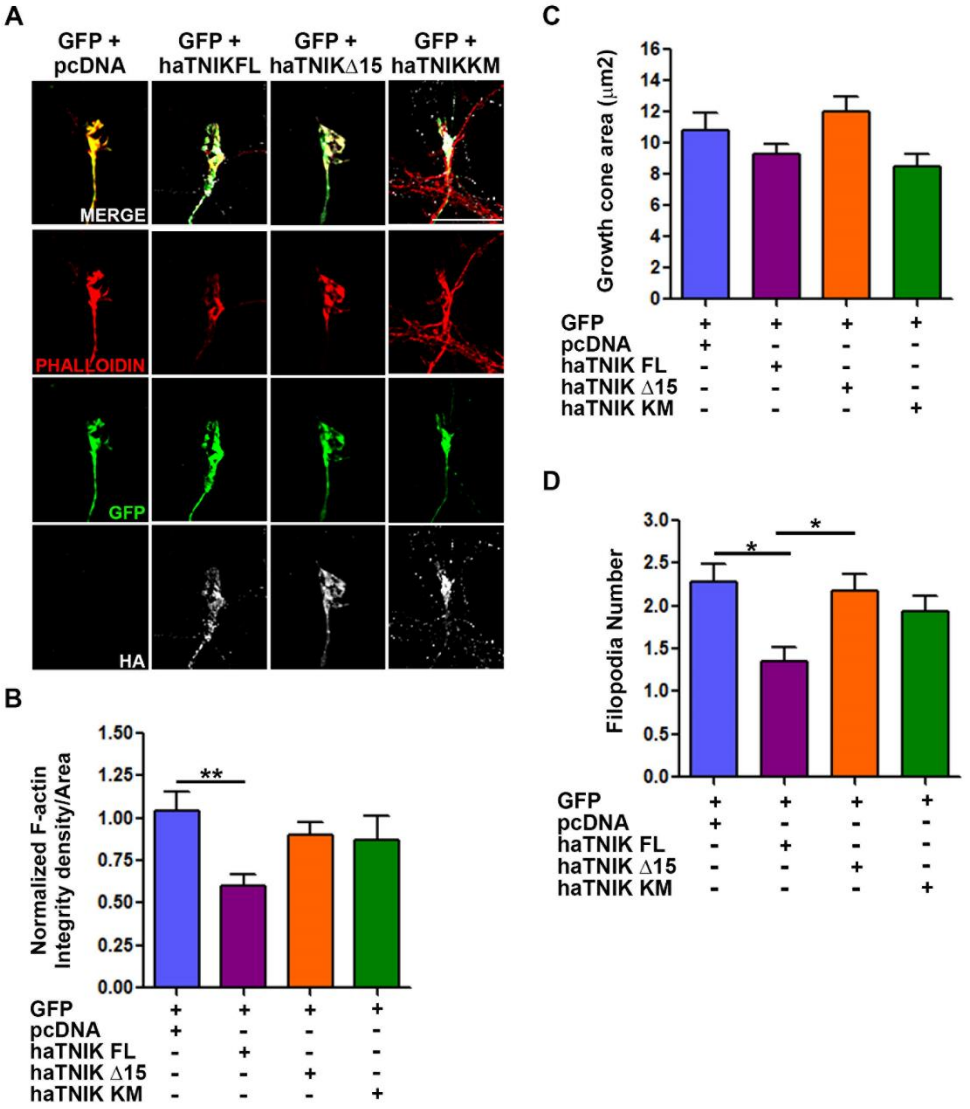

Figure 4.18 TNIK effect on growth cones morphology and F-actin levels in primary murine cortical neurons. ***A)*** Representative IF images of growth cones of murine cortical neurons (DIV7) transfected with human TNIK plasmids and GFP to label the cell morphology. Phalloidin (red) was used to stain and quantify filamentous F-actin. Ha (grey) antibody was used to visualized transfected cells. Bar 10μm. Quantification of growth cones ***B)*** F-actin levels and ***C)*** area of TNIK FL (n=45), TNIKΔ15 (n=65), TNIK KM-expressing neurons (n=39) or control cells (n=65) performed by ImageJ NIH software. ***D)*** Filopodia number for growth cone was quantified (mean ± s.e.m.; n is referred to total cells analyzed for each condition from four indipendent experiments; one-way ANOVA Kruskal-Wallis, Dunn's post hoc test; * $p < 0.05$; ** $p < 0.01$).

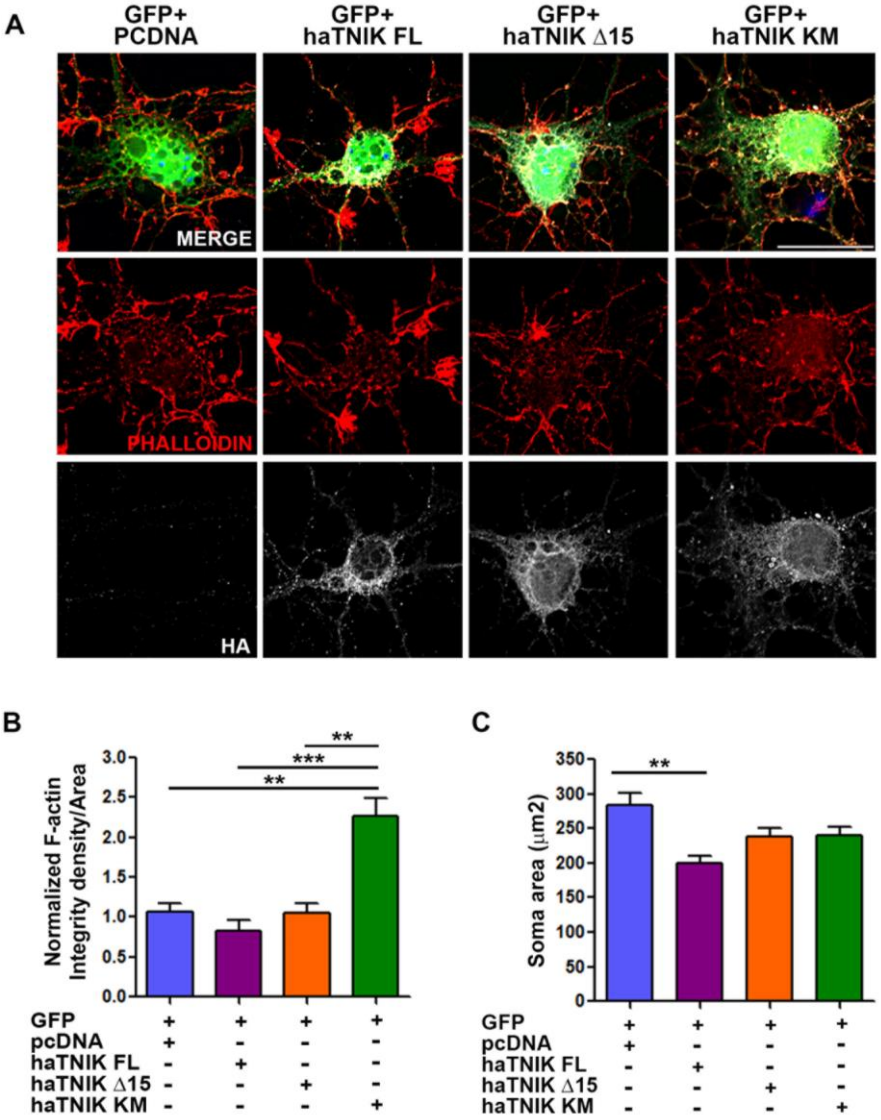

Figure 4.19 TNIK effects on soma morphology and F-actin levels in primary murine cortical neurons. ***A)*** Representative iIF images of somas of DIV7 cortical neurons transfected with human TNIK plasmids. GFP protein was used to label the cell morphology. Phalloidin (red) staining was used to quantify filamentous F-actin. Ha (grey) antibody shows the expression of transfected plasmid and nuclear staining (DAPI) is shown in merged images. Bar 20μm. Quantification of soma F-actin levels ***B)*** and area ***C)*** of cells transfected with TNIK FL (n=35), TNIKΔ15 (n=46), TNIK KM cells (n=42) or empty vector (n=46) was performed by ImageJ NIH software (mean ± s.e.m.; n is referred to total cells analyzed for each condition from four indipendent experiments; one-way ANOVA Kruskal-Wallis, Dunn's post hoc test; ** $p < 0.01$; *** $p<0.001$).

5 DISCUSSION

5.1 *TNIK* alternative splicing in human adult tissues and in neuronal differentiation models *in vitro*

The ubiquitous RBP TDP-43, the neuropathological hallmark of ALS and FTLD diseases, is involved in different steps of RNA metabolism, including the alternative splicing regulation [181]. Our group has recently demonstrated that, upon TDP-43 knock-down in neuroblastoma cells, to mimic a *loss-of-function* mechanism, *TNIK* alternative splicing is altered with an increased exon 15 inclusion and an up-regulation of the corresponding protein isoform [21]. The Ser/Thr kinase TNIK is highly expressed in the brain and plays an important role in neuronal functions, such as dendrites organization, neurogenesis and synaptic structure and functionality [108–110]. Moreover, it is a genetic risk factors for schizophrenia [124–126] and null-mutations in *TNIK* gene were identified in families with intellectual disability [131].

In this study, we characterized *TNIK* alternative splicing in human adult tissues and in neuronal differentiation models *in vitro* to define *TNIK* splicing pattern in neurons.

So far, only one study analysed *TNIK* expression in different human adult tissues showing higher *TNIK* mRNA levels in brain [103]. This study also described that *TNIK* pre-mRNA is alternatively spliced in three exons (exon 15, 17 and 22) encoding for amino-acid sequences inserted *in frame* in the TNIK intermediate region [103]. To date, a characterization of the different *TNIK* isoforms expression is still missing. We demonstrated that *TNIK* exon 15 alternative splicing is differently regulated in human adult tissues, showing

exon 15 inclusion as the only splicing event occurring in brain and spinal cord. Our results suggest a potential role of the specific *TNIKex15* isoforms in the central nervous system, supported also by literature data where the function of the full-length TNIK protein isoform is widely described in neuronal models [104,109,110]. We also observed a prevalent *TNIKex15* expression in skeletal muscle, a tissue in which TNIK function has not been reported yet. For a full characterization of *TNIK* alternative splicing, we also analysed the other two alternative splicing events (exon 17 and 22) in human adult tissues. We found that exon 17 is not regulated in a tissue-specific manner, as it was prevalently included in all tissues analysed, suggesting that the 55 amino-acid-long sequence encoded by this exon may be necessary for the main TNIK functions independently on the tissue type. Regarding exon 22, in neuronal tissues both *TNIKex22* and *TNIKex21-23* isoforms were expressed showing, however, a different splicing pattern between brain and spinal cord, as exon 22 is mostly included in brain, while it is mainly skipped in spinal cord. Indeed, we also found that *TNIKex22* isoforms were less expressed that *TNIKex21-23* ones in all the non-neuronal tissues analysed. *TNIK* exon 22 is a 24-nucleotide-long exon and, according to recent literature classifications [179,180], it is defined as a “microexon”, whose inclusion has been described to increase during neuronal maturation by RNA-Seq analysis [182]. Microexons are particularly enriched in the brain and their dysregulation has been associated to the autism spectrum [182], so that also the analysis of *TNIK* exon 22 alternative splicing would warrant further investigation in association with this disease.

All these findings support a prevalent neuronal role of TDP-43-regulated exon 15, as all the *TNIK* isoforms expressed in both brain and spinal cord always include exon 15 sequence, unlike exon 22, that is contemporary included or skipped, and exon 17, that is mainly expressed in all tissues analysed.

The neuronal relevance of *TNIK* exon 15 inclusion is further supported by our *TNIK* alternative splicing analyses during neuronal differentiation *in vitro*. In neuroblastoma SK-N-BE cells treated with RA to induce neurites outgrowth and branching, we found an increased *TNIKex15* expression together with an overall increase of total *TNIK* mRNA content. We confirmed these findings in another differentiation model *in vitro*, using human iPSCs. In this model, a clear change of *TNIK* exon 15 splicing pattern was observed, showing 5.8% of inclusion in the undifferentiated iPSCs and more than 50% of inclusion in iPSC-neurons.

The translation of splicing studies from RNA to protein level to assess if the alternatively spliced mRNAs are also translated into different proteins, thus having an impact on cell biology, is usually limited, mainly due to the absence of isoform-specific antibodies. In a previous work, for the first time, we analysed *TNIK* exon 15 splicing at protein level, using a home-made antibody generated against the 29-amino-acid region encoded by exon 15 [21]. Therefore, using this TNIK-exon15 specific antibody in immunofluorescence assay, we confirmed the specific *TNIKex15* isoforms expression also at protein levels at the late stage of neuroblastoma cell differentiation (6 days-treatment) and in iPSC-neurons. TNIKex15 protein showed a diffuse cytoplasmic localization enriched in the perinuclear region and a weaker distribution along neurites. Literature data report that the TNIK longer isoform (1360 aa), including exon 15, localizes in the cytoplasm of different cellular models [104,105,109,110] and, when over-expressed with the small GTP-binding protein Rap2A, a functional TNIK partner, it specifically localizes in the perinuclear region and regulates the actin cytoskeleton organization [111].

All these findings suggest a specific regulation of *TNIK* exon 15 alternative splicing in neurons and a neuron-specific function for TNIKex15 isoforms.

5.2 TDP-43 and NOVA-1 interplay in regulating *TNIK* exon 15 splicing

As TDP-43 inhibits *TNIK* exon 15 inclusion [21, 28] and as our results showed that exon 15 inclusion increased during neuronal differentiation *in vitro*, we assessed if TDP-43 protein levels decreased during the neuronal differentiation process. TDP-43 protein content did not change in both differentiated neuroblastoma cells and iPSC-Neurons, suggesting the possible involvement of other splicing factors in regulating *TNIK* exon15 processing.

In the nervous system, the integrated regulatory activity of ubiquitous and neuron-specific splicing factors defines tissue-specific splicing patterns [151,152] and NOVA-1 is one of the main RBPs specifically expressed in neurons [163,164], where it regulates the alternative splicing of several genes involved in synaptic architecture and activity [170]. To test our hypothesis of NOVA-1 as a *TNIK* splicing regulator, we first confirmed the neuron-specific NOVA-1 expression in our neuronal differentiation models *in vitro*, where an increased exon 15 inclusion was observed. Moreover, we demonstrated that *TNIK* exon 15 inclusion is increased upon NOVA-1 over-expression in HEK293T cells, a non-neuronal cell line where NOVA-1 is not physiologically expressed and exon 15 is prevalently skipped. Furthermore, TDP-43 protein levels were unchanged upon NOVA-1 over-expression, thereby also excluding that NOVA-1 indirectly influences *TNIK* exon 15 splicing by affecting negatively TDP-43 expression. While our results showed that NOVA-1 does not alter TDP-43 protein levels, literature data have evidenced that TDP-43 depletion is associated to a decreased *NOVA-1* and *NOVA-2* expression in mouse brain and human neuroblastoma cell models [48,63], suggesting also a TDP-43-mediated regulation of *NOVA* gene expression in neurons.

As in our neuronal differentiation models *in vitro*, *TNIK* exon 15 inclusion is associated to the contemporary presence of NOVA-1 and TDP-43 proteins, we investigate the interplay between these two RBPs in *TNIK* exon 15 splicing regulation. Literature data already described NOVA-1 interplay with other ubiquitous RBPs to regulate alternative splicing of specific genes, such as *Dopamine D2 receptor (DR2)* exon 6 inclusion, which is favoured by NOVA-1 counteracting the hnRNPM splicing inhibition [174], or the *NMDA receptor 1* exon 19, which is regulated by NOVA-1 and hnRNPA1 interplay in spinal cord and cerebral cortex [152].

Also TDP-43 was already described to regulate alternative splicing cooperating with other ubiquitous RBPs. For example, the *SMN2* exon 7 inclusion is promoted by TDP-43 together with hnRNPG and Htra2-β1, counteracting hnRNPA1-mediated *SMN2* exon 7 skipping [184]. TDP-43, together with hnRNPH, was shown to promote *Apo-II* exon 3 skipping [50] and together with hnRNPA2, hnRNPL and PTBP, to regulate human *Sortilin* exon 17b [56]. Moreover, the ubiquitously expressed RBPs hnRNPQ, hnRNPR and DAZAP1 have been recently demonstrated to modulate TDP-43 splicing activity although for few target transcripts, including also *TNIK* pre-mRNA [63]. However, studies reporting modulation of TDP-43 splicing activity by tissue-specific RBPs are missing.

For the first time, we demonstrated that the neuron-specific NOVA-1 is able to counteract TDP-43 skipping activity on *TNIK* exon 15, as in our minigene assay NOVA-1 over-expression completely inhibited TDP-43-mediated exon 15 exclusion.

TDP-43 skipping activity is described to be improved by the cooperation with several hnRNP family members [72], like hnRNPA2B1 in the regulation of *CFTR* exon 9 splicing [9,10]. We found that the ubiquitous hnRNPA2B1 was also involved in regulating *TNIK* splicing in our minigene assay, by synergistically cooperating with TDP-43 in promoting exon 15 skipping. The

combined hnRNPA2B1/TDP-43 splicing activity was fully inhibited upon NOVA-1 overexpression.

Therefore, our results show that the TDP-43-mediated *TNIK* exon 15 skipping is increased by the ubiquitous hnRNPA2B1 and completely blocked by the neuron-specific NOVA-1 RBP.

We further investigated the molecular mechanisms of such competition between TDP-43 and NOVA-1, by the hypothesis of a competitive binding on *TNIK* pre-mRNA. NOVA-1 mainly binds its target transcripts by recognizing a stem-loop YCAY-cluster motif (Y=pyrimidine), containing a minimum of three clusters in the loop region [167] and NOVA-1 binding consensus motifs were previously identified in *TNIK* intron 2, not likely involved in exon 15 splicing regulation [170]. By *in silico* analysis using the RBPmap software, we did not evidence any NOVA-1 consensus binding motif in *TNIK* exon 15 and within the upstream and downstream intronic regions used in the minigene construct (data not shown). Moreover, also by UV-CLIP assay we demonstrated that NOVA-1 does not bind such sequences in contrast to TDP-43, suggesting an indirect NOVA-1 regulation of this exon splicing.

To address this issue, we evaluated NOVA-1 binding to both TDP-43 and hnRNPA2B1 proteins by co-IP experiments. Proteomic studies already identified as main TDP-43 interactors, proteins involved in RNA metabolism, including several splicing factors such as hnRNP proteins, PTBP1, SFRS6 or SFRS7 [38,47,61], and these interactions may occur both in a RNA-dependent or independent manner [38]. We demonstrated that NOVA-1 binds TDP-43 in a RNA-dependent manner and that the TDP-43 C-terminal domain, which is mainly involved in protein-protein interaction, like for hnRNPA2B1 binding [9], is not necessary for NOVA-1 interaction. In particular, we demonstrated that TDP-43 binding to RNA is needed for its interaction with NOVA-1, as our co-IP experiments showed that the recombinant TDP-43 proteins unable to recognize RNA (TDP-43 ΔRRM1

and 4FL) both failed to bind NOVA-1, in a condition where total RNA was preserved by RNAse inhibitor treatment.

Moreover, we demonstrated NOVA-1 RNA-dependent binding also to hnRNPA2B1, suggesting that NOVA-1 might promote *TNIK* exon 15 inclusion by interacting and competing with both TDP-43 and hnRNPA2B1 RBPs.

According to our minigene and co-IP results, we propose the neuron-specific NOVA-1 RBP as a TDP-43 modifier in *TNIK* exon 15 splicing regulation. Excluding the direct NOVA-1 binding to *TNIK* intronic regions 14 and 15, we may suggest a model whereby, in a neuronal environment, the specific expression of NOVA-1 may drive the formation of new ribonucleoprotein complex(es) that, probably by sequestering the ubiquitous TDP-43 and hnRNPA2/B1 RBPs, repress their inhibitory splicing activity on *TNIK* pre-mRNA, favouring exon 15 inclusion. Alternatively, NOVA-1 by binding to TDP-43 and hnRNPA2B1 may promote a conformational change in the bound *TNIK* pre-mRNA, favouring spliceosome assembly and, as a consequence, exon 15 inclusion.

However, further studies are needed to confirm these two hypotheses, in order to define the molecular mechanisms regulating *TNIK* alternative splicing.

5.3 Role of TNIKex15 protein isoforms in neurite development and cell spreading

The *TNIK* alternative exon 15 encodes for a 29 amino-acid-long sequence in the TNIK intermediate protein region where no functional domains are annotated. The functional role of this long intermediate region is poorly investigated, although it is described to be necessary for TNIK interaction

with Traf2, NCK [103] and Nedd4-1 proteins [110]. Our study, by demonstrating a neuronal-specific *TNIK* exon 15 inclusion both at transcript and protein levels, suggests a potential neuronal relevance for TNIKex15 isoforms.

The TNIK full-length protein is necessary for dendrite organization in primary murine and rat neurons and both *TNIK* silencing or over-expression were described to affect negatively dendrite development [110]. Here, we demonstrated that the short amino-acid sequence encoded by *TNIK* exon 15 is responsible for TNIK-mediated neurite development, because we found that, in primary murine cortical neurons, TNIKΔ15 over-expression did not affect neurite outgrowth in contrast to the full-length TNIK protein that reduced neurite number since the soma emergence. Moreover, our results suggest that TNIK exon 15-encoded amino-acid sequence might influence TNIK kinase activity, as the over-expression of TNIKΔ15 and the mutant kinase TNIK KM proteins had similar effects on neurite arborisation.

Neurite development is tightly dependent on cytoskeleton dynamics [185], as developing neurites properly form synaptic connections thanks to growth cones motility which is strictly dependent on F-actin organization and dynamics [183,184]. As TNIK kinase activity regulates actin dynamics, promoting F-actin disassembly through Rap2A pathway [110,111], we also assessed if TNIK protein affects neurite development influencing actin dynamics by measuring F-actin levels and growth cones morphology. In transfected primary cortical neurons, recombinant TNIK proteins localized at growth cones, indicating that they may be actively involved in this subcellular compartment. In particular, TNIKex15 protein impaired growth cones dynamics by reducing F-actin levels and filopodia numbers, while TNIKΔ15 did not affect either growth cones morphology or F-actin levels similarly to the mutant kinase TNIK protein. A similar analysis of F-actin levels and morphology of the soma, as another cellular region representative of actin

dynamics, showed unchanged F-actin levels of TNIK FL-transfected cortical neurons, although the area were smaller compared to control cells. TNIKΔ15-transfected neurons showed normal soma F-actin and morphology, while, unexpectedly, somatic F-actin levels increased upon TNIK KM over-expression, although soma morphology was unchanged. To try to explain this result, we speculate that the increased F-actin levels observed in the soma of TNIK KM-positive cells might be the early step of a more active neurite formation that we were not able to detect in our cortical neurons cultures at DIV7. To support this hypothesis, in fact, in primary rat neurons at DIV 10, TNIK KM over-expression was shown to promote dendrite growth [110].

Our characterization of *TNIK* alternative splicing in human adult tissues showed TNIKex15 expression also in non-neuronal tissues, although at lower levels, suggesting also a non-neuronal function for TNIKex15 isoforms. In HEK293T cells, the over-expression of full-length TNIK was previously described to affect cell spreading, inducing the change to a round cell shape contrarily to the mutant kinase TNIK KM that was not able to influence cell morphology [103,111]. Our analysis of cell spreading in HEK293T cells showed that TNIKΔ15 over-expressing cells had an intermediate phenotype between TNIKex15 and TNIK KM-expressing cells, suggesting that TNIK exon 15-encoded amino-acid sequence is important also to affect cell spreading in non-neuronal cells, likely due to F-actin disassembly induced by Rap2A/TNIK signalling [111].

Taking into account all our results, we can assert that the 29-amino acidic sequence encoded by TNIK exon 15 seems to influence TNIK kinase activity that, regulating F-actin dynamics through the Rap2A pathway, is important both for neurite development in neuronal cells and for cell spreading in non-neuronal cells.

However, future studies are needed to address the specific TNIKex15 functions in neurons, such as crystallography and NMR studies to clarify the structural differences between TNIK protein including and excluding exon-15-amino-acid sequence, and the investigation of other neurobiological aspects already described for TNIK, such as post-synaptic organization and signalling or neurogenesis.

6 CONCLUSIONS

In this study, we have shown for the first time that the alternative splicing of *TNIK* exon 15 is differentially regulated in human adult tissues, highlighting the neuronal relevance of TNIKex15 isoforms. Moreover, we showed that *TNIK* exon 15 splicing pattern changes during neuronal differentiation *in vitro* and TNIKex15 protein is specifically expressed in neuronal differentiated cells. In other species, such as *Mus musculus* and *Danio rerio*, *TNIK* isoforms alternatively spliced in exon 15 are reported in genome databases, suggesting a phylogenetic conservation of this alternative splicing event. A deeper investigation of *TNIK* alternative splicing during the central nervous system development of these animal models might help to further clarify the biological mechanisms occurring during neurodevelopment, whose impairment may lead in humans to cognitive dysfunctions, like in intellectual disability and autism, or to psychiatric disorders, such as schizophrenia and bipolar disorders.

Genetic data support *TNIK* as a risk factor for schizophrenia even if apparently independently from the *TNIK* exon 15 splicing dysregulation, as SNPs identified in the *TNIK* gene map in regions (introns 2, 3 and intergenic region upstream the *TNIK* gene) not likely associated to exon 15 splicing. Nonetheless, two RNA-Seq studies investigated the alternative splicing in post-mortem schizophrenia brains and did not identify splicing alterations in *TNIK* gene in comparison to healthy tissues [185,186]. In the general population, the genetic polymorphism rs369149036 (MAF 0.05), a $(GT)_8(GC)_3$ deletion, is reported to overlap the TDP-43 consensus binding sequence $(TG)_{18}$ and may modify TDP-43 binding affinity to *TNIK* pre-mRNA. Furthermore, since one study reported NOVA-1 binding to *TNIK* intron 2

[170], it would be interesting to study if the reported risk SNPs, mapping in intron 2 and not functionally investigated yet, may affect NOVA-1 recognition of *TNIK* pre-mRNA.

Although the current genetic literature seems not to support *TNIK* alternative splicing dysregulation in association to schizophrenia, experimental data strongly suggest that *TNIK* dysfunction in neurons may play a role in schizophrenia pathogenesis. In fact, a dysregulation of dentate gyrus neurogenesis and dendrite spines organization and activity, processes in which the role of the full-length TNIK protein has been documented, may occur in schizophrenia patients [119,121], showing also an altered *TNIK* gene expression [128] and a severe loss of dendritic spines in the affected dorsolateral prefrontal cortex [190]. Moreover, TNIK interaction with DISC1 protein [104], another well-described schizophrenia genetic risk factor [123], is important for the proper AMPA receptor activity [104]. In this scenario, our study, by demonstrating that *TNIK* exon 15 inclusion is exclusively promoted in neurons and that the 29-amino-acid sequence encoded by exon 15 is responsible for TNIK-mediate neurite development, gives new insights supporting a possible role of *TNIK* alternative splicing regulation in schizophrenia pathogenesis.

From another point of view, for the first time, this study highlights a neuron-specific modulation of TDP-43 splicing activity, completely suppressed by the neuron-specific splicing factor NOVA-1, although our findings are restricted to only one TDP-43 RNA target so far.

Since 2006, when TDP-43 was first identified as a major component of the neuropathological aggregates in ALS and FTLD patients [45,46], several studies have investigated TDP-43 biological functions mainly focusing on its splicing activity [191]. It will be of great interest to extend the analysis of NOVA-1 and TDP-43 interplay in the splicing regulation of other TDP-43 RNA targets. This will help to define if, in a neuronal environment, the ubiquitous

TDP-43 RBP remains a fundamental player in splicing regulation or if it is mainly required for other neurobiological functions whose impairment may better account for the neurodegenerative processes. A similar example is represented by survival of motor neuron (SMN), a RBP whose reduced levels due to homozygous deletion of the *SMN1* gene causes spinal muscular atrophy (SMA), an infantile motor neuron disease. Although the ubiquitously expressed SMN protein is mainly involved in spliceosome formation, in motor neurons the pathogenic mechanisms that lead to SMA seem to be more associated to its specific neuronal function of axonal RNA transport [192].
In line with this hypothesis, clarifying TDP-43 functions in a neuronal environment may help understand the pathogenetic mechanisms associated to TDP-43 proteinopathy in ALS and FTLD diseases.

REFERENCES

[1] N. F. Garci, S. I. Ou, F. Wu, D. Harrich, and R. B. Gaynor, “Cloning and Characterization of a Novel Cellular Protein , TDP-43 , That Binds to Human Immunodeficiency Virus Type 1 TAR DNA Sequence Motifs,” *J. Virol.*, vol. 69, no. 6, pp. 3584–3596, 1995.

[2] Y. Zhang, T. Caulfield, Y. Xu, T. F. Gendron, J. Hubbard, C. Stetler, H. Sasaguri, E. C. Whitelaw, S. Cai, W. C. Lee, and L. Petrucelli, “The dual functions of the extreme N-terminus of TDP-43 in regulating its biological activity and inclusion formation,” *Hum. Mol. Genet.*, vol. 22, no. 15, pp. 3112–3122, 2013.

[3] L. Jiang, W. Xue, J. Hon, J. Zhang, M. Li, and S. Yu, “The N-terminal dimerization is required for TDP-43 splicing activity,” *Sci. Rep.*, vol. 7, no. February, pp. 1–12, 2017.

[4] M. Mompeán, V. Romano, X. D. Pantoja-uceda, C. Stuani, X. F. E. Baralle, X. E. Buratti, and X. D. V Laurents, “Point mutations in the N-terminal domain of transactive response DNA-binding protein 43 kDa (TDP-43) compromise its stability , dimerization , and functions,” vol. 292, pp. 11992–12006, 2017.

[5] E. Buratti and F. E. Baralle, “Characterization and Functional Implications of the RNA Binding Properties of Nuclear Factor TDP-43 , a Novel Splicing Regulator of CFTR Exon 9 *,” *J. Biol. Chem.*, vol. 276, no. 39, pp. 36337–36343, 2001.

[6] P. J. Lukavsky, D. Daujotyte, J. R. Tollervey, J. Ule, C. Stuani, E. Buratti, F. E. Baralle, F. F. Damberger, and F. H. T. Allain, “Molecular basis of UG-rich RNA recognition by the human splicing factor TDP-43,” *Nat. Struct. Mol. Biol.*, vol. 20, no. 12, pp. 1443–1449, 2013.

[7] M. J. Winton, L. M. Igaz, M. M. Wong, L. K. Kwong, J. Q. Trojanowski, and V. M. Lee, “Disturbance of Nuclear and Cytoplasmic TAR DNA-binding Protein (TDP-43) Induces Disease-like Redistribution , Sequestration , and Aggregate Formation,” *J. Biol. Chem.*, vol. 283, no. 19, pp. 13302–13309, 2008.

[8] L. Lim, Y. Wei, Y. Lu, and J. Song, “ALS-Causing Mutations Significantly Perturb the Self-Assembly and Interaction with Nucleic Acid of the Intrinsically Disordered Prion-Like Domain of TDP-43,” *PLoS Biol.*, vol. 14, no. 1, pp. 1–35, 2016.

[9] E. Buratti, A. Brindisi, M. Giombi, S. Tisminetzky, Y. M. Ayala, and F. E. Baralle, “TDP-43 Binds Heterogeneous Nuclear Ribonucleoprotein A / B through Its C-terminal Tail AN IMPORTANT REGION FOR THE INHIBITION OF CYSTIC FIBROSIS TRANSMEMBRANE,” *J. Biol. Chem.*, vol. 280, no. 45, pp. 37572–37584, 2005.

[10] A. D. Ambrogio, E. Buratti, C. Stuani, C. Guarnaccia, M. Romano, Y. M. Ayala, and F. E. Baralle, “Functional mapping of the interaction between TDP-43 and hnRNP A2 in vivo,” *Nucleic Acids Res.*, vol. 37, no. 12, pp. 4116–4126, 2009.

[11] R. A. Fuentealba, M. Udan, S. Bell, I. Wegorzewska, J. Shao, M. I. Diamond, C. C. Weihl, and R. H. Baloh, “Interaction with polyglutamine aggregates reveals a Q/N-rich domain in TDP-43,” *J. Biol. Chem.*, vol. 285, no. 34, pp. 26304–26314, 2010.

[12] M. Budini, E. Buratti, C. Stuani, C. Guarnaccia, V. Romano, L. De Conti, and F. E. Baralle, “Cellular Model of TAR DNA-binding Protein 43 (TDP-43) Aggregation Based on Its C-terminal Gln / Asn-rich Region,” *J. Biol. Chem.*, vol. 287, no. 10, pp. 7512–7525, 2012.

[13] M. Mompeán, E. Buratti, C. Guarnaccia, R. M. M. Brito, A. Chakrabartty, F. E. Baralle, and D. V. Laurents, “Structural characterization of the minimal segment of TDP-43 competent for aggregation,” *Arch. Biochem. Biophys.*, vol. 545, pp. 53–62, 2014.

[14] A. E. Conicella, G. H. Zerze, J. Mittal, and N. L. Fawzi, “ALS Mutations Disrupt Phase Separation Mediated by α-Helical Structure in the TDP-43 Low-Complexity C-Terminal Domain,” *Structure*, vol. 24, no. 9, pp. 1537–1549, 2016.

[15] E. L. Guenther, Q. Cao, H. Trinh, J. Lu, M. R. Sawaya, D. Cascio, D. R. Boyer, J. A. Rodriguez, M. P. Hughes, and D. S. Eisenberg, “Atomic structures of TDP-43 LCD segments and insights into reversible or pathogenic aggregation,” *Nat. Struct. Mol. Biol.*, vol. 25, no. 6, pp. 463–471, 2018.

[16] M. M. Abhyankar, C. Urekar, and P. P. Reddi, “A Novel CpG-free Vertebrate Insulator Silences the Testis-specific SP-10 Gene in Somatic Tissues,” *J. Biol. Chem.*, vol. 282, no. 50, pp. 36143–36154, 2007.

[17] B. M. Schwenk, H. Hartmann, A. Serdaroglu, M. H. Schludi, F. Meissner, D. Orozco, A. Colombo, S. Tahirovic, M. Michaelsen, F. Schreiber, S. Haupt, M. Peitz, O. Brüstle, C. Küpper, M. Otto, A. C. Ludolph, T. Arzberger, and P. Kuhn, “TDP- 43 loss of function inhibits endosomal trafficking and alters trophic signaling in neurons,” *EMBO J.*, vol. 35, no. 21, pp. 2350–2370, 2016.

[18] J. R. Thorpe and N. J. Cairns, “Fine structural analysis of the neuronal inclusions of frontotemporal lobar degeneration with TDP-43 proteinopathy,” *J. Neural Transm.*, vol. 115, no. 12, pp. 1661–1671, 2008.

[19] I. Casafont, R. Bengoechea, O. Tapia, M. T. Berciano, and M. Lafarga, “TDP-43 localizes in mRNA transcription and processing sites in mammalian neurons,” *J. Struct. Biol.*, vol. 167, no. 3, pp. 235–241, 2009.

[20] Y. Kawahara and A. Mieda-sato, “TDP-43 promotes microRNA biogenesis as a component of the Drosha and Dicer complexes,” *Proc. Natl. Acad. Sci. U. S. A.*, vol. 109, no. 9, pp. 3347–3352, 2012.

[21] C. Colombrita, E. Onesto, E. Buratti, P. de la Grange, V. Gumina, F. E. Baralle, V. Silani, and A. Ratti, “From transcriptomic to protein level changes in TDP-43 and FUS loss-of-function cell models,” *Biochim. Biophys. Acta - Gene Regul. Mech.*, vol. 1849, no. 12, pp. 1398–1410, 2015.

[22] E. Buratti, L. De Conti, C. Stuani, M. Romano, M. Baralle, and F. Baralle, “Nuclear factor TDP-43 can affect selected microRNA levels,” *FEBS J.*, vol. 1, pp. 2268–2281, 2010.

[23] Y.-Y. Park, S. B. Kim, H. D. Han, B.-H. Sohn, J.-H. Kim, J. Liang, Y. Lu, G. B. Mills, A. K. Sood, and J.-S. Lee, “TARDBP regulates glycolysis in hepatocellular carcinoma by regulating PFKP through miR-520,” *Hepatology*, vol. 58, no. 1, pp. 182–191, 2013.

[24] Z. Zhang, S. Almeida, Y. Lu, A. L. Nishimura, L. Peng, D. Sun, B. Wu, A. M. Karydas, M. C. Tartaglia, J. C. Fong, B. L. Miller, R. V Farese, M. J. Moore, C. E. Shaw, and F. Gao, "Downregulation of MicroRNA-9 in iPSC-Derived Neurons of FTD / ALS Patients with TDP-43 Mutations," *PLoS One*, vol. 8, no. 10, p. e76055, 2013.

[25] Z. Fan, X. Chen, and R. Chen, "Genomics Transcriptome-wide analysis of TDP-43 binding small RNAs identi fi es miR-NID1 (miR-8485), a novel miRNA that represses NRXN1 expression," *Genomics*, vol. 103, no. 1, pp. 76–82, 2014.

[26] I. N. King, V. Yartseva, D. Salas, A. Kumar, A. Heidersbach, D. M. Ando, N. R. Stallings, J. L. Elliott, D. Srivastava, and K. N. Ivey, "The RNA-binding Protein TDP-43 Selectively Disrupts MicroRNA-1 / 206 Incorporation into the RNA-induced Silencing Complex," *J. Biol. Chem.*, vol. 289, no. 20, pp. 14263–14271, 2014.

[27] X. Liu, D. Li, W. Zhang, M. Guo, and Q. Zhan, "Long non-coding RNA gadd7interacts with TDP-43 and regulates Cdk6 mRNA decay," *EMBO J.*, vol. 31, no. 23, pp. 4415–4427, 2012.

[28] J. R. Tollervey, T. Curk, B. Rogelj, M. Briese, M. Cereda, M. Kayikci, J. König, T. Hortobágyi, A. L. Nishimura, V. Župunski, R. Patani, S. Chandran, G. Rot, B. Zupan, C. E. Shaw, and J. Ule, "Characterizing the RNA targets and position- dependent splicing regulation by TDP-43," *Nat. Publ. Gr.*, vol. 14, no. 4, pp. 452–458, 2011.

[29] F. Guo, F. Jiao, Z. Song, S. Li, B. Liu, H. Yang, Q. Zhou, and Z. Li, "Biochemical and Biophysical Research Communications Regulation of MALAT1 expression by TDP43 controls the migration and invasion of non-small cell lung cancer cells in vitro," *Biochem. Biophys. Res. Commun.*, vol. 465, no. 2, pp. 293–298, 2015.

[30] P. Li, X. Ruan, L. Yang, K. Kiesewetter, Y. Zhao, H. Luo, Y. Chen, and M. Gucek, "Article A Liver-Enriched Long Non-Coding RNA , lncLSTR ," *Cell Metab.*, vol. 21, no. 3, pp. 455–467, 2015.

[31] C. Colombrita, E. Onesto, F. Megiorni, A. Pizzuti, F. E. Baralle, E. Buratti, V. Silani, and A. Ratti, "TDP-43 and FUS RNA-binding Proteins Bind Distinct Sets of Cytoplasmic Messenger RNAs and Differently Regulate Their Post-transcriptional Fate in Motoneuron-like Cells," *J. Biol. Chem.*, vol. 287, no. 19, pp. 15635–15647, 2012.

[32] L. Costessi, F. Porro, and A. Iaconcig, “TDP-43 regulates b -adducin (Add2) transcript stability,” *RNA Biol.*, vol. 11, no. 10, pp. 1280–1290, 2014.

[33] S. Lee, T. A. Lee, E. Lee, S. Kang, A. Park, S. W. Kim, H. J. Park, J. Yoon, S. Ha, T. Park, J. Lee, J. H. Cheon, and B. Park, “Identification of a subnuclear body involved in sequence-specific cytokine RNA processing,” *Nat. Commun.*, vol. 6, no. May 2014, pp. 1–14, 2015.

[34] Swanger Sharon A and Bassel Gary j, “Making and breaking synapses through local mRNA regulation,” *Curr. Opin. Genet Dev*, vol. 21, no. 4, pp. 414–421, 2011.

[35] I. F. Wang, L. S. Wu, H. Y. Chang, and C. K. J. Shen, “TDP-43, the signature protein of FTLD-U, is a neuronal activity-responsive factor,” *J. Neurochem.*, vol. 105, no. 3, pp. 797–806, 2008.

[36] C. Fallini, G. J. Bassell, and W. Rossoll, “The ALS disease protein TDP-43 is actively transported in motor neuron axons and regulates axon outgrowth,” *Hum. Mol. Genet.*, vol. 21, no. 16, pp. 3703–3718, 2012.

[37] N. H. Alami, R. B. Smith, M. A. Carrasco, L. A. Williams, S. Christina, S. S. W. Han, E. Kiskinis, B. Winborn, B. D. Freibaum, A. Kanagaraj, A. J. Clare, N. M. Badders, B. Bilican, S. Chandran, C. E. Shaw, K. C. Eggan, T. Maniatis, and J. P. Taylor, “Axonal transport of TDP-43 mRNA granules in neurons is impaired by ALS-causing mutations,” *Neuron*, vol. 81, no. 3, pp. 536–543, 2014.

[38] B. D. Freibaum, R. K. Chitta, A. A. High, and J. P. Taylor, “Global Analysis of TDP-43 Interacting Proteins Reveals Strong Association with RNA Splicing and Translation Machinery research articles,” *J. Proteome Res.*, vol. 9, pp. 1104–1120, 2010.

[39] V. K. Godena, G. Romano, M. Romano, C. Appocher, R. Klima, F. E. Baralle, and F. Feiguin, “TDP-43 Regulates Drosophila Neuromuscular Junctions Growth by Modulating Futsch / MAP1B Levels and Synaptic Microtubules Organization,” *PLoS Biol.*, vol. 6, no. 3, p. e17808, 2011.

[40] P. Majumder, Y. C. Jayarama, and K. Bose, “TDP-43 regulates the mammalian spinogenesis through translational repression of Rac1,” *Acta Neuropathol.*, vol. 124, pp. 231–245, 2012.

[41] A. N. Coyne, B. B. Siddegowda, P. S. Estes, J. Johannesmeyer, T. Kovalik, S. G. Daniel, A. Pearson, R. Bowser, and X. D. C. Zarnescu, “Futsch / MAP1B mRNA Is a Translational Target of TDP-43 and Is Neuroprotective in a Drosophila Model of Amyotrophic Lateral Sclerosis,” *J. Neurosci.*, vol. 34, no. 48, pp. 15962–15974, 2014.

[42] M. Romano, F. Feiguin, and E. Buratti, “TBPH / TDP-43 modulates translation of Drosophila futsch mRNA through an UG-rich sequence within its 5′ UTR,” *Brain Res.*, vol. 1647, pp. 50–56, 2016.

[43] C. Colombrita, E. Zennaro, C. Fallini, M. Weber, A. Sommacal, E. Buratti, V. Silani, and A. Ratti, “TDP-43 is recruited to stress granules in conditions of oxidative insult,” *J. Neurochem.*, vol. 111, pp. 1051–1061, 2009.

[44] E. Buratti, T. Dork, E. Zuccato, F. Pagani, M. Romano, and F. E. Baralle, “Nuclear factor TDP-43 and SR proteins promote in vitro and in vivo CFTR exon 9 skipping,” *EMBO J.*, vol. 20, no. 7, pp. 1774–1784, 2001.

[45] T. Arai, M. Hasegawa, H. Akiyama, K. Ikeda, Y. Hashizume, and T. Oda, “TDP-43 is a component of ubiquitin-positive tau-negative inclusions in frontotemporal lobar degeneration and amyotrophic lateral sclerosis,” *Biochem. Biophys. Res. Commun.*, vol. 351, pp. 602–611, 2006.

[46] M. Neumann, D. M. Sampathu, L. K. Kwong, A. C. Truax, M. C. Micsenyi, T. T. Chou, J. Bruce, T. Schuck, M. Grossman, C. M. Clark, L. F. McCluskey, B. L. Miller, E. Masliah, I. R. Mackenzie, H. Feldman, W. Feiden, H. A. Kretzschmar, J. Q. Trojanowski, and V. M. Y. Lee, “Ubiquitinated TDP-43 in frontotemporal lobar degeneration and amyotrophic lateral sclerosis,” *Science (80-.).*, vol. 314, no. 5796, pp. 130–133, 2006.

[47] C. F. Sephton, C. Cenik, A. Kucukural, E. B. Dammer, B. Cenik, Y. Han, C. M. Dewey, F. P. Roth, J. Herz, J. Peng, M. J. Moore, and G. Yu, “Identification of Neuronal RNA Targets of TDP-43-containing Ribonucleoprotein Complexes,” *J. Biol. Chem.*, vol. 286, no. 2, pp. 1204–1215, 2011.

[48] M. Polymenidou, C. Lagier-tourenne, K. R. Hutt, S. C. Huelga, J. Moran, T. Y. Liang, S. Ling, E. Sun, E. Wancewicz, C. Mazur, H. Kordasiewicz, Y. Sedaghat, J. P. Donohue, L. Shiue, C. F. Bennett, G. W. Yeo, and D. W. Cleveland, "Long pre-mRNA depletion and RNA missplicing contribute to neuronal vulnerability from loss of TDP-43," *Nat. nauroscience*, vol. 14, no. 4, pp. 459–468, 2011.

[49] S. Xiao, T. Sanelli, S. Dib, D. Sheps, J. Findlater, J. Bilbao, J. Keith, L. Zinman, E. Rogaeva, and J. Robertson, "Molecular and Cellular Neuroscience RNA targets of TDP-43 identified by UV-CLIP are deregulated in ALS," *Mol. Cell. Neurosci.*, vol. 47, pp. 167–180, 2011.

[50] P. A. Mercado, Y. M. Ayala, M. Romano, E. Buratti, and F. E. Baralle, "Depletion of TDP 43 overrides the need for exonic and intronic splicing enhancers in the human apoA-II gene," *Nucleic Acids Res.*, vol. 33, no. 18, pp. 6000–6010, 2005.

[51] F. C. Fiesel, S. S. Weber, J. Supper, A. Zell, and P. J. Kahle, "TDP-43 regulates global translational yield by splicing of exon junction complex component SKAR," *Nucleic Acids Res.*, vol. 40, no. 6, pp. 2668–2682, 2012.

[52] A. Shiga, T. Ishihara, A. Miyashita, M. Kuwabara, and T. Kato, "Alteration of POLDIP3 Splicing Associated with Loss of Function of TDP-43 in Tissues Affected with ALS," *PLoS One*, vol. 7, no. 8, p. e43120, 2012.

[53] M. Passoni, L. De Conti, M. Baralle, and E. Buratti, "UG Repeats / TDP-43 Interactions near 5 ′ Splice Sites Exert Unpredictable Effects on Splicing Modulation," *J. Mol. Biol.*, vol. 415, no. 1, pp. 46–60, 2012.

[54] L. De Conti, M. V Akinyi, R. Mendoza-maldonado, M. Romano, M. Baralle, and E. Buratti, "TDP-43 affects splicing profiles and isoform production of genes involved in the apoptotic and mitotic cellular pathways," *Nucleic Acids Res.*, vol. 43, no. 18, pp. 8990–9005, 2015.

[55] M. Prudencio, K. R. Jansen-west, W. C. Lee, T. F. Gendron, Y. Zhang, and Y. Xu, "Misregulation of human sortilin splicing leads to the generation of a nonfunctional progranulin receptor," *Pnas*, vol. 109, no. 52, pp. 21510–21515, 2012.

[56] F. Mohagheghi, M. Prudencio, C. Stuani, C. Cook, K. Jansen-west, D. W. Dickson, L. Petrucelli, and E. Buratti, “TDP-43 functions within a network of hnRNP proteins to inhibit the production of a truncated human SORT1 receptor,” *Hum. Mol. Genet.*, vol. 25, no. 3, pp. 534–545, 2016.

[57] Y. M. Ayala, L. De Conti, A. Dhir, M. Romano, A. D. Ambrogio, J. Tollervey, J. Ule, M. Baralle, and F. E. Baralle, “TDP-43 regulates its mRNA levels through a negative feedback loop,” *EMBO J.*, vol. 30, no. 2, pp. 277–288, 2011.

[58] S. Eréndira Avendaño-Vázquez, A. Dhir, S. Bembich, E. Buratti, N. Proudfoot, and F. E. Baralle, “Autoregulation of TDP-43 mRNA levels involves interplay between transcription, splicing, and alternative polyA site selection,” *Genes Dev.*, vol. 26, no. 15, pp. 1679–1684, 2012.

[59] S. Bembich, J. S. Herzog, L. De Conti, C. Stuani, S. E. Avendaño-Vázquez, E. Buratti, M. Baralle, and F. E. Baralle, “Predominance of spliceosomal complex formation over polyadenylation site selection in TDP-43 autoregulation,” *Nucleic Acids Res.*, vol. 42, no. 5, pp. 3362–3371, 2014.

[60] J. Ule, G. Stefani, A. Mele, M. Ruggiu, X. Wang, B. Taneri, T. Gaasterland, B. J. Blencowe, and R. B. Darnell, “An RNA map predicting Nova-dependent splicing regulation,” *Nature*, vol. 444, no. 7119, pp. 580–586, 2006.

[61] S. Ling, C. P. Albuquerque, J. Seok, C. Lagier-tourenne, and S. Tokunaga, “ALS-associated mutations in TDP-43 increase its stability and promote TDP-43 complexes with FUS / TLS,” *Pnas*, vol. 107, no. 30, pp. 13318–13323, 2010.

[62] A. M. Blokhuis, M. Koppers, E. J. N. Groen, D. M. A. van den Heuvel, S. Dini Modigliani, J. J. Anink, K. Fumoto, F. van Diggelen, A. Snelting, P. Sodaar, B. M. Verheijen, J. A. A. Demmers, J. H. Veldink, E. Aronica, I. Bozzoni, J. den Hertog, L. H. van den Berg, and R. J. Pasterkamp, “Comparative interactomics analysis of different ALS-associated proteins identifies converging molecular pathways,” *Acta Neuropathol.*, vol. 132, no. 2, pp. 175–196, 2016.

[63] C. Appocher, F. Mohagheghi, S. Cappelli, C. Stuani, M. Romano, F. Feiguin, and E. Buratti, “Major hnRNP proteins act as general TDP-43 functional modifiers both in Drosophila and human neuronal cells,” *Nucleic Acids Res.*, vol. 45, no. 13, pp. 8026–8045, 2017.

[64] C. Chang, T. Wu, C. Wu, M. Chiang, E. K. Toh, Y. Hsu, K. Lin, Y. Liao, T. Huang, and J. J. Huang, “Biochemical and Biophysical Research Communications The N-terminus of TDP-43 promotes its oligomerization and enhances DNA binding affinity,” *Biochem. Biophys. Res. Commun.*, vol. 425, no. 2, pp. 219–224, 2012.

[65] S. Ling, M. Polymenidou, and D. W. Cleveland, “Review Converging Mechanisms in ALS and FTD : Disrupted RNA and Protein Homeostasis,” *Neuron*, vol. 79, no. 3, pp. 416–438, 2013.

[66] M. Zufiria, F. Gil-Bea, R. Fernandez-Torron, J. J. Poza, J. L. Munoz-balnco, R. Rojas-garcı, and J. Riancho, “Progress in Neurobiology Review article ALS : A bucket of genes , environment , metabolism and unknown ingredients,” *Prog. Neurobiol.*, vol. 142, pp. 104–129, 2016.

[67] E. B. Lee, V. M. Y. Lee, and J. Q. Trojanowski, “Gains or losses : molecular mechanisms of TDP43 - mediated neurodegeneration,” *Nat. Rev. Neurosci.*, vol. 13, no. January 2012, pp. 38–50, 2011.

[68] Y. T. Wang, P. H. Kuo, C. H. Chiang, J. R. Liang, Y. R. Chen, S. Wang, J. C. K. Shen, and H. S. Yuan, “The truncated C-terminal RNA recognition motif of TDP-43 protein plays a key role in forming proteinaceous aggregates,” *J. Biol. Chem.*, vol. 288, no. 13, pp. 9049–9057, 2013.

[69] V. Romano, Z. Quadri, F. E. Baralle, and E. Buratti, “The structural integrity of TDP-43 N-terminus is required for efficient aggregate entrapment and consequent loss of protein function,” *Prion*, vol. 9, no. 1, pp. 1–9, 2015.

[70] Y. R. Li, O. D. King, J. Shorter, and A. D. Gitler, “Stress granules as crucibles of ALS pathogenesis,” *J. Cell Biol.*, vol. 201, no. 3, pp. 361–372, 2013.

[71] Y. Sun and A. Chakrabartty, “Phase to Phase with TDP-43,” *Biochemistry*, vol. 56, no. 6, pp. 809–823, 2018.

[72] E. Buratti and F. E. Baralle, “TDP-43 : gumming up neurons through protein – protein and protein – RNA interactions,” *Trends Biochem. Sci.*, vol. 37, no. 6, pp. 237–247, 2012.

[73] D. Dormann and C. Haass, “TDP-43 and FUS : a nuclear affair,” *Trends Neurosci.*, vol. 34, no. 7, pp. 339–348, 2011.

[74] L. Cragnaz, R. Klima, N. Skoko, M. Budini, F. Feiguin, and F. E. Baralle, “Aggregate formation prevents dTDP-43 neurotoxicity in the Drosophila melanogaster eye,” *Neurobiol. Dis.*, vol. 71, pp. 74–80, 2014.

[75] M. Collins, D. Riascos, T. Kovalik, J. An, K. Krupa, B. J. Traynor, and R. Bowser, “The RNA-binding motif 45 (RBM45) protein accumulates in inclusion bodies in amyotrophic lateral sclerosis (ALS) and frontotemporal lobar degeneration with TDP-43 inclusions (FTLD-TDP) patients,” *Acta Neuropathol.*, vol. 124, no. 5, pp. 717–732, 2012.

[76] E. B. Dammer, C. Fallini, Y. M. Gozal, D. M. Duong, W. Rossoll, P. Xu, J. J. Lah, A. I. Levey, J. Peng, G. J. Bassell, and N. T. Seyfried, “Coaggregation of RNA-Binding Proteins in a Model of TDP-43 Proteinopathy with Selective RGG Motif Methylation and a Role for RRM1 Ubiquitination,” *PLoS One*, vol. 7, no. 6, p. e38658, 2012.

[77] D. Tsuboi, K. Kuroda, M. Tanaka, T. Namba, Y. Iizuka, S. Taya, T. Shinoda, T. Hikita, S. Muraoka, M. Iizuka, A. Nimura, A. Mizoguchi, N. Shiina, M. Sokabe, H. Okano, K. Mikoshiba, and K. Kaibuchi, “Disrupted-in-schizophrenia 1 regulates transport of ITPR1 mRNA for synaptic plasticity,” *Nat. Neurosci.*, vol. 18, no. 5, pp. 698–707, 2015.

[78] R. Endo, N. Takashima, Y. Nekooki-machida, Y. Komi, K. K. Hui, M. Takao, H. Akatsu, S. Murayama, A. Sawa, and M. Tanaka, “Archival Report TAR DNA-Binding Protein 43 and Disrupted in Schizophrenia 1 Coaggregation Disrupts Dendritic Local Translation and Mental Function in Frontotemporal Lobar Degeneration,” *Biol. Psychiatry*, vol. 43, pp. 1–13, 2018.

[79] L. I. Grad, S. M. Fernando, and N. R. Cashman, “From molecule to molecule and cell to cell : Prion-like mechanisms in amyotrophic lateral sclerosis,” *Neurobiol. Dis.*, vol. 77, pp. 257–265, 2015.

[80] P.-F. Pradat, E. Kabashi, and C. Desnuelle, “Deciphering spreading mechanisms in amyotrophic lateral sclerosis,” *Curr. Opin. Neurol.*, vol. 28, no. 5, pp. 455–461, 2015.

[81] M. Neumann, L. K. Kwong, E. B. Lee, E. Kremmer, Y. Xu, M. Forman, D. Troost, H. A. Kretzschmar, Q. John, and V. M. Lee, "Phosphorylation of S409/410 of TDP-43 is a consistent feature in all sporadic and familial forms of TDP-43 proteinopathies," *Acta Neuropathol.*, vol. 117, no. 2, pp. 137–149, 2009.

[82] L. M. Igaz, L. K. Kwong, Y. Xu, A. C. Truax, K. Uryu, M. Neumann, C. M. Clark, L. B. Elman, B. L. Miller, M. Grossman, L. F. McCluskey, J. Q. Trojanowski, and V. M. Y. Lee, "Enrichment of C-terminal fragments in TAR DNA-binding protein-43 cytoplasmic inclusions in brain but not in spinal cord of frontotemporal lobar degeneration and amyotrophic lateral sclerosis," *Am. J. Pathol.*, vol. 173, no. 1, pp. 182–194, 2008.

[83] T. J. Cohen, A. W. Hwang, C. R. Restrepo, C. X. Yuan, J. Q. Trojanowski, and V. M. Y. Lee, "An acetylation switch controls TDP-43 function and aggregation propensity," *Nat. Commun.*, vol. 6, pp. 1–13, 2015.

[84] M. A. Gitcho, R. H. Baloh, S. Chakraverty, K. Mayo, C. L. W. Iii, E. H. Bigio, R. Caselli, M. Baker, M. T. Al-Iozi, J. C. Morris, A. Pestronk, R. Rademakers, and A. M. Goate, "TDP-43 A315T Mutation in Familial Motor Neuron Disease," *Ann Neurol*, vol. 3, no. 4, pp. 535–538, 2008.

[85] E. Kabashi, P. N. Valdmanis, P. Dion, D. Spiegelman, B. J. Mcconkey, C. Vande Velde, J. Bouchard, L. Lacomblez, K. Pochigaeva, F. Salachas, P. Pradat, W. Camu, V. Meininger, N. Dupre, and G. A. Rouleau, "TARDBP mutations in individuals with sporadic and familial amyotrophic lateral sclerosis," *Nat. Genet.*, vol. 40, no. 5, pp. 572–574, 2008.

[86] J. Sreedharan, I. P. Blair, V. B. Tripathi, X. Hu, C. Vance, B. Rogelj, S. Ackerley, J. C. Durnall, K. L. Williams, E. Buratti, F. Baralle, J. De Belleroche, J. D. Mitchell, P. N. Leigh, A. Al-Chalabi, C. C. Miller, G. Nicholson, and C. E. Shaw, "TDP-43 mutations in familial and sporadic amyotrophic lateral sclerosis," *Science (80-.).*, vol. 319, no. 5870, pp. 1668–1672, 2008.

[87] S. Lattante, G. A. Rouleau, and E. Kabashi, "TARDBP and FUS Mutations Associated with Amyotrophic Lateral Sclerosis : Summary and Update," *Hum. Mutat.*, vol. 34, no. 6, pp. 812–826, 2013.

[88] E. Buratti, "Functional Significance of TDP-43 Mutations in Disease," *Adv. Genet.*, vol. 91, pp. 1–53, 2015.

[89] H. R. Li, T. C. Chen, C. L. Hsiao, L. Shi, C. Y. Chou, and J. rong Huang, “The physical forces mediating self-association and phase-separation in the C-terminal domain of TDP-43,” *Biochim. Biophys. Acta - Proteins Proteomics*, vol. 1866, no. 2, pp. 214–223, 2018.

[90] E. S. Arnold, S.-C. Ling, S. C. Huelga, C. Lagier-Tourenne, M. Polymenidou, D. Ditsworth, H. B. Kordasiewicz, M. McAlonis-Downes, O. Platoshyn, P. A. Parone, S. Da Cruz, K. M. Clutario, D. Swing, L. Tessarollo, M. Marsala, C. E. Shaw, G. W. Yeo, and D. W. Cleveland, “ALS-linked TDP-43 mutations produce aberrant RNA splicing and adult-onset motor neuron disease without aggregation or loss of nuclear TDP-43,” *Proc. Natl. Acad. Sci.*, vol. 110, no. 8, pp. E736–E745, 2013.

[91] M. Budini, V. Romano, S. E. Avendaño-Vázquez, S. Bembich, E. Buratti, and F. E. Baralle, “Role of selected mutations in the Q/N rich region of TDP-43 in EGFP-12xQ/N-induced aggregate formation,” *Brain Res.*, vol. 1462, pp. 139–150, 2012.

[92] C. Amador-Ortiz, W.-L. Lin, Z. Ahmed, D. Personett, P. Davies, R. Duara, G.-R. N. R, H. M. L, and D. W. Dickson, “TDP-43 immunoreactivity in hippocampal sclerosis and Alzheimer’s disease,” *Ann Neurol*, vol. 61, no. 5, pp. 435–445, 2007.

[93] M. Hasegawa, T. Arai, H. Akiyama, T. Nonaka, H. Mori, T. Hashimoto, M. Yamazaki, and K. Oyanagi, “TDP-43 is deposited in the Guam parkinsonism-dementia complex brains,” *Brain*, vol. 130, no. 5, pp. 1386–1394, 2007.

[94] H. Nakashima-Yasuda, K. Uryu, J. Robinson, S. X. Xie, H. Hurtig, J. E. Duda, S. E. Arnold, A. Siderowf, M. Grossman, J. B. Leverenz, R. Woltjer, O. L. Lopez, R. Hamilton, D. W. Tsuang, D. Galasko, E. Masliah, J. Kaye, C. M. Clark, T. J. Montine, V. M. Y. Lee, and J. Q. Trojanowski, “Co-morbidity of TDP-43 proteinopathy in Lewy body related diseases,” *Acta Neuropathol.*, vol. 114, no. 3, pp. 221–229, 2007.

[95] A. Probst, K. I. Taylor, and M. Tolnay, “Hippocampal sclerosis dementia: A reappraisal,” *Acta Neuropathol.*, vol. 114, no. 4, pp. 335–345, 2007.

[96] M. J. Farrer, M. M. Hulihan, J. M. Kachergus, J. Dächsel, A. Jon, L. L. Grantier, S. Calne, D. B. Calne, B. Lechevalier, F. Chapon, Y. Tsuboi, T. Yamada, L. Gutmann, B. Elibol, K. P. Bhatia, C. W. Wider, C. Vilariño-güell, O. A. Ross, A. Laura, M. Castanedes-casey, D. W. Dickson, and Z. K. Wszolek, "DCTN1 mutations in Perry syndrome," *Nat. Genet.*, vol. 41, no. 2, pp. 163–165, 2009.

[97] B. Ziso, T. L. Williams, R. J. L. Walters, S. R. Jaiser, J. Attems, U. C. Wieshmann, A. J. Larner, and A. Jacob, "Facial onset sensory and motor neuronopathy: Further evidence for a TDP-43 proteinopathy," *Case Rep. Neurol.*, vol. 7, no. 1, pp. 95–100, 2015.

[98] A. Dardis, S. Zampieri, S. Canterini, K. L. Newell, C. Stuani, J. R. Murrell, B. Ghetti, M. T. Fiorenza, B. Bembi, and E. Buratti, "Altered localization and functionality of TAR DNA binding protein 43 (TDP-43) in niemann-pick disease type C," *Acta Neuropathol. Commun.*, vol. 4, no. 1, pp. 1–13, 2016.

[99] R. Juntas Morales, N. Pageot, G. Taieb, and W. Camu, "Adult-onset spinal muscular atrophy: An update," *Rev. Neurol. (Paris).*, vol. 173, no. 5, pp. 308–319, 2017.

[100] M. Salajegheh, J. L. Pinkus, J. P. Taylor, A. Amato, R. Nazareno, R. H. Baloh, and A. Steven, "Sarcoplasmic Redistribution of Nuclear TDP-43 in Inclusion Body Myositis," *Muscle Nerve*, vol. 40, no. 1, pp. 19–31, 2009.

[101] S. Homma, M. Lou Beermann, B. Yu, F. M. Boyce, and J. B. Miller, "Nuclear bodies reorganize during myogenesis in vitro and are differentially disrupted by expression of FSHD-associated DUX4," *Skelet. Muscle*, vol. 6, no. 1, pp. 1–16, 2016.

[102] A. C. Wilson, B. N. Dugger, D. W. Dickson, and D. Wang, "TDP-43 in aging and Alzheimer ' s disease – a review," *Int J Clin Exp Pathol*, vol. 4, no. 2, pp. 147–155, 2011.

[103] C. A. Fu, M. Shen, B. C. B. Huang, J. Lasaga, D. G. Payan, and Y. Luo, "TNIK , a Novel Member of the Germinal Center Kinase Family That Activates the c-Jun N-terminal Kinase Pathway and Regulates the Cytoskeleton," *J. Biol. Chem.*, vol. 274, no. 43, pp. 30729–30737, 1999.

[104] Q. Wang, E. I. Charych, V. L. Pulito, J. B. Lee, N. M. Graziane, R. A. Crozier, R. Revilla-Sanchez, M. P. Kelly, A. J. Dunlop, H. Murdoch, N. Taylor, Y. Xie, M. Pausch, A. Hayashi-Takagi, K. Ishizuka, S. Seshadri, B. Bates, K. Kariya, A. Sawa, R. J. Weinberg, S. J. Moss, M. D. Houslay, Z. Yan, and N. J. Brandon, "The psychiatric disease risk factors DISC1 and TNIK interact to regulate synapse composition and function," *Mol. Psychiatry*, vol. 16, no. 10, pp. 1006–1023, 2011.

[105] A. C. Burette, K. D. Phend, S. Burette, Q. Lin, M. Liang, G. Foltz, Q. Wang, N. J. Brandon, B. Bates, M. D. Ehlers, and R. J. Weinberg, "Organization of TNIK in Dendritic Spines," *J. Comp. Neurol.*, vol. 523, no. 13, pp. 1913–1924, 2015.

[106] J. Peng, M. Jong, D. Cheng, D. M. Duong, S. P. Gygi, and M. Sheng, "Semiquantitative Proteomic Analysis of Rat Forebrain Postsynaptic Density Fractions by Mass Spectrometry," *J. Biol. Chem.*, vol. 279, no. 20, pp. 21003–21011, 2004.

[107] M. O. Collins, H. Husi, L. Yu, J. M. Brandon, C. N. G. Anderson, W. P. Blackstock, J. S. Choudhary, and S. G. N. Grant, "Molecular characterization and comparison of the components and multiprotein complexes in the postsynaptic proteome," *J. Neurochem.*, vol. 97, no. Suppl 1, pp. 16–23, 2006.

[108] N. K. Hussain, H. Hsin, R. L. Huganir, and M. Sheng, "MINK and TNIK Differentially Act on Rap2-Mediated Signal Transduction to Regulate Neuronal Structure and AMPA Receptor Function," *J. Neurosci.*, vol. 30, no. 44, pp. 14786–14794, 2010.

[109] M. P. Coba, N. H. Komiyama, J. Nithianantharajah, M. V. Kopanitsa, T. Indersmitten, N. G. Skene, E. J. Tuck, D. G. Fricker, K. A. Elsegood, L. E. Stanford, N. O. Afinowi, L. M. Saksida, T. J. Bussey, T. J. O'Dell, and S. G. N. Grant, "TNiK Is Required for Postsynaptic and Nuclear Signaling Pathways and Cognitive Function," *J. Neurosci.*, vol. 32, no. 40, pp. 13987–13999, 2012.

[110] H. Kawabe, A. Neeb, K. Dimova, S. M. Young, M. Takeda, S. Katsurabayashi, M. Mitkovski, O. A. Malakhova, D. Zhang, M. Umikawa, K. Kariya, S. Goebbels, K. Nave, C. Rosenmund, O. Jahn, J. Rhee, and N. Brose, "Regulation of Rap2A by the Ubiquitin Ligase Nedd4-1 Controls Neurite Development," *Neuron*, vol. 65, no. 3, pp. 358–372, 2010.

[111] K. Taira, M. Umikawa, K. Takei, B. Myagmar, M. Shinzato, N. Machida, H. Uezato, S. Nonaka, and K. Kariya, “The Traf2- and Nck-interacting Kinase as a Putative Effector of Rap2 to Regulate Actin Cytoskeleton,” *J. Biol. Chem.*, vol. 279, no. 47, pp. 49488–49496, 2004.

[112] Y. Zhu, D. Pak, Y. Qin, S. G. Mccormack, M. J. Kim, J. P. Baumgart, V. Velamoor, Y. P. Auberson, P. Osten, L. Van Aelst, M. Sheng, and J. J. Zhu, “Rap2-JNK Removes Synaptic AMPA Receptors during Depotentiation,” *Neuron*, vol. 46, no. 6, pp. 905–916, 2005.

[113] X. M. Larhammar, S. Huntwork-rodriguez, Y. Rudhard, A. Sengupta-ghosh, X. J. W. Lewcock, S. Francisco, I. V. Pharmacology, E. Ag, and M. E. Campus, “Converge to Regulate Stress-Induced JNK Signaling in Neurons,” *J. Neurosci.*, vol. 37, no. 46, pp. 11074–11084, 2017.

[114] S. M. Lee, S. Tole, E. Grove, and a P. McMahon, “A local Wnt-3a signal is required for development of the mammalian hippocampus.,” *Development*, vol. 127, no. 3, pp. 457–467, 2000.

[115] X. Gao, P. Arlotta, J. D. Macklis, and J. Chen, “Conditional Knock-Out of -Catenin in Postnatal-Born Dentate Gyrus Granule Neurons Results in Dendritic Malformation,” *J. Neurosci.*, vol. 27, no. 52, pp. 14317–14325, 2007.

[116] H. Shu, S. Chen, Q. Bi, M. Mumby, and D. L. Brekken, “Identification of phosphoproteins and their phosphorylation sites in the WEHI-231 B lymphoma cell line,” *Mol. Cell. Proteomics*, vol. 3, no. 3, pp. 279–286, 2004.

[117] F. S. Oppermann, F. Gnad, J. V. Olsen, R. Hornberger, Z. Greff, G. Kéri, M. Mann, and H. Daub, “Large-scale Proteomics Analysis of the Human Kinome,” *Mol. Cell. Proteomics*, vol. 8, no. 7, pp. 1751–1764, 2009.

[118] Q. Wang, S. P. Amato, D. M. Rubitski, M. M. Hayward, B. L. Kormos, P. R. Verhoest, L. Xu, N. J. Brandon, and M. D. Ehlers, “Identification of Phosphorylation Consensus Sequences and Endogenous Neuronal Substrates of the Psychiatric Risk Kinase TNIK,” *J. Pharmacol. Exp. Ther.*, vol. 356, no. 2, pp. 410–423, 2016.

[119] N. A. DeCarolis and A. J. Eisch, “Hippocampal neurogenesis as a target for the treatment of mental illness: A critical evaluation,” *Neuropharmacology*, vol. 58, no. 6, pp. 884–893, 2010.

[120] M. A. Snyder and W.-J. Gao, “NMDA hypofunction as a convergence point for progression and symptoms of schizophrenia,” *Front. Cell. Neurosci.*, vol. 7, pp. 1–12, 2013.

[121] A. A. Coley and W.-J. Gao, “PSD95: A synaptic protein implicated in schizophrenia or autism?,” *Prog. Neuro-Psychopharmacology Biol. Psychiatry*, vol. 82, pp. 187–194, 2018.

[122] J. H. Barnett, T. W. Robbins, V. C. Leeson, B. J. Sahakian, E. M. Joyce, and A. D. Blackwell, “Neuroscience and Biobehavioral Reviews Assessing cognitive function in clinical trials of schizophrenia,” *Neurosci. Biobehav. Rev.*, vol. 34, no. 8, pp. 1161–1177, 2010.

[123] N. J. Brandon, J. K. Millar, C. Korth, H. Sive, K. K. Singh, and A. Sawa, “Understanding the Role of DISC1 in Psychiatric Disease and during Normal Development,” *J. Neurosci.*, vol. 29, no. 41, pp. 12768–12775, 2009.

[124] S. G. Potkin, J. A. Turner, G. Guffanti, A. Lakatos, J. H. Fallon, D. D. Nguyen, D. Mathalon, J. Ford, J. Lauriello, and F. Macciardi, “A genome-wide association study of schizophrenia using brain activation as a quantitative phenotype,” *Schizophr. Bull.*, vol. 35, no. 1, pp. 96–108, 2009.

[125] J. Shi, D. F. Levinson, J. Duan, A. R. Sanders, Y. Zheng, I. Péer, F. Dudbridge, P. A. Holmans, A. S. Whittemore, B. J. Mowry, A. Olincy, F. Amin, C. R. Cloninger, J. M. Silverman, N. G. Buccola, W. F. Byerley, D. W. Black, R. R. Crowe, J. R. Oksenberg, D. B. Mirel, K. S. Kendler, R. Freedman, and P. V. Gejman, “Common variants on chromosome 6p22.1 are associated with schizophrenia,” *Nature*, vol. 460, no. 7256, pp. 753–757, 2009.

[126] M. Ayalew, D. F. Levey, N. Jain, B. Changala, S. D. Patel, E. Winiger, A. Breier, A. Shekhar, R. Amdur, D. Koller, J. I. Nurnberger, A. Corvin, M. Geyer, M. T. Tsuang, D. Salomon, N. J. Schork, A. H. Fanous, and M. C. O. Donovan, “Convergent functional genomics of schizophrenia : from comprehensive understanding to genetic risk prediction,” *Mol. ps*, vol. 17, no. 9, pp. 887–905, 2012.

[127] H. Yu, H. Yan, L. Wang, J. Li, L. Tan, W. Deng, Q. Chen, G. Yang, F. Zhang, T. Lu, J. Yang, K. Li, and L. Lv, “Articles Five novel loci associated with antipsychotic treatment response in patients with schizophrenia : a genome-wide association study,” *The Lancet Psychiatry*, vol. 0366, no. 18, pp. 1–12, 2018.

[128] S. J. Glatt, I. P. Everall, W. S. Kremen, J. Corbeil, R. Sa, N. Khanlou, M. Han, C. Liew, and M. T. Tsuang, “Comparative gene expression analysis of blood and brain provides concurrent validation of SELENBP1 up-regulation in schizophrenia,” *Proc. Natl. Acad. Sci. U. S. A.*, vol. 102, no. 43, pp. 15533–15538, 2005.

[129] S. G. Potkin, F. Macciardi, G. Guffanti, Q. Wang, J. A. Turner, M. F. Miles, A. Lander, M. P. Vawter, and X. Xie, “Identifying Gene Regulatory Networks in Schizophrenia,” *Neuroimage*, vol. 53, no. 3, pp. 839–847, 2010.

[130] N. Matigian, L. Windus, H. Smith, C. Filippich, C. Pantelis, J. Mcgrath, and B. Mowry, “Expression profiling in monozygotic twins discordant for bipolar disorder reveals dysregulation of the WNT signalling pathway,” *Mol. Psychiatry*, vol. 12, no. 9, pp. 815–825, 2007.

[131] S. Anazi, H. E. Shamseldin, D. Alnaqeb, and M. Abouelhoda, “A null mutation in TNIK defines a novel locus for intellectual disability,” *Hum. Genet.*, vol. 135, no. 7, pp. 773–778, 2016.

[132] E. T. Wang, R. Sandberg, S. Luo, I. Khrebtukova, L. Zhang, C. Mayr, S. F. Kingsmore, G. P. Schroth, and C. B. Burge, “Alternative isoform regulation in human tissue transcriptomes,” *Nature*, vol. 456, no. 7221, pp. 470–476, 2008.

[133] B. J. Blencowe, “Alternative Splicing: New Insights from Global Analyses,” *Cell*, vol. 126, no. 1, pp. 37–47, 2006.

[134] A. G. Matera and Z. Wang, “A day in the life of the spliceosome,” *Nat. Rev. Mol. Cell Biol.*, vol. 15, no. 2, pp. 108–121, 2014.

[135] A. R. Kornblihtt, M. De La Mata, J. P. Fededa, M. J. Muñoz, and G. Nogués, “Multiple links between transcription and splicing,” *Rna*, vol. 10, no. 10, pp. 1489–1498, 2004.

[136] R. Luco, Q. Pan, and K. Tominaga, “Regulation of alternative splicing by histone modifications,” *Science (80-.).*, vol. 327, no. 5968, pp. 996–1000, 2010.

[137] A. J. Matlin, F. Clark, and C. W. J. Smith, “Understanding alternative splicing: Towards a cellular code,” *Nat. Rev. Mol. Cell Biol.*, vol. 6, no. 5, pp. 386–398, 2005.

[138] T. W. Nilsen and B. R. Graveley, “Expansion of the eukaryotic proteome by alternative splicing,” *Nature*, vol. 463, no. 7280, pp. 457–463, 2010.

[139] G. Yeo, D. Holste, G. Kreiman, and C. B. Burge, “Variation in alternative splicing across human tissues.,” *Genome Biol.*, vol. 5, no. 10, p. R74, 2004.

[140] N. L. Barbosa-Morais, M. Irimia, Q. Pan, H. Y. Xiong, S. Gueroussov, L. J. Lee, V. Slobodeniuc, C. Kutter, S. Watt, R. Çolak, T. H. Kim, C. M. Misquitta-Ali, M. D. Wilson, P. M. Kim, D. T. Odom, B. J. Frey, and B. J. Blencowe, “The evolutionary landscape of alternative splicing in vertebrate species,” *Science (80-.).*, vol. 338, no. 6114, pp. 1587–1593, 2012.

[141] J. Merkin, C. Russell, P. Chen, and C. B. Burge, “Evolutionary dynamics of gene and isoform regulation in mammalian tissues,” *Science (80-.).*, vol. 338, no. 6114, pp. 1593–1599, 2012.

[142] S. Zheng and D. L. Black, “Alternative pre-mRNA splicing in neurons: Growing up and extending its reach,” *Trends Genet.*, vol. 29, no. 8, pp. 442–448, 2013.

[143] S. M. Weyn-vanhentenryck, H. Feng, D. Ustianenko, R. Duf, Q. Yan, M. Jacko, J. C. Martinez, M. Goodwin, X. Zhang, U. Hengst, S. Lomvardas, M. S. Swanson, and C. Zhang, “Precise temporal regulation of alternative splicing during neural development,” *Nat. Commun.*, vol. 9, no. 1, p. 2189, 2018.

[144] G. Hermey, N. Blüthgen, and D. Kuhl, “Neuronal activity-regulated alternative mRNA splicing,” *Int. J. Biochem. Cell Biol.*, vol. 91, pp. 184–193, 2017.

[145] R. Daoud, M. Da Penha Berzaghi, F. Siedler, M. Hubener, and S. Stamm, “Activity-dependent regulation of alternative splicing patterns in the rat brain,” *Eur J Neurosci*, vol. 11, no. 3, p. 788–802., 1999.

[146] J. Xie and D. L. Black, “A CaMK IV responsive RNA element mediates depolarization-induced alternative splicing of ion channels,” *Nature*, vol. 410, no. 831, pp. 936–939, 2001.

[147] P. R. Brakeman, A. A. Lanahan, R. O'Brien, K. Roche, C. A. Barnes, R. L. Huganir, and P. F. Worley, "Homer: A protein that selectively binds metabotropic glutamate receptors," *Nature*, vol. 386, no. 6622. pp. 284–288, 1997.

[148] R. Hepp, J. Dupont, D. Aunis, K. Langley, and N. Grant, "NGF enhances depolarization effects on SNAP-25 expression: induction of SNAP-25b isoform," *Neuroreport*, vol. 12, no. 4, pp. 673–677, 2001.

[149] T. Iijima, K. Wu, H. Witte, Y. Hanno-Iijima, T. Glatter, S. Richard, and P. Scheiffele, "SAM68 regulates neuronal activity-dependent alternative splicing of neurexin-1," *Cell*, vol. 147, no. 7, pp. 1601–1614, 2011.

[150] X. Liu, R. Bates, D.-M. Yin, C. Shen, F. Wang, N. Su, S. A. Kirov, Y. Luo, J.-Z. Wang, W.-C. Xiong, and L. Mei, "Specific Regulation of NRG1 Isoform Expression by Neuronal Activity," *J. Neurosci.*, vol. 31, no. 23, pp. 8491–8501, 2011.

[151] D. L. Black, "Mechanisms of Alternative Pre-Messenger RNA Splicing," *Annu. Rev. Biochem.*, vol. 72, no. 1, pp. 291–336, 2003.

[152] J. Ule and R. B. Darnell, "RNA binding proteins and the regulation of neuronal synaptic plasticity," *Curr. Opin. Neurobiol.*, vol. 16, no. 1, pp. 102–110, 2006.

[153] J. A. Calarco, S. Superina, D. O'Hanlon, M. Gabut, B. Raj, Q. Pan, U. Skalska, L. Clarke, D. Gelinas, D. van der Kooy, M. Zhen, B. Ciruna, and B. J. Blencowe, "Regulation of Vertebrate Nervous System Alternative Splicing and Development by an SR-Related Protein," *Cell*, vol. 138, no. 5, pp. 898–910, 2009.

[154] B. Raj, D. O'Hanlon, J. P. Vessey, Q. Pan, D. Ray, N. J. Buckley, F. D. Miller, and B. J. Blencowe, "Cross-Regulation between an Alternative Splicing Activator and a Transcription Repressor Controls Neurogenesis," *Mol. Cell*, vol. 43, no. 5, pp. 843–850, 2011.

[155] C. Zhang, Z. Zhang, J. Castle, S. Sun, J. Johnson, A. R. Krainer, and M. Q. Zhang, "Defining the splicing regulatory network of tissue-specific splicing factors Fox-1/2," *Genes Dev*, vol. 22, pp. 2550–2563, 2008.

[156] S. M. Weyn-Vanhentenryck, A. Mele, Q. Yan, S. Sun, N. Farny, Z. Zhang, C. Xue, M. Herre, P. A. Silver, M. Q. Zhang, A. R. Krainer, R. B. Darnell, and C. Zhang, "HITS-CLIP and Integrative Modeling Define the Rbfox Splicing-Regulatory Network Linked to Brain Development and Autism," *Cell Rep.*, vol. 6, no. 6, pp. 1139–1152, 2014.

[157] P. L. Boutz, P. Stoilov, Q. Li, C. H. Lin, G. Chawla, K. Ostrow, L. Shiue, M. Ares, and D. L. Black, "A post-transcriptional regulatory switch in polypyrimidine tract-binding proteins reprograms alternative splicing in developing neurons," *Genes Dev.*, vol. 21, no. 13, pp. 1636–1652, 2007.

[158] E. V. Makeyev, J. Zhang, M. A. Carrasco, and T. Maniatis, "The MicroRNA miR-124 Promotes Neuronal Differentiation by Triggering Brain-Specific Alternative Pre-mRNA Splicing," *Mol. Cell*, vol. 27, no. 3, pp. 435–448, 2007.

[159] H. J. Okano and R. B. Darnell, "A hierarchy of Hu RNA binding proteins in developing and adult neurons.," *J. Neurosci.*, vol. 17, no. 9, pp. 3024–3037, 1997.

[160] C. Colombrita, V. Silani, and A. Ratti, "ELAV proteins along evolution: Back to the nucleus?," *Mol. Cell. Neurosci.*, vol. 56, pp. 447–455, 2013.

[161] H. Zhu, R. A. Hasman, V. A. Barron, G. Luo, and H. Lou, "A Nuclear Function of Hu Proteins as Neuron-specific Alternative RNA Processing Regulators," *Mol. Biol. Cell*, vol. 17, no. 12, pp. 5105–5114, 2006.

[162] R. J. Buckanovich, J. B. Posner, and R. B. Darnell, "Nova, the papraneoplastic Ri antigen, is homologous to an RNA-binding protein and is specifically expressed in the developing motor system," *Neuron*, vol. 11, no. 4, pp. 657–672, 1993.

[163] Y. Y. L. Yang, G. L. Yin, and R. B. Darnell, "The neuronal RNA-binding protein Nova-2 is implicated as the autoantigen targeted in POMA patients with dementia," *Proc. Natl. Acad. Sci.*, vol. 95, no. 22, pp. 13254–13259, 1998.

[164] K. B. Jensen, B. K. Dredge, G. Stefani, R. Zhong, R. J. Buckanovich, H. J. Okano, Y. Y. L. Yang, and R. B. Darnell, "Nova-1 regulates neuron-specific alternative splicing and is essential for neuronal viability," *Neuron*, vol. 25, no. 2, pp. 359–371, 2000.

[165] C. S. Huang, S. H. Shi, J. Ule, M. Ruggiu, L. A. Barker, R. B. Darnell, N. J. Yuh, and L. Y. Jan, “Common molecular pathways mediate long-term potentiation of synaptic excitation and slow synaptic inhibition,” *Cell*, vol. 123, no. 1, pp. 105–118, 2005.

[166] M. Ruggiu, R. Herbst, N. Kim, M. Jevsek, J. J. Fak, M. A. Mann, G. Fischbach, S. J. Burden, and R. B. Darnell, “Rescuing Z+ agrin splicing in Nova null mice restores synapse formation and unmasks a physiologic defect in motor neuron firing,” *Proc. Natl. Acad. Sci. U. S. A.*, vol. 106, no. 9, pp. 3513–3518, 2009.

[167] R. J. Buckanovich and R. B. Darnell, “The neuronal RNA binding protein Nova-1 recognizes specific RNA targets in vitro and in vivo,” *Mol. Cell. Biol.*, vol. 17, no. 6, pp. 3194–3201, 1997.

[168] R. J. Buckanovich, Y. Y. Yang, and R. B. Darnell, “The onconeural antigen Nova-1 is a neuron-specific RNA-binding protein, the activity of which is inhibited by paraneoplastic antibodies,” *J. Neurosci.*, vol. 16, no. 3, pp. 1114–1122, 1996.

[169] Racca, “The neuronal splicing factor Nova co-localizes with target RNAs in the dendrite,” *Front. Neural Circuits*, vol. 4, no. March, pp. 1–16, 2010.

[170] J. Ule, K. B. Jensen, M. Ruggiu, A. Mele, and R. B. Darnell, “CLIP Identifes Nova-Regulated RNA Networks in the Brain,” *Science (80-.).*, vol. 302, no. 5648, pp. 1212–1215, 2003.

[171] J. Ule, A. Ule, J. Spencer, A. Williams, J. S. Hu, M. Cline, H. Wang, T. Clark, C. Fraser, M. Ruggiu, B. R. Zeeberg, D. Kane, J. N. Weinstein, J. Blume, and R. B. Darnell, “Nova regulates brain-specific splicing to shape the synapse,” *Nat. Genet.*, vol. 37, no. 8, pp. 844–852, 2005.

[172] C. Zhang, M. A. Frias, A. Mele, M. Ruggiu, T. Eom, C. B. Marney, H. Wang, D. D. Licatalosi, J. J. Fak, and R. B. Darnell, “Integrative modeling defines the nova splicing-regulatory network and its combinatorial controls,” *Science (80-.).*, vol. 329, no. 5990, pp. 439–443, 2010.

[173] K. Han, G. Yeo, P. An, C. B. Burge, and P. J. Grabowski, “A combinatorial code for splicing silencing: UAGG and GGGG motifs,” *PLoS Biol.*, vol. 3, no. 5, pp. 0843–0860, 2005.

[174] E. Park, C. Iaccarino, J. Lee, I. Kwon, S. M. Baik, M. Kim, J. Y. Seong, G. H. Son, E. Borrelli, and K. Kim, "Regulatory Roles of Heterogeneous Nuclear Ribonucleoprotein M and Nova-1 Protein in Alternative Splicing of Dopamine D2 Receptor Pre-mRNA," *J. Biol. Chem.*, vol. 286, no. 28, pp. 25301–25308, 2011.

[175] P. Bossolasco, F. Sassone, V. Gumina, S. Peverelli, M. Garzo, and V. Silani, "Motor neuron differentiation of iPSCs obtained from peripheral blood of a mutant TARDBP ALS patient," *Stem Cell Res.*, vol. 30, no. May, pp. 61–68, 2018.

[176] M. W. Amoroso, G. F. Croft, D. J. Williams, S. O'Keeffe, M. A. Carrasco, A. R. Davis, L. Roybon, D. H. Oakley, T. Maniatis, C. E. Henderson, and H. Wichterle, "Accelerated high-yield generation of limb-innervating motor neurons from human stem cells," *J Neurosci*, vol. 33, no. 2, pp. 574–586, 2013.

[177] F. Pagani, E. Buratti, C. Stuani, M. Romano, E. Zuccato, M. Niksic, L. Giglio, D. Faraguna, and F. E. Baralle, "Splicing factors induce cystic fibrosis transmembrane regulator exon 9 skipping through a nonevolutionary conserved intronic element," *J. Biol. Chem.*, vol. 275, no. 28, pp. 21041–21047, 2000.

[178] K. Takahashi, K. Tanabe, M. Ohnuki, M. Narita, T. Ichisaka, K. Tomoda, and S. Yamanaka, "Induction of Pluripotent Stem Cells from Adult Human Fibroblasts by Defined Factors," *Cell*, vol. 131, no. 5, pp. 861–872, 2007.

[179] A. Ratti, C. Falini, L. Cova, R. Fantozzi, C. Calzarossa, E. Zennaro, A. Pascale, A. Quattrone, and V. Silani, "A role for the ELAV RNA-binding proteins in neural stem cells: stabilization of Msi1 mRNA," *J. Cell Sci.*, vol. 119, no. 7, pp. 1442–1452, 2006.

[180] I. Paz, I. Kosti, M. Ares, M. Cline, and Y. Mandel-Gutfreund, "RBPmap: A web server for mapping binding sites of RNA-binding proteins," *Nucleic Acids Res.*, vol. 42, no. W1, pp. 1–7, 2014.

[181] A. Ratti and E. Buratti, "Physiological functions and pathobiology of TDP-43 and FUS/TLS proteins," *J. Neurochem.*, vol. 138, pp. 95–111, 2016.

[182] M. Irimia, R. J. Weatheritt, J. D. Ellis, N. N. Parikshak, T. Gonatopoulos-Pournatzis, M. Babor, M. Quesnel-Vallières, J. Tapial, B. Raj, D. O'Hanlon, M. Barrios-Rodiles, M. J. E. Sternberg, S. P. Cordes, F. P. Roth, J. L. Wrana, D. H. Geschwind, and B. J. Blencowe, "A highly conserved program of neuronal microexons is misregulated in autistic brains," *Cell*, vol. 159, no. 7, pp. 1511–1523, 2014.

[183] Y. I. Li, L. Sanchez-Pulido, W. Haerty, and C. P. Ponting, "RBFOXand PTBP1 proteins regulate the alternative splicing of micro-exons in human brain transcripts," *Genome Res.*, vol. 25, no. 1, pp. 1–13, 2015.

[184] J. K. Bose, I. F. Wang, L. Hung, W. Y. Tarn, and C. K. J. Shen, "TDP-43 overexpression enhances exon 7 inclusion during the survival of motor neuron pre-mRNA splicing," *J. Biol. Chem.*, vol. 283, no. 43, pp. 28852–28859, 2008.

[185] K. C. Flynn, "The cytoskeleton and neurite initiation," *Bioarchitecture*, vol. 3, no. 4, pp. 86–109, 2013.

[186] E. W. Dent, S. L. Gupton, and F. B. Gertler, "The Growth Cone Cytoskeleton in Axon outgrowth and guidance.pdf," *Cold Spring Harb. Perspect. Biol.*, pp. 1–40, 2011.

[187] T. M. Gomez and P. C. Letourneau, "Actin Dynamics in Growth Cone Motility and Navigation," *J Neurochem*, vol. 129, no. 2, pp. 221–234, 2014.

[188] J. Q. Wu, X. Wang, N. J. Beveridge, P. A. Tooney, R. J. Scott, V. J. Carr, and M. J. Cairns, "Transcriptome sequencing revealed significant alteration of cortical promoter usage and splicing in schizophrenia," *PLoS One*, vol. 7, no. 4, 2012.

[189] S. G. Fillman, N. Cloonan, V. S. Catts, L. C. Miller, J. Wong, T. Mccrossin, M. Cairns, and C. S. Weickert, "Increased inflammatory markers identified in the dorsolateral prefrontal cortex of individuals with schizophrenia," *Mol. Psychiatry*, vol. 18, no. 2, pp. 206–214, 2013.

[190] L. A. Glantz and D. A. Lewis, "Decreased dendritic spine density on prefrontal cortical pyramidal neurons in schizophrenia.," *Arch. Gen. Psychiatry*, vol. 57, no. 1, pp. 65–73, 2000.

[191] E. Buratti, M. Romano, and F. E. Baralle, “TDP-43 high throughput screening analyses in neurodegeneration: Advantages and pitfalls,” *Mol. Cell. Neurosci.*, vol. 56, pp. 465–474, 2013.

[192] P. Price, D. Mordered, and W. Rossoll, “RNP Assembly Defects in Spinal Muscular Atrophy,” *Adv Neurobiol*, vol. 20, pp. 143–171, 2018.

SCIENTIFIC PRODUCTION

PUBLICATIONS ON JOURNALS

1) Onesto E, Colombrita C, **Gumina V**, Borghi MO, Dusi S, Doretti A, Fagiolari G, Invernizzi F, Moggio M, Tiranti V, Silani V, Ratti A. "Gene-specific mitochondria dysfunctions in human TARDBP and C9ORF72 fibroblasts". Acta Neuropathol Commun. 2016 May 5; 4(1):47. doi: 10.1186/s40478-016-0316-5.

2) Bossolasco P, Sassone F, **Gumina V**, Peverelli S, Garzo M, Silani V. "Motor neuron differentiation of iPSCs obtained from peripheral blood of a mutant TARDBP ALS patient". Stem Cell Res., 2018 Jul; 30:61-68. doi: 10.1016/j.scr.2018.05.009.

3) Giampetruzzi A, Danielson EW, Jeon M, **Gumina V**, Boopathy S, Brown RH, Landers JE, Fallini C. "Modulation of actin polymerization affects nucleocytoplasmic transport in multiple forms of Amyotrophic Lateral Sclerosis" (*submitted Nature Communication*)

4) Fogh I, Lin K, Tiloca C, Van Rheenen W, Jones A, Ratti A, Van Damme P, Corrado L, McLaughlin RL, Sorarù G, Pensato V, Shatunov A, Iacoangeli A, Calvo A, Corcia P, Del Bo R, Cereda C, Gentilini D, De Blasio A, Bertolini C, Ticozzi N, Dekker A, Rooney J, Vajda A, Verde F, Martin S, Sproviero W, Orrell R, Moisse M, Bossolasco P, **Gumina V**, Peverelli S, Nigel Leigh P, Traynor BJ, Meininger V, Melki J, Comi GP, Lewis CM, Robberecht W, Hardy J, Fratta P, Mazzini L, Taroni F, Gellera C, D'Alfonso S, Chiò A, Hardiman O, van den Berg LH, Veldink JH, Al-Chalabi A, Shaw CE, Silani V and Powell J. "Genetic Modifiers of Age of Onset in ALS Patients with Repeat Expansions in C9orf72 Gene: a genome-wide association study". (*submitted Brain*)

5) **Gumina V**, Colombrita C, Bossolasco P, Fallini C, Buratti E, Maraschi AM, Landers JE, Silani V, Ratti A. "TDP-43 and NOVA-1 as alternative splicing regulators of *TNIK* gene, a schizophrenia genetic risk factor" (*in preparation*)

POSTERS

1) **Gumina V**, Colombrita C, Maraschi AM, Buratti E, Baralle FE, Silani V, Ratti A. “Characterization of TDP-43 splicing target TNIK in neuronal differentiation”. ENCALS meeting, Milan, 19-21 May, 2016

2) Maraschi AM, **Gumina V**, Colombrita C, Feligioni M, Silani V, Ratti A. “TDP-43 post-translational modifications: what role for SUMOylation?” ENCALS meeting, Milan, 19-21 May 2016

3) **Gumina V**, Colombrita C, Maraschi AM, Buratti E, Baralle FE, Silani V, Ratti A. “Characterization of TNIK alternative splicing, a TDP-43 target, in neuronal differentiation”. MNDA Symposium, Dublin, December 7-9, 2016

4) Maraschi AM, **Gumina V**, Colombrita C, Feligioni M, Silani V, Ratti A. “Analysis of SUMOylation as a posttranslational modification of TDP-43 protein”. MNDA Symposium, Dublin, December 7-9, 2016

5) Colombrita C, **Gumina V**, Maraschi AM, Doretti A, Tiloca C, Silani V, Ratti A. “Stress granules formation upon condition of chronic stress in human ALS fibroblasts” ENCALS meeting, Ljubljana (Slovenia), 18-20 May, 2017

6) **Gumina V**, Colombrita C, Bossolasco P, Maraschi AM, Sassone F, Buratti E, Silani V, Ratti A. “TNIK and its alternative splicing regulation during neuronal differentiation”. SiNAPSA Neuroscience Conference, Ljubljana (Slovenia), September 29-30, 2017

7) **Gumina V**, Colombrita C, Bossolasco P, Maraschi AM, Sassone F, Buratti E, Silani V, Ratti A. “Regulation of Traf2 and NcK interacting Kinase (TNIK) alternative splicing in human tissues and during neuronal differentiation”. Society for Neuroscience, Washington, November 10-16, 2017

8) Colombrita C, **Gumina V**, Maraschi AM, Doretti A, Sassone F, Bossolasco P, Ratti A, Silani V. “Stress granules formation upon condition of chronic stress in human ALS disease models”. Society for Neuroscience, Washington, November 10-16, 2017

9) Maraschi AM, **Gumina V**, Colombrita C, Volpe C, Feligioni M, Silani V, Ratti A. “TDP-43 protein and SUMOylation”. ENCALS meeting, Oxford, 20-22 May, 2018

10) Bossolasco P, Sassone F, **Gumina V**, Silani V. “Motor neuron differentiation of iPSCs from peripheral blood of a TARDBP mutated ALS patient”. ENCALS meeting, Oxford, 20-22 May, 2018

11) **Gumina V**, Colombrita C, Bossolasco P, Maraschi A, Sassone F, Buratti E, Silani V, Ratti A. “Role of TDP-43 and NOVA1 RNA-binding proteins in the regulation of TNIK alternative splicing in neuronal cells”. 2nd International Caparica Conference in Splicing 2018, Caparica, July 16-19, 2018

Acknowledgements

This project was financially supported by the Laboratory of Neuroscience of IRCSS Istituto Auxologico Italiano (Ricerca Corrente, Ministero della Salute).
I am particularly grateful to my supervisor Dr. Antonia Ratti, who followed and support me during my entire PhD program. I would thank her also for the emblematic sentence “Chi ha tempo, non perda tempo”, that sometimes drove me crazy, but always spurred me to achieve new goals important for my professional growth.
I wish to thank Prof. Vincenzo Silani and all my colleagues of the Laboratory of Neuroscience of IRCCS Istituto Auxologico Italiano for the scientific support.
Part of this project was conducted during my training experience at the Department of Neurology of UMASS Medical School in Worcester, USA. In particular, I would like to thank Claudia Fallini, who gave me the opportunity of a significant professional and personal growth, who welcomed me in her sweet family and daily saved me with a good Italian Espresso.
At last, but not least, I want to heartily dedicate this work to my husband, my family and all my friends who love me and make my life definitely better, believing in me and encouraging me every day.